DOI: 10.31577/ahs-2020-0021.02.0016

ACTA HYDROLOGICA SLOVACA

Volume 21, No. 2, 2020, 133 – 138

CHANGES IN SOIL MOISTURE VALUES TWO YEARS AFTER BIOCHAR REAPPLICATION

Justína Vitková*, Peter Šurda, Anton Zvala

Biochar, as a carbon rich material, has properties which are similar to water repellent material. Its application into the soil changes these properties, but it takes a few years. Our research was focused on soil moisture values comparison at plots with aged biochar (applied into the soil in 2014) and fresh biochar (aged biochar applied in 2014 + reapplied biochar applied into soil in 2018). Results indicated that fresh biochar had water repellent properties in first year after its application into the silt loam soil, which were changed in second year after its application. Our measurements show positive effect of biochar on soil water regime in a longer time horizon.

KEY WORDS: biochar reapplication, soil moisture, barley, maize

Introduction

Biochar is a solid porous material with high carbon content. It is the product of thermal degradation of organic materials in the absence of air (pyrolysis). During pyrolysis, between 50% and 80% of biomass is converted into combustible liquids and vapours, which can be used to produce bioenergy (Laird et al., 2009). The remaining biomass is converted into biochar, which retains some residual feedstock properties but is essentially composed of amorphous carbon, turbostratic crystallites of polycondensed aromatic sheets, and interspersed voids (Keiluweit et al., 2010). Feedstock selection and pyrolysis conditions affect biochar properties (Rutherford et al., 2012). Functional surface groups of biochars create hydrophobic hot-spots thereby increasing spatial heterogeneity of the water repellency of the soil (Kinney et al., 2012). It has been reported that water repellency is linked to the abundance of non-polar aliphatic and aromatic groups of organic compounds (Ellerbrock et al., 2005).
The hydraulic system becomes more complex when biochars are added to soil. The impact of soil water repellency on hydraulic properties including infiltration capacity, surface runoff and erosion has been studied intensively during the last two decades (e.g., Bachmann et al., 2013). Water repellency depends on the initial moisture content and time. Biochars tend to decompose slowly in the environment and are thus considered temporal sinks for atmospheric CO_2 (Glaser et al., 2002). Water repellency and delayed wetting are commonly causing higher fractions of entrapped air and thus decrease the fraction of saturated soil pores, which should reduce both, the available water capacity and hydraulic conductivity. Therefore, the development of chars with low water repellency has been proposed for optimizing the positive effects on soil hydraulic properties (Kinney et al., 2012).
Biochar produced at low temperature contains more aliphatic compounds in the biochar pores that increase the hydrophobicity (Chen et al., 2008; Gray et al., 2014), while high temperature pyrolysis allows a much smaller number of aliphatic compounds remaining in the pores (Chen et al., 2008). The addition of hydrophobic biochar can turn hydrophilic soil into water repellent. Addition of hydrophobic biochar to soil could change soil hydrophobicity that influences soil hydraulic properties (Jeffery et al., 2015). Therefore, biochar hydrophobicity should be considered for biochar application to soil amendment. The effects of biochar on soil hydrophobicity concerning physical structure change of soil have been discussed. However, regarding to chemical properties of soil and characteristics of biochar, the effects of biochar on soil hydrophobicity remain unclear (Mao et al., 2019).
In last year's began accrue number of articles aimed on impact of biochar on different research topics: soil moisture (Vitkova et al., 2017), grain yields (Horák et al., 2020), CO_2 production (Horák and Šimanský, 2017) or soil structure (Juriga and Šimanský, 2018) in Slovakia. Biochar hydrophobicity (or water repellency) is one of the topics, which has not been studied yet. Therefore, our article is focused on possible biochar's water repellency effect on soil moisture in field conditions.

Material and methods

Our measurements were conducted at the experimental site in Malanta (Fig. 1), which belongs to the Slovak University of Agriculture in Nitra, Slovakia. The research site is located approximately 5 km north-east of Nitra city (N 48°19'00"; E 18°09'00") in the Nitra river basin, where there is a deficit of soil water available to plants due to dry years (Tarnik and Leitmanova, 2017). The locality is 175 MASL and the soil is classified as Haplic Luvisol with soil organic carbon content of 9.13 g.kg^{-1}, with pH of 5.71 and silt loam soil texture. The site is in the temperate region with the mean annual air temperature of 9.8°C and average precipitation amounting to 540 mm (30-year climate normal, 1961–1990) (Horák et al., 2019).
The biochar experiment was established in March, 2014 when whole area was separated at plots (6x4 m) separated by 0.5 m buffer zone. Certificated biochar (Table 1) in amount of 0, 10 and 20 t ha^{-1} was applied on soil surface and incorporated into the depth of 0–10 cm. The biochar was produced from paper fiber sludge and grain husks in a ratio of 1:1 per weight, at a pyrolysis temperature of 550°C (Domanová et al., 2015). Research on various aspects of biochar application into the soil was studied at this area. In 2018, the original plots with former biochar application were divided in halves (4x3 m) and the same biochar with the same dose (0, 10 and 20 t ha^{-1}) was reapplied to one of these halves (Toková et al., 2020).
In this paper we focused on impact of biochar application at the dose of 20 t ha^{-1}. Soil moisture was measured at plots with aged biochar – applied in 2014 (B20) and at plots with fresh biochar – consisting from aged biochar + new biochar applied in 2018 (B20 reap.). These measurements were compared with plots without biochar (Control).
Soil moisture was measured by 5TM dielectric sensors (Decagon Devices, USA) and data was collected in five-minute interval and stored using the EM 50 data loggers. Two sensors were installed to the depth of 5–10 cm below the soil surface at two plots with aged biochar and two plots with fresh biochar. Four sensors were installed to the depth of 5–10 cm below the soil surface at two Control plots. We present the average value for each variant. The measurements were carried out during the 2018 and 2019 growing seasons where cultivated crop was spring barley (*Hordeum vulgare L.*) and maize (*Zea mays L.*), respectively. The monitoring period lasted from June 22, 2018 to July 24, 2018 and from May 3, 2019 to October 23, 2019.
Significance was tested with a two-way analysis of variance. The significance limit was set to 0.05.

Fig. 1. Studied area at Malanta site (© Google maps 2019).

Table 1. Characteristics of used biochar

C	N	H	O	$pH_{(CaCl_2)}$	Ash	SSA
[%]	[%]	[%]	[%]	[-]	[%]	[m^2 g^{-1}]
53.1	1.4	1.84	5.3	8.8	38.3	21.7

Note: (C–carbon, N–nitrogen, H–hydrogen, O–oxygen, pH determined by $CaCl_2$, SSA–specific surface area)

Results and discussion

Meteorological characteristics are very important factors for soil moisture in top soil layer. The monitoring period (as well as the vegetation period) was very dry in 2018 and it was the warmest or equally warmest in the history of measurements in the meteorological station Nitra–Janíkovce according to SHMÚ (2019). According to SHMÚ (2020), the year 2019 was very warm especially in far east of Slovakia. Table 2 shows average monthly air temperatures and precipitation totals during monitoring days and their comparison to climatic normal 1961–1990 according to Šiška et al. (2005). Meteorological data from 2018 and 2019 were provided by Slovak Hydrometeorological Institute from Nitra–Janíkovce meteorological station, which is located approximately 6 km from studied area at Malanta site. In 2018, monitoring period starts on June, 22 and finished on July, 24, so only 9 days (9 values) were calculated as average value for air temperature or precipitation totals in VI./2018 and 24 values (24 days) were calculated for VII./2018 (Table 2). In 2019, monitoring period starts on May, 3 and finished on October, 23, so 29 values (29 days) were calculated for V./2019 and 23 values (23 days) were calculated for X./2019. The month June in Table 2 is not good to compare because of unequal number of values. Average value of air temperature and precipitation totals during other months was calculated from more than 23 days. Measured soil moisture was higher during monitoring period in 2019 because of higher amount of precipitation totals during spring months (Table 3).

Sensors 5TM reacted very well on precipitation in top soil layer. In 2018 (Fig. 2), soil moisture at B20 plots and B20 reap. plots was statistically insignificant during or in a short time after rain episodes (June, 28–30; July, 8; or July, 11–12). Larger differences (statistically significant) were occurred during longer time of non-precipitation days, when soil moisture at B20 reap. plots was lower in about 2–6% vol. in comparison to B20 plots. Soil moisture at Control plots was the lowest almost during the whole monitoring period except the end of monitoring period (July 16–22, 2018). In 2019 (Fig. 3), soil moisture values were completely different. The highest values were measured at B20 reap. plots. Soil moisture at B20 and Control plots was very similar (statistically insignificant) during non-precipitation days (June, 17–23; July, 3–6; or August, 2–6), but smaller at B20 plot in comparison to Control plot (statistically significant) during some rainy days (July, 7–August, 1; or September, 21–October, 2).

Our results showed differences in soil moisture values during monitoring period 2018 and 2019. While in 2018 soil moisture was lower at plots with fresh biochar than at plots with aged biochar, the situation was opposite in 2019. Soil moisture at Control plots was the lowest almost in all months during monitoring periods in 2018 and 2019. Similar results at the same experimental site in 2018 measured also Tarnik (2019) with different sensors. Few studies investigated the particular role of biochar water repellency on hydraulic properties of amended soils. In soil water infiltration experiments the observed reduction of the infiltration rate was attributed to hydrophobic properties of pyrochars (Githinji, 2014).

Table 2. **Average monthly air temperature and precipitation totals at Nitra area during monitoring days in comparison to the climatic normal (CN) 1961–1990**

	TEMPERATURE [°C]			PRECIPITATION [mm]		
	CN	2018	2019	CN	2018	2019
V.	9		13	135		116
VI.	19	18	23	29	26	63
VII.	22	21	22	52	42	41
VIII.	22		23	64		107
IX.	16		16	53		67
X.	12		13	18		16

Table 3. **Average monthly soil moisture values at Malanta area during monitoring days**

	2018 [$cm^3.cm^{-3}$]			2019 [$cm^3.cm^{-3}$]		
	Control	B20	B20 reap.	Control	B20	B20 reap.
V.				0.209	0.238	0.259
VI.	0.080	0.143	0.137	0.178	0.195	0.211
VII.	0.101	0.144	0.120	0.158	0.143	0.169
VIII.				0.166	0.173	0.194
IX.				0.187	0.192	0.208
X.				0.183	0.188	0.207

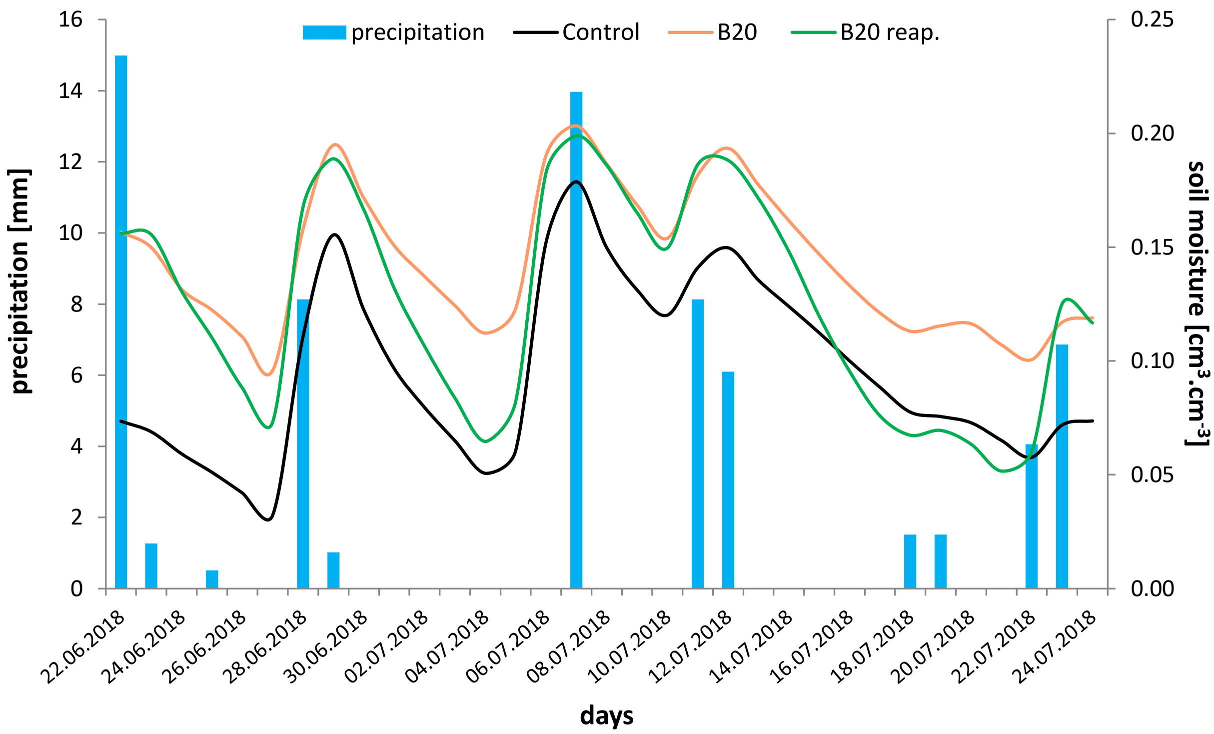

Fig. 2. Measured soil moisture at plots without biochar (Control) and plots with aged biochar (B20) and fresh biochar (B20 reap.) in comparison to daily precipitation totals during monitoring period 2018.

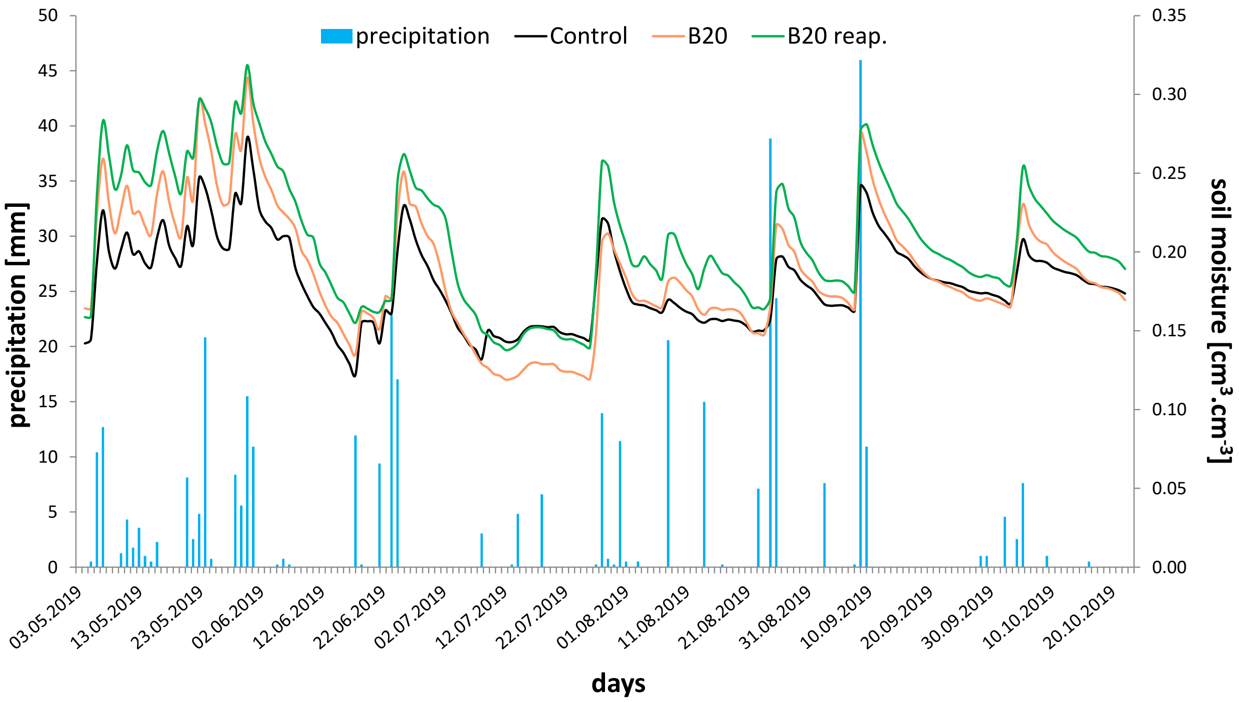

Fig. 3. Measured soil moisture at plots without biochar (Control) and plots with aged biochar (B20) and fresh biochar (B20 reap.) in comparison to daily precipitation totals during monitoring period 2019.

In another study, the water repellency of pyrochars decreased with increasing pyrolysis temperature resulting in higher field capacities (Kinney et al., 2012). In contrast, Baronti et al. (2014) did not find any effects on wettability in a two-year field experiment when sandy clay loam was amended with pyrochar. Our results showed that this type of fresh biochar reduced the soil moisture during non-precipitation days in comparison to plots with aged biochar and Control in 2018. But in 2019 soil moisture was the highest at plots with fresh biochar in comparison to Control and aged biochar. Fresh biochar becomes a part of soil aggregates gradually and its properties are changing by meteorological changes; root system of vegetation; soil animals etc. The results showed that biochar's water repellency properties were lower two years after its reapplication into the silt loam soil. Biochar degradation is a natural process and properties of aged biochar are now different than it was in 2014 and also properties of fresh biochar are different than it was in 2018. It may also been some reasons of our results.

Conclusion

In this paper we focused on biochar application and its reapplication into silt loam soil at Malanta site (Slovakia). We measured soil moisture in short time intervals to have a good overview of impact of precipitation totals and air temperature on soil moisture changes. Our results confirmed that biochar has water repellent properties and with soil moisture being lower at B20 reap. plots (with fresh biochar) than at B20 plots (with aged biochar, applied 5 years ago) first year of its reapplication (in 2018) into the soil. Soil moisture was still higher at B20 plots compared to Control plots (without biochar). It was caused by aged biochar particles (applied in 2014) which are situated at B20 reap. plots and in this time they are part of soil aggregates. The soil moisture was higher at B20 reap. plots two years after biochar reapplication (in 2019) almost the whole monitoring period. These results show positive effect of this type of biochar on soil water regime in a longer time horizon. Authors are aware of the fact that two years after biochar reapplication in field conditions is not long enough to make a strict conclusion, but the results indicate that biochar application into the soil has more benefits in a longer time horizon. Therefore, it is necessary to continue with this research.

Acknowledgement

This work was supported by Scientific Grant Agency No. VEGA 2/0053/18.

References

Bachmann, J., Goebel, M.-O., Woche, S. K. (2013): Small-scale contact anglemapping on undisturbed soil surfaces. J. Hydrol. Hydromech., vol. 61, no. 1, 3–8.

Baronti, S., Vaccari, F. P., Miglietta, F., Calzolari, C., Lugato, E., Orlandini, S., Pini, R., Zulian, C., Genesio, L. (2014): Impact of biochar application on plant water relations in Vitis vinifera (L.). Eur. J. Agron., vol. 53, 38–44.

Chen, B., Zhou, D., Zhu, L. (2008): Transitional adsorption and partition of nonpolar and polar aromatic contaminants by biochars of pine needles with different pyrolytic temperatures. Environ. Sci. Technol., vol. 42, 5137–5143.

Domanová, J., Igaz, D., Borza, T., Horák, J. (2015): Retenčné charakteristiky pôdy po aplikácii biouhlia. Acta Hydrologica Slovaca, vol. 16, No. 2, 193–198.

Ellerbrock, R., Gerke, H. H., Bachmann, J., Goebel, M.-O. (2005): Composition of organic matter fractions for explaining wettability of three forest soils. Soil Sci. Soc. Am. J., vol. 69, 57–66.

Githinji, L. (2014): Effect of biochar application rate on soil physical and hydraulic properties of a sandy loam. Arch. Agron. Soil Sci., vol. 60, 457–470.

Glaser, B., Lehmann, J., Zech, W. (2002): Ameliorating physical and chemical properties of highly weathered soils in the tropics with charcoal e a review. Biol Fert Soils, vol. 35, no. 4, 219–230.

Gray, M., Johnson, M. G., Dragila, M. I., Kleber, M. (2014): Water uptake in biochars: the roles of porosity and hydrophobicity. Biomass Bioenergy, vol. 61, 196–205.

Horák, J. Šimanský, V., Aydin, E. (2020): Benefits of biochar and its combination with nitrogen fertilization for soil quality and grain yields of barley, wheat and corn. J. Elem., vol. 25, no. 2, 443–458.

Horák, J., Šimanský, V. (2017): Effect of biochar on soil CO_2 production. Acta fytotechn zootech, vol. 20, no. 4, 72–77.

Horák, J., Šimanský, V., Igaz, D. (2019): Biochar and Biochar with N Fertilizer Impact on Soil Physical Properties in a Silty Loam Haplic Luvisol. Journal of Ecological Engineering, vol. 20, no. 7, 31–38.

Jeffery, S., Meinders, M. B. J., Stoof, C. R., Bezemer, T. M., van de Voorde, T. F. J., Mommer, L., Van Groenigen, J. W. (2015): Biochar application does not improve the soil hydrological function of a sandy soil. Geoderma, vol. 251–252, 47–54.

Juriga, M., Šimanský, V. (2018): Effect of biochar on soil structure – review. Acta fytotechn zootechn, vol. 21, no. 1, 11–19.

Keiluweit, M., Nico, P. S., Johnson, M. G., Kleber, M. (2010): Dynamic molecular structure of plant biomass-derived black carbon (biochar). Environ Sci Technol, vol. 44, no. 4, 1247–1253.

Kinney, T. J., Masiello, C. A., Dugan, B., Hockaday, W. C., Dean, M. R., Zygourakis, K., Barnes, R. T. (2012): Hydrologic properties of biochars produced at different temperatures. Biomass Bioenergy, vol. 41, 34–43.

Laird, D. A., Brown, R. C., Amonette, J. E., Lehmann, J. (2009): Review of the pyrolysis platform for coproducing bio-oil and biochar. Biofuel Bioprod Bior, vol. 3, no. 5, 547–562.

Mao, J., Zhang, K., Chen, B. (2019): Linking hydrophobicity of biochar to the water repellency and water holding capacity of biochar-amended soil. Environmental Pollution, vol. 253, 779–789.

Rutherford, D. W., Wershaw, R. L., Rostad, C. E., Kelly, C. N. (2012): Effect of formation conditions on biochars: compositional and structural properties of cellulose, lignin, and pine biochars. Biomass Bioenergy, vol. 46, 693–701.

SHMU (2019): The year 2018 – the hottest year in several places in Slovakia (in Slovak language). Available online: <http://www.shmu.sk/sk/?page=2049&id=972> (accessed on 3 March 2019).

SHMÚ (2020): The year 2019 is the warmest in the history of observations in the far east of Slovakia (in Slovak language). Available online: <http://www.shmu.sk/sk/?page=2049&id=1037> (accessed on 8 October 2020).

Šiška, B., Špánik, F., Repa, Š., Gálik, M. (2005): Praktická Biometeorológia (Practical Biometeorology); Slovenská Pol'nohospodárska Univerzita: Nitra, Slovakia. p. 102.

Tarnik, A. (2019): Impact of Biochar Reapplication on Physical Soil Properties. IOP Conf. Series: Materials Science and Engineering, vol. 603, issue 2 (022068).

Tarnik, A., Leitmanova, M. (2017): Analysis of the Development of Available Soil Water Storage in the Nitra River Catchment. IOP Conference Series: Materials Science and Engineering, WMCAUS, 245, art No. 062017.

Toková, L., Igaz, D., Horák, J., Aydin, E. (2020): Effect of Biochar Application and Re-Application on Soil Bulk Density, Porosity, Saturated Hydraulic Conductivity, Water Content and Soil Water Availability in a Silty Loam Haplic Luvisol. Agronomy, vol. 10, no. 7, 1005.

Vitkova, J., Kondrlova, E., Rodny, M., Surda, P., Horak, J. (2017): Analysis of soil water content and crop yield after biochar application in field conditions. Plant, Soil and Environ, vol. 63, no. 12, 569–573.

Ing. Justína Vitková, PhD. (*corresponding author, e-mail: vitkova@uh.savba.sk)
Ing. Peter Šurda, PhD.
Mgr. Anton Zvala, PhD.
Institute of Hydrology SAS
Dúbravská cesta 9
84104 Bratislava
Slovak Republic

DOI: 10.31577/ahs-2020-0021.02.0017

ACTA HYDROLOGICA SLOVACA

Volume 21, No. 2, 2020, 139 – 144

DETERMINATION AND COMPARISON OF HYDRAULIC CONDUCTIVITY VALUES OF BED SILTS ALONG CHOTÁRNY CHANNEL USING GRAIN SIZE ANALYSIS

Renáta Dulovičová*, Yvetta Velísková, Radoslav Schűgerl

This paper goes in for the evaluation of permeability of the bed silts located along the Chotárny channel at the Žitný ostrov (ŽO), Slovakia. The Chotárny channel is one of three main channels at the ŽO area – the flat lowland with channel network. Whole ŽO area has very low slope, so longitudinal slopes of all channels are negligible. This fact influences the formation of silts on the channel bottom. The bed silt permeability impacts water flow between surface water in the channel and surrounding groundwater in the scope of their interaction at this area. It is expressed by value of hydraulic conductivity, for our case, inasmuch as the bed silts are located in saturated zone under water level, by value of saturated hydraulic conductivity. This paper deals with disturbed samples extracted from the Chotárny channel and for that reason only the empirical formulas based on the grain size analysis were used for assessment of saturated hydraulic conductivity value. The disturbed samples were extracted in three different vertical parts of silt – top, middle and bottom part of silt layer and subsequently as mixed samples in each selected profile of the Chotárny channel. The selection of sampling place was made by thickness of bed silt in the measured profiles. The values of saturated hydraulic conductivity obtained from disturbed samples of bed silt – K_d were calculated according to three empirical formulas: 1. Bayer – Schweiger formula; 2. Špaček I formula and 3. Špaček II formula, firstly for samples from the single vertical parts of the silt layer (top, middle and bottom) and then for mixed samples. The valid values K_d from single parts of the silt layers reached from 1.29×10^{-08} to 1.19×10^{-04} m s^{-1}, the valid values K_d from mixed samples reached from 1.38×10^{-08} to 4.11×10^{-06} m s^{-1}. All values obtained using grain size analysis are only approximate, but the only possible ones in case of impossibility to take an undisturbed samples. According to results of comparison of K_d from single vertical parts of silt layers and K_d from mixed samples it is not possible to assess explicitly which values set of saturated hydraulic conductivity are more suitable to use in calculation or modelling. Next analysis of obtained datasets and comparison with the values of saturated hydraulic conductivity from undisturbed samples of bed silt will be necessary.

KEY WORDS: bed silts, disturbed samples, grain size analysis, silt permeability, hydraulic conductivity

Introduction

Žitný ostrov (ŽO) – a part of the Danube Lowland – was created by sediments transport from upper part of the Danube River (Fig. 1a). This area formed as a flat plain with only small differences in altitude. Its average slope is about 0.25‰ and it was one of the reasons for building channel network here. The longitudinal slopes of its channels are also very low. This fact had impact to production of bed silts on the channel bottom. The bed silts have been created by the surface runoff (or overland flow) and soil erosion from adjacent territory, as a results of manipulation with water-gates in the channel network and as a result of the decomposition of aquatic vegetation. The thickness and structure of bed silts influence the interaction between groundwater and water level in channel network. The rate of this interaction is important for agricultural production in this area, but also for regime of groundwater in this area. As important characteristics influencing this mutual interaction were determined the thickness and permeability of silts, which is often expressed by saturated hydraulic conductivity value. The channel network aggradation has been monitored and studied – many specialists dealt with it (Kosorin, 1997; Burger and Čelková, 2004; Mucha et al, 2006; Štekauerová et al., 2009; Baroková and Šoltész, 2014; Čelková, 2014; Kováčová, 2017; etc.). This paper shows some results of field measurements along the Chotárny channel – one of three main channels at the ŽO area (Fig. 1b).

Material and methods

Channel network at the ŽO area is created by several bigger channels – e.g. the channel Gabčíkovo–Topoľníky, the Chotárny channel, the Komárňanský channel, the channel Čalovo–Holiare–Kosihy, the channel Aszód –Čergov, the channel Čergov–Komárno, the channel Dudváh and by network of several smaller channels. Our research of channel network silting up has been concen-

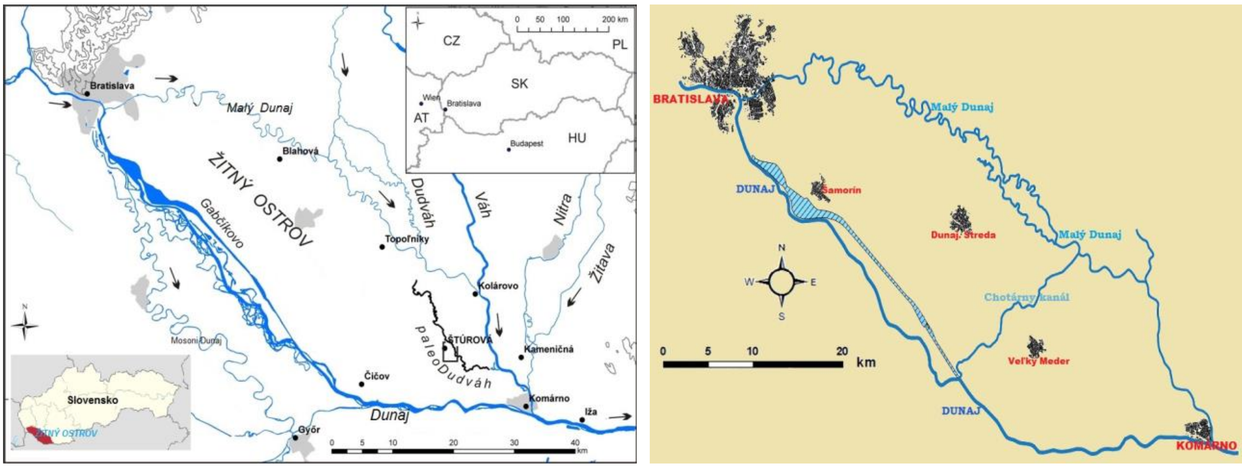

a) *b)*

Fig. 1. a) Localisation of the ŽO area (left), b) Location of the Chotárny channel at the ŽO area (right).

trated to three main channels of this network: the channel Gabčíkovo–Topoľníky, the Chotárny channel and the Komárňanský channel (Dulovičová, 2014; Dulovičová et al., 2016).

Chotárny channel is one from these three main channels of the ŽO channel network. Geometrical parameters of this channel observed during the measurements were: the channel length was approximately 27 km, the channel width was in range 11–17.5 m, the channel depth run into maximal values up to 3.15 m (according to cross-section profiles location). The values of hydraulic conductivity in aquifers nearby this channel K_{fs} were 0.40–3.4x10^{-3} m s^{-1} (Mišigová, 1988).

The measurements of bed silts thickness along the Chotárny channel were performed from the displaceable inflatable dinghy by simple drill hole. The distance of cross-section profiles along the channel varied between 1.0–1.5 km. In all channel cross-section profiles there was measured the water depth and bed silts thickness with step 1.0–2.0 m along the channel width. The samples of channel bed silt were taken in these selected cross-section profiles where the largest channel bed silt thickness was noticed. The extraction of samples was done by sediment beeker sampler device. The silt sample was taken from each selected cross-section profile and then from each whole sample a part from top, middle and bottom layer was extracted. Finally, these separated samples were combined into a mixed sample (from all three layers). Next, the granularity analysis for each disturbed sample was performed, from which the value of saturated hydraulic conductivity was determined.

Determination of saturated hydraulic conductivity of bed silts from granularity analysis

Determination of hydraulic conductivity from disturbed samples of bed silts can be calculated by empirical formulas coming out from grain size analysis (Kutílek, 1978).

Several empirical formulas for determination of hydraulic conductivity from granularity exist, but it is possible to apply only a few of them because their limited validity. Therefore we used for our determination of saturated hydraulic conductivity of bed silts the relationships by Beyer-Schweiger and Špaček (Špaček, 1987). These relationships are functions of d_{10} – particle diameter in 10% of soil mass (m) and d_{60} – particle diameter in 60% of soil mass [m]. Both of them were determined from granularity curves of all extracted samples of bed silts. The formula of Beyer-Schweiger, used for assessment of saturated hydraulic conductivity from disturbed samples of the Chotárny channel – K_{dBS} [m s^{-1}], has a form:

$$K_{dBS} = 7.5x10^6\, C\left(d_{10}\right)^2 \tag{1}$$

where
C=1.5961x10^{-3} $(d_{60}/d_{10})^{-0.20371}$;
d_{10} – particle diameter in 10% of soil mass [m];
d_{60} – particle diameter in 60% of soil mass [m];

and conditions of validity are:

$$0.06 \le d_{10} \le 0.6 \quad \text{and} \quad 1 \le \frac{d_{60}}{d_{10}} \le 20$$

Špaček formulas I, II [m d^{-1}] for saturated hydraulic conductivity from disturbed samples of the Chotárny channel K_d are as follows:

$$K_{d\,ŠI.} = 20.577\,\left(d_{10}\right)^{1.013}\left(\frac{0,5}{d_{60}-d_{10}}\right)^{0.059} \tag{2}$$

$$K_{d\,ŠII.} = 108.4386\left(d_{10}\right)^{0.8866}\left(d_{60}\right)^{0.7726} \tag{3}$$

where
conditions of validity for application of eq.(2) are:

1. $d_{10} < 0.01$mm

or

2. $0.01 \le d_{10} < 0.13 \wedge d_{60} < 0.0576 + 0.5765 d_{10}$

and conditions of validity for application of eq.(3) are:

1. $d_{10} \ge 0.13$ mm

or

2. $0.01 \le d_{10} < 0.13 \wedge d_{60} > 0.0576 + 0.5765 d_{10}$

Results and discussion

Sometime it is not possible to take away undisturbed samples of bed silts or sediments and in the same moment it is necessary to know the rate of permeability of them. For this reason a way how to make it was searched. One way is the determination from granularity analysis. There are a lot of empirical relationships based on this analysis, but with a lot of limitations of validity, as well. As it was mentioned and described above, the value of saturated hydraulic conductivity as the indicator of channel bed silt permeability was determined for disturbed samples by the Beyer-Schweiger and two Špaček´s formulas. Each of them determines this variable quantity as a function of d_{10} and d_{60} .Conditions of validity for application of these formulas also depends on value of d_{10} and d_{60} (Šurda et al., 2013). The both values were determined separately for the top, middle and bottom part of extracted samples and then for mixed samples from measured sample points along the Chotárny channel. The obtained and determined values of saturated hydraulic conductivity of disturbed samples K_d extracted from top, middle and bottom layer of bed silt are summed in Table 1. The valid values of channel bed silt saturated hydraulic conductivity from single parts of the silt layers reached from 1.29x10^{-08} to 1.19x10^{-04} m s^{-1}. The graphical interpretation of results is in Fig. 2.

The values of saturated hydraulic conductivity of disturbed samples K_d extracted from mixed samples of bed silt along the Chotárny channel are summed in Table 2. The valid values of channel bed silt saturated hydraulic conductivity from mixed samples reached from 1.38x10^{-08} to 4.11x10^{-06} m s^{-1}. The graphical interpretation of these results is in Fig. 3.

Table 1. Chotárny channel – valid values of K_d from single parts of the silt layers in 2018

Channel	**Chotárny**			
Channel stationing [rkm]	**Silt layer**	**K_d [m s^{-1}]**		
		Bayer-Schweiger	**Špaček I.**	**Špaček II.**
1.2	top	3.81x10^{-08}	6.03x10^{-07}	-
	middle	-	-	1.02x10^{-06}
	bottom	-	5.06x10^{-07}	-
6.0	top	4.13x10^{-06}	-	2.62x10^{-05}
	middle	1.80x10^{-08}	4.23x10^{-07}	-
	bottom	6.30x10^{-05}	-	1.19x10^{-04}
8.6	top	-	7.64x10^{-07}	1.69x10^{-06}
	middle	-	-	2.04x10^{-05}
	bottom	1.68x10^{-07}	1.24x10^{-06}	1.70x10^{-06}
16.3	top	1.99x10^{-08}	4.45x10^{-07}	-
	middle	-	5.05x10^{-07}	-
	bottom	3.32x10^{-08}	5.69x10^{-07}	-
18.0	top	2.15x10^{-08}	4.61x10^{-07}	-
	middle	-	4.11x10^{-07}	-
	bottom	1.59x10^{-08}	3.99x10^{-07}	-
20.0	top	1.97x10^{-08}	4.44x10^{-07}	-
	middle	1.29x10^{-08}	3.66x10^{-07}	-
	bottom	1.37x10^{-08}	3.72x10^{-07}	-
24.6	top	-	5.50x10^{-07}	6.29x10^{-07}
	middle	-	1.66x10^{-06}	4.28x10^{-06}
	bottom	-	5.16x10^{-07}	2.61x10^{-06}
25.5	top	1.06x10^{-07}	9.95x10^{-07}	1.27x10^{-06}
	middle	-	6.60x10^{-07}	1.03x10^{-06}
	bottom	-	-	1.29x10^{-05}

Table 2. **Chotárny channel – valid values of K_d from mixed samples of the silt in year 2018**

Channel	Chotárny			
Channel stationing [rkm]	**Silt layer**	**K_d [m s^{-1}]** Bayer-Schweiger	**Špaček I.**	**Špaček II.**
1.2 –1.3	mixed sample (top + middle + bottom)	$1.89x10^{-08}$	$4.39x10^{-07}$	-
6.0	mixed sample (top + middle + bottom)	-	$4.65x10^{-07}$	$6.90x10^{-07}$
8.7	mixed sample (top + middle + bottom)	-	$6.44x10^{-07}$	$3.88x10^{-06}$
16.3	mixed sample (top + middle + bottom)	$4.32x10^{-08}$	$6.45x10^{-07}$	-
18.0	mixed sample (top + middle + bottom)	-	$4.34x10^{-07}$	-
20.0	mixed sample (top + middle + bottom)	$1.38x10^{-08}$	$3.73x10^{-07}$	-
24.6	mixed sample (top + middle + bottom)	-	$1.03x10^{-06}$	$4.11x10^{-06}$
25.5	mixed sample (top + middle + bottom)	-	$9.54x10^{-07}$	$2.17x10^{-06}$

– unkept conditions of validity for aplication of Beyer-Schweiger´s and Špaček´s formulas

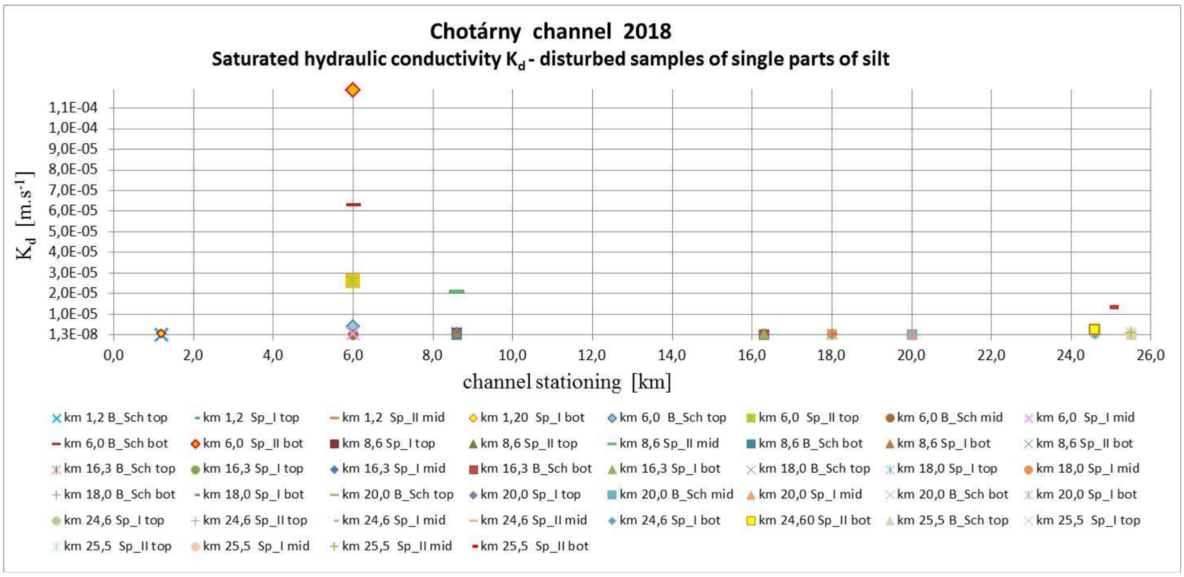

Fig. 2. The graphical presentation of K_d for disturbed samples from single parts of silt layer.

Comparing K_d value of single parts of silt layers extracted along the Chotárny channel, the various ranges among top, middle and bottom layer were identified. In rkm 1.2 the valid values of saturated hydraulic conductivity K_d in single layers were from 10^{-08} to 10^{-06} m s^{-1}, withal the value 10^{-7} m s^{-1}predominated. In rkm 6.0 was larger range of values K_d – from 10^{-08} to 10^{-04} m s^{-1}, in rkm 8.6 the values of K_d were from 10^{-07} to 10^{-05} m s^{-1}. From rkm 16.3 to rkm 20.0 the values of K_d changed from 10^{-08} to 10^{-07} m s^{-1}, withal the value 10^{-7} m s^{-1} (calculated by Špaček I) predominated. In km 24.6 was range of K_d only from 10^{-07} to 10^{-06} m s^{-1} (by Špaček I, II). In rkm 25.5 the values K_d varied from 10^{-07} to 10^{-05} m s^{-1}.

In the case of mixed disturbed samples of bed silt extracted along the Chotárny channel, the valid values K_d ranged from 10^{-08} to 10^{-06} m s^{-1}. In rkm 1.2–1.3 the valid values K_d, calculated by Bayer-Schweiger (Eq.1) and Špaček I (Eq. 2) formulas, varied only from 10^{-08} to 10^{-07} m s^{-1}. From rkm 6.0 to rkm 8.7 the valid values K_d ranged from 10^{-07} to 10^{-06} m s^{-1}, the value 10^{-7} m s^{-1} predominated

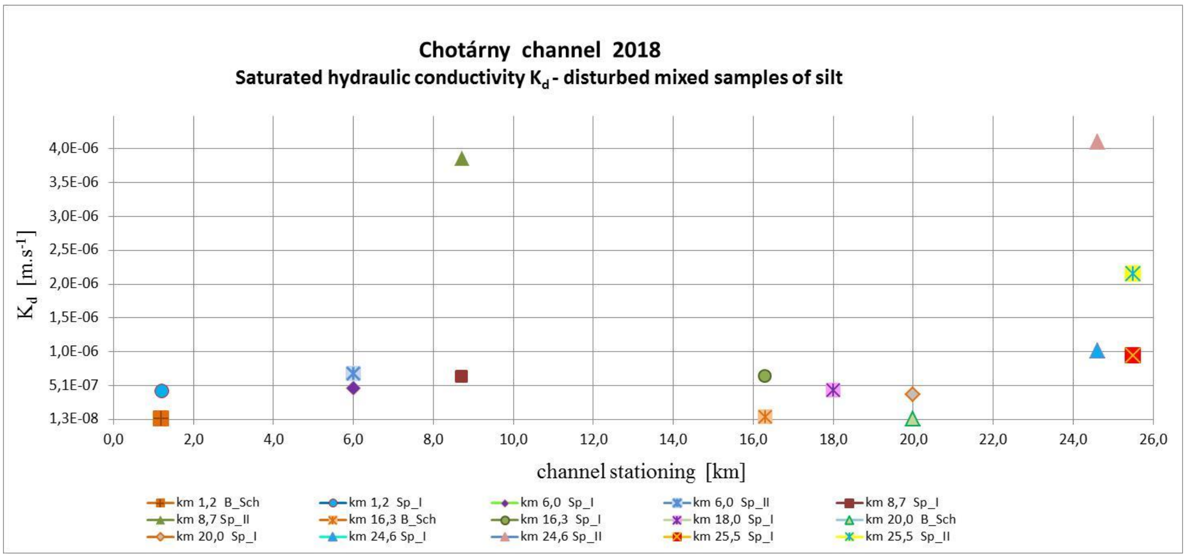

Fig. 3. The graphical presentation of K_d for mixed disturbed samples of silt.

(calculated by Špaček I (Eq. 2) and Špaček II (Eq.3)). From rkm 16.3 to rkm 20.0 the values of K_d varied from 10^{-08} to 10^{-07} m s^{-1}, with dominance 10^{-07} m s^{-1} (by Špaček I (Eq. 2)). In rkm 24.6 and 25.5 were the valid values K_d in range only from 10^{-07} to 10^{-06} m s^{-1}, where the value 10^{-06} m s^{-1} predominated.

Comparing of the values K_d, extracted from single parts of silt layers and from mixed samples of silt, some small differences were detected. The values K_d according Bayer-Schweiger formula (Eq. 1) were mostly 10^{-08}, but the possibility to apply this formula for mixed samples was only in rkm 1.2, 16.3 and 20.0. The values K_d according Špaček I formula (Eq. 2) were mostly 10^{-07} m s^{-1} and its applicability was nearly in the same extent, except rkm 8.6 and rkm 24.6 for single silt layers, and rkm 24.6 for mixed samples of silt (here the K_d values were 10^{-06} m s^{-1}). The values K_d according Špaček II formula (Eq. 3) varied from 10^{-07} to 10^{-04} m s^{-1}, mostly 10^{-06} m s^{-1}. The application of Eq. 3 was not valid from rkm 16.3 to rkm 20.0 for both cases (single layers of silt and mixed silt samples). At comparison of the values of saturated hydraulic conductivity K_d of bed silts extracted from single silt layers and K_d from mixed silt samples are evident only very small differences or variation.

Comparing of obtained range of values of saturated hydraulic conductivity and values of this characteristic for typical fresh groundwater conditions with using standard values of viscosity and specific gravity for water at 20 °C and 1 atm, the values of K_d determined for the Chotárny channel bed silts represent a semi-pervious to impervious conditions of bed sediments (Bear, 1972).

Conclusion

This paper is aimed to the evaluation of bed silt permeability along the Chotárny channel on base of field measurements performed during the year 2018 at the ŽO area. The thickness of bed silt and the permeability of channel bed silt fundamentally influence and determine the rate of mutual interaction between surface water in the Chotárny channel and groundwater in its surroundings. For this reason, it is important to research and monitor continuously the state of channel bed aggradation and to know the permeability of bed silt, expressed by its value of saturated hydraulic conductivity.

The values of saturated hydraulic conductivity of bed silt along the Chotárny channel were determined according to three formulas applicable for disturbed samples of bed silts, which are based on granularity analysis of samples. The resultant values are presented in Table 1 and Table 2. The valid values of saturated hydraulic conductivity of the channel bed silt for single parts of bed silt layers reached from 1.29×10^{-08} to 1.19×10^{-04} m s^{-1}, the valid values of channel bed silt saturated hydraulic conductivity from mixed samples reached from 1.38×10^{-08} to 4.11×10^{-06} m s^{-1}. These values mean semi-pervious to impervious environment.

Comparison of values of saturated hydraulic conductivity between top, middle and bottom parts of bed silt layers did not appear significantly marked differences. The value of decimal order 10^{-07} prevailed in all layers. The values of saturated hydraulic conductivity of mixed disturbed samples of bed silt were also analysed and the value 10^{-07} prevailed again. Comparison of the values of saturated hydraulic conductivity K_d from single parts of silt layers and K_d from mixed silt samples showed only small differences. On the base of analysis of these results it can be taken a note that it is not possible to assess explicitly the reliability of saturated hydraulic conductivity value set by this way. In the next level of our research is needful to compare these results with the values obtained from undisturbed samples of bed silts determined by the laboratory falling head method.

However, all obtained information about bed silt thicknesses supplemented by values of saturated hydraulic conductivity of bed silt will be usable for numerical simulation models and simultaneously they represent rare information for any future way of groundwater level regulation in surroundings of the Chotárny channel or other channels at the ŽO area.

Acknowledgement

This work is support by the contract VEGA–02/0025/19 and APVV–14–0735.

References

Baroková, D., Šoltész, A. (2014): Analysis of surface and groundwater interaction in the Danube river branch system., SGEM Conference Proceedings, 14th SGEM Geo-Conference on Water Resources. Forest, Marine and Ocean Ecosystems, Vol. I., www.sgem.org, ISBN 978-619-7105-13-1 / ISSN 1314-2704, 51–58.

Bear, J. (1972): Dynamics of Fluids in Porous Media. Dover Publications, ISBN 0-486-65675-6.

Burger, F. Čelková, A. (2004): Simulation of aquifer feeding processes during dry period. Acta Hydrologica Slovaca, Vol. 5, No.2, 348–357. (in Slovak)

Čelková, A. (2014): The influence of groundwater on soil salinization in the alluvium in the left bank side of Danube river between Komárno and Štúrovo. Acta Hydrologica Slovaca, Vol. 15, No. 2, 413–423 (in Slovak)

Dulovičová, R. (2014): Aggradation changes at Komárňanský channel during period 1993–2013. Acta Hydrologica Slovaca, Vol. 15, Temat. No., 103–111 (in Slovak)

Dulovičová, R., Velísková, Y., Schűgerl, R. (2016): Hydraulic conductivity of silts in Chotárny channel at Žitný ostrov. Acta Hydrol. Slovaca, Vol. 17, No. 2, 149–156 (in Slovak)

Kosorin, K. (1997): Spatial groundwater dynamics of the Rye Island aquifer. J. Hydrol. Hydromech., Vol. 45, 348–364.

Kováčová, V. (2017): Trends of nitrate ions content in Žitný Ostrov channel network. Acta Hydrologica Slovaca, Vol. 18, No. 1, 57–67 (in Slovak)

Kutílek, M. (1978): Vodohospodářská pedologie, Alfa Bratislava, SNTL 04-721-78, 296 p., (in Czech)

Mišigová, I., (1988): Methods of regional assessment of hydraulic properties of the rocks on the Žitný Ostrov. Report IHH SAS, (in Slovak)

Mucha, I., Banský Ľ., Hlavatý Z., Rodák D (2006): Impact of riverbed clogging colmatation on ground water, Riverbank Filtration Hydrology: Impacts on System Capacity and Water Quality. NATO Science Series: IV. Earth and Environmental Sciences – Vol. 60, Springer, 43–72. (printed in the Netherlands)

Špaček, J. (1987): Determination of filtration coefficient from total grain-size curves. J. Meliorace, Vol. 23, No.1, 1–13 (in Czech)

Šurda, P., Štekauerová, V., Nagy, V. (2013): Variability of the saturated hydraulic conductivity of the individual soil types in the area of the Hron catchment. Nővénytermelés, Vol. 62, supplement, 323–326.

Štekauerová, V., Nagy V., Šútor J., Milics G., Neményi M. (2009): Influence of groundwater level on soil water regime of Žitný ostrov. In V. Növénytermesztési Tudományos Nap – Növénytermesztés: Gazdálkodás – Klímaváltozás – Társadalom, Akadémiai Kiadó, Budapest, 197–200

Ing. Renáta Dulovičová (*corresponding author, e-mail: dulovicova@uh.savba.sk)
Ing. Yvetta Velísková, PhD.
Mgr. Radoslav Schűgerl, PhD.
Institute of Hydrology SAS
Dúbravská cesta 9
84104 Bratislava
Slovak Republic

DOI: 10.31577/ahs-2020-0021.02.0018

ACTA HYDROLOGICA SLOVACA

Volume 21, No. 2, 2020, 145 – 151

IMPACT OF ROUGHNESS CHANGES ON CONTAMINANT TRANSPORT IN SEWERS

Marek Sokáč*, Yvetta Velísková

The paper deals with question how the bed sediment or deposits impact transport processes in conditions of flow with low velocity and water depth. This is often a problem especially in case of flow in sewer network. For this reason, there were performed several tests in laboratory flume having the shape of a pipe with circular cross-section. To simulate the hydraulic condition in sewer pipe with sediments and deposits, some sand was inserted in the pipe with various layer thickness and granularity. It was used a sand of fraction 0.6–1.2 mm. In total, 4 sets of experiments with different layer thickness were performed: with layer thickness of 0 mm (no sediments), 8.5 mm (3.4% of the pipe diameter), 25 mm (10%) and 35 mm (14%) of sand sediment. For each thickness of the sediment layer a set of tracer experiment was performed with different discharges ranging approximately (0.14–2.5) l s^{-1}. Results of the tracer experiments show, that the value of the longitudinal dispersion coefficient D_x in the hydraulic conditions of circular sewer pipe with sediment and deposits decreases when the Reynolds number is decreasing too. The value of D_x reaches its minimal value in the range of the Reynolds number between 4500 up to 10 000. With Reynolds number below this range the value of D_x start to rise.

KEY WORDS: contaminant transport, longitudinal dispersion, bed sediment, roughness, sewers

Introduction

Flowing water in any natural conditions is connected with substances transport. This process consists basically of advection and dispersion. Substances transport is due primarily to advection, but there are many situations in which dispersion plays an important role and cannot be neglected. Knowledge of the rate at which substances disperse in streams is essential to stream management especially if the carried substance is toxic and means contamination for the stream.

Predicting of pollution spread is important for the environmental protection. In the field of water quality modelling, several authors (Chapra, 1997; Fischer et al., 1979; Graf, 1998; Runkel and Broshears, 1991; Marsalek, et al., 2004; Meddah, et al., 2015) presented different approaches to understand and interpret the basic concept of water quality problems. In a case an accidental discharge in a stream, the prediction of the pollutant transport is crucial in effective and rapid decision-making. On the other hand, in the case of an illegal release of a toxic substance, the determination of the source of the pollution is even more complicated, since it is an inverse task with a high degree of uncertainty. A way to solve that can be finding a simple, precise, a reduced computational time and a minimum input data consuming solution – equation. But in natural condition dispersion process is impacted by several hydrodynamic parameters of flow. One of them is occurrence of bottom sediment which changes the roughness. This effect can be significant especially at low speeds and water depths. These conditions often occur in sewer networks.

This paper describes partial results of the research of the influence of bottom deposits in a circular pipeline in laboratory conditions to the value of longitudinal dispersion coefficient as a parameter of dispersion rate.

Theoretical background

Dispersion is a combination of molecular and turbulent diffusion, advection and shear (Meddah, et al., 2015). It is created by the non-uniformity of velocity fields related to the different characteristics of the stream such as geometry, roughness, and kinematics. The dispersion zones are usually (Rutherford, 1994): the initial mixing zone, the mid-field mixing zone and the „far” field zone, where dispersion is considered longitudinal and one-dimensional in the flow direction. In the mathematical models, the effect of dispersion is accounted by means of the dispersion coefficient, for the evaluation of which several procedures are proposed, supported by experimental studies.

One-dimensional advection-dispersion equation (ADE) describes the mixing and transport phenomena, where the following assumptions are considered:

- Vertical and transversal dispersions are very small;
- The pollutant is completely miscible in water;
- Chemical reactions between the pollutant and its environment are absent;
- The overall mass of pollutant is maintained during transport.

The form of this equation is then as follows:

$$\frac{\partial C}{\partial t} + v_x \frac{\partial C}{\partial x} = D_x \left(\frac{\partial^2 C}{\partial x^2}\right) + M \tag{1}$$

where
C – substance concentration [kg m^{-3}];
v_x – fluid velocity in longitudinal direction [m s^{-1}];
D_x – dispersion coefficient in the longitudinal direction [m^2 s^{-1}];
t – time [s];
M_s – express the substance sources or sinks [kg m^{-3} s^{-1}];
x – distance in the longitudinal direction [m].

Relatively simple analytical solution of Eq. (1) can be obtained by using various mathematical approaches. One of the most used approach is the general solution of the ADE by (Socolofsky and Jirka, 2005), and eventually by (Fischer et al., 1979; Martin and McCutcheon, 1998), and it could be written as

$$C = \frac{M}{A\sqrt{D_x t}} \; f\left(\frac{x}{\sqrt{D_x t}}\right) \tag{2}$$

where
M – substance mass [kg];
A – cross-sectional area of the stream [m^2];
f – unknown function ("similarity solution ").

Other symbols meanings are the same as in the previous equation. The most-used one-dimensional analytical solution of the equation (2) for simplified conditions and immediate solute input has the form (Martin and McCutcheon, 1998)

$$c(x,t) = \frac{M}{2A\sqrt{\pi D_x t}} \; exp\left(-\frac{(x-v_x t)^2}{4\, D_x\, t}\right) \tag{3}$$

where
v_x – velocity of water flow in x direction of flow [m s^{-1}].

Unfortunately, the analytical solution used in Eq. (3) is based on the assumption of symmetrical substance spreading up- and downstream (Gauss distribution) and thus it does not take into account the temporary storage zones (dead zones) (Weitbrecht, 2004; Gualtieri, 2008; Valentine & Wood, 1977; 1979) or other singularities influencing substance spreading. Use of this approximation in streams with large presence of those singularities can be problematic. Because of this, we used in our research also alternative formulation of the one-dimensional analytic solution of the ADE based on the assumption of asymmetrical substance spreading. This alternative solution is based on the Gumbel statistical distribution and it has the form (Sokáč et al., 2019):

$$c(x,t) = \frac{M}{A\sqrt{D_{x,G} t}} \exp\left[\frac{x-v_x t}{\sqrt{D_{x,G} t}} - \exp\left(\frac{x-v_x t}{\sqrt{D_{x,G} t}}\right)\right] \tag{4}$$

where
$D_{x,G}$ – dispersion coefficient in the longitudinal direction [m^2 s^{-1}] used in the Gumbel distribution model.

Materials and Methods

The experiments were performed in the hydraulic laboratory of the WUT (Warsaw University of Technology). In aim to simulate the hydraulic conditions of a real sewer, experiments were conducted in a hydraulic flume with form of the pipe with circular cross-section. The inner diameter of the pipe was 250 mm, length was 12 m, slope of the pipe was 0.5 % (5 ‰). The pipe material was transparent plastic; every 2 m there were holes at the top of the pipe, enabling the access into the pipe (measuring devices, sediment insertion and retrieval). At the pipe inlet there was a storage tank with water inlet in the bottom part of the storage tank. After the water level rises above the pipe bottom, water starts to flow into the circular pipe. At the downstream end of the pipe was a free outfall into another storage tank with outflow in the tank bed (Fig. 1).
A drinking water was used for all the experiments, without recirculation, so there was no problem with the tracer background concentration increase. The inflow into the system was regulated with a lever valve; using this device it was very difficult to set up the same discharge in the experiments. Because of this, in all the experiments the discharge was measured individually for each individual experiment, using a simple volumetric method below the water free outfall in the downstream storage tank.
To simulate the hydraulic condition in sewer pipe with sediments and deposits, some sand was inserted in the pipe with various layer thickness and granularity. It was used a commercially available sand of fraction 0.6–1.2 mm; coarser material – fine gravel – was spread on the bottom of the sand layer to create hydraulic conditions similar to the real sewer pipes. After each insertion the sand was spread and finely compacted; then water was discharged approximately 20 minutes through the pipe to saturate the sand layer and to naturally form the top of the sand layer. To stabilise the velocity and to prevent the water level drop connected with sand outwash, it was necessary to form a small weir at the end of the pipe.
In total, 4 sets of hydraulic experiments were performed with layer thickness of 0 mm (no sediments), 8.5 mm of sand sediment (3.4% of the pipe diameter), 25 mm (10%) and 35 mm (14%) of sand sediment. The layer thickness was measured with a portable calliper at the locations of the openings in the experimental circular flume with accuracy of 0.1 mm. For each thickness of the sand layer sediment a set of tracer experiment was performed with different discharges ranging approximately from 0.14 l s^{-1} up to 2.5 l s^{-1}. The upper discharge limit was set up individually for each experiment and with respect the sand wash-out.
The dispersion (tracer) experiments were performed

using the Rhodamine and the salt as tracers, for the concentration measurement there were used a fluorometric and a conductivity probe. The fluorometric probe (Turner designs, Inc.) has declared mini-mum detection limit 0.01 ppb and linear range 0–1000 ppb (linearity 0.99 R^2). The conductivity probe has a detection range from 1 $\mu S\ cm^{-1}$ up to 1000 $mS\ cm^{-1}$, manufacturer (WTW) typically declares the accuracy for the probes of this type ±0.5% of measured value. The probes were placed at the pipe end, approximately 200 mm prior the weir at the pipe end. Tracers were dosed manually at the pipe beginning.

Each tracer experiment (for each combination of the layer thickness and discharge) was repeated five times. The data were measured in one second interval and they were saved automatically in the storage unit of the corresponding measuring device.

During evaluation of the measured data we noticed, that the fluorometric probe responded better to the concentration changes, its response time was minimal, whereas the conductivity probe had the response time about 2–3 secs. Moreover, the measured values were probably time-averaged by the device software. Because of this, we used only the measured data from the fluorometric probe in the evaluation process.

Results and discussion

Five tracer experiments, measured for the same discharge and deposit layer thickness, form one dataset. The example of such dataset is on the Fig. 2. Each measured tracer experiment was evaluated to determine the dispersion parameters according the Eq. (3) and Eq. (4). For the numeric evaluation, the statistical approach was used. The best approximation between measured and modelled data, i.e. the optimal set of dispersion parameters was determined searching the minimal root square mean error (RMSE). For the numeric optimisation procedure, the built-in function Solver in MS Excel environment was used.

The dispersion parameters, evaluated from five tracer experiments were averaged. The complete results are shown in Table 1. Graphical evaluation of the experiment results can be seen on the Fig. 3, 4, 5 and 6.

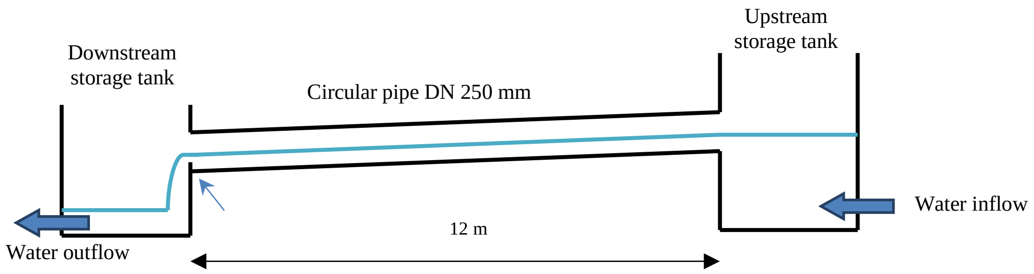

Fig. 1. Hydraulic scheme of the experimental device.

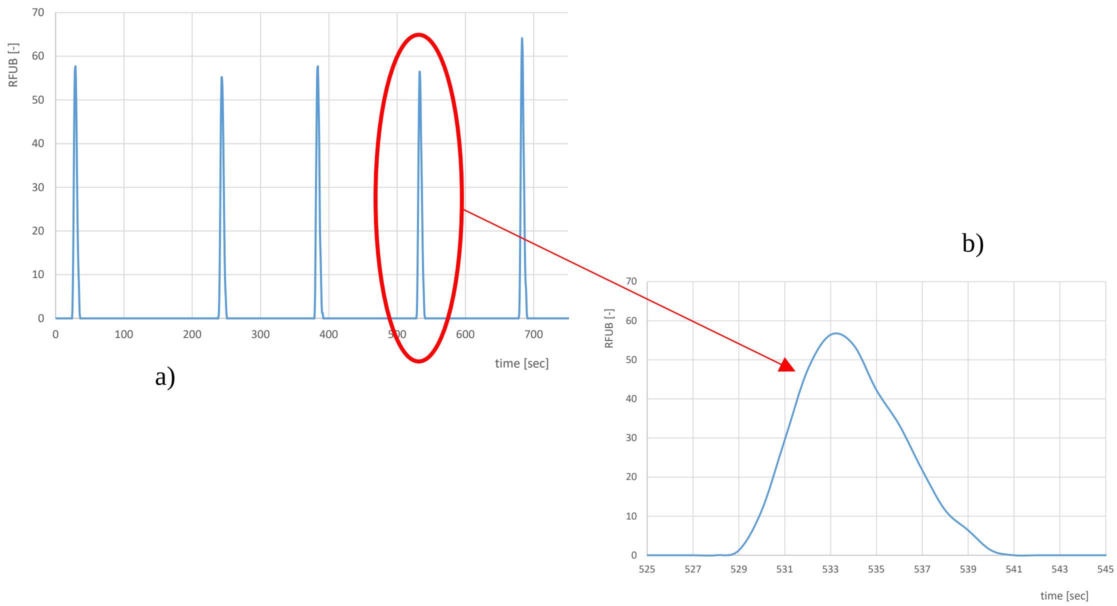

Fig. 2. Example of a dataset (a) and detail of a single experiment concentration time-course (b).

Table 1. Results of the tracer experiments

sediment	Dataset Nr.	Water depth	Discharge	Velocity	D_x	$D_{x,G}$
	[-]	[mm]	[l s^{-1}]	[m s^{-1}]	[m^2 s^{-1}]	[m^2 s^{-1}]
sediment 0 mm	37	10.4	0.145	0.211	0.011	0.016
	38	15.5	0.422	0.293	0.008	0.013
	11	19.6	0.505	0.324	0.008	0.014
	12	24	0.839	0.361	0.008	0.013
	13	29.6	1.170	0.385	0.009	0.015
	14	34.4	1.628	0.397	0.011	0.018
	15	40.3	2.237	0.458	0.014	0.023
sediment 8.5 mm	20	7.7	0.147	0.181	0.015	0.026
	20.1	16.6	0.410	0.232	0.010	0.016
	21	20.6	0.589	0.270	0.008	0.014
	22	24.7	0.799	0.306	0.008	0.013
	23	30.7	1.114	0.343	0.008	0.013
sediment 25 mm	28	5.9	0.140	0.157	0.021	0.038
	24	14.3	0.392	0.181	0.013	0.022
	25	18.1	0.600	0.220	0.008	0.013
	26	20.2	0.794	0.260	0.007	0.012
	27	24.6	1.227	0.330	0.007	0.013
sediment 35 mm	31	9.1	0.141	0.084	0.044	0.072
	32	14.2	0.410	0.155	0.015	0.024
	33	18.2	0.633	0.188	0.010	0.017
	34	21.1	0.876	0.224	0.008	0.014
	35	25.6	1.280	0.270	0.009	0.015
	36	30.2	2.070	0.370	0.012	0.021

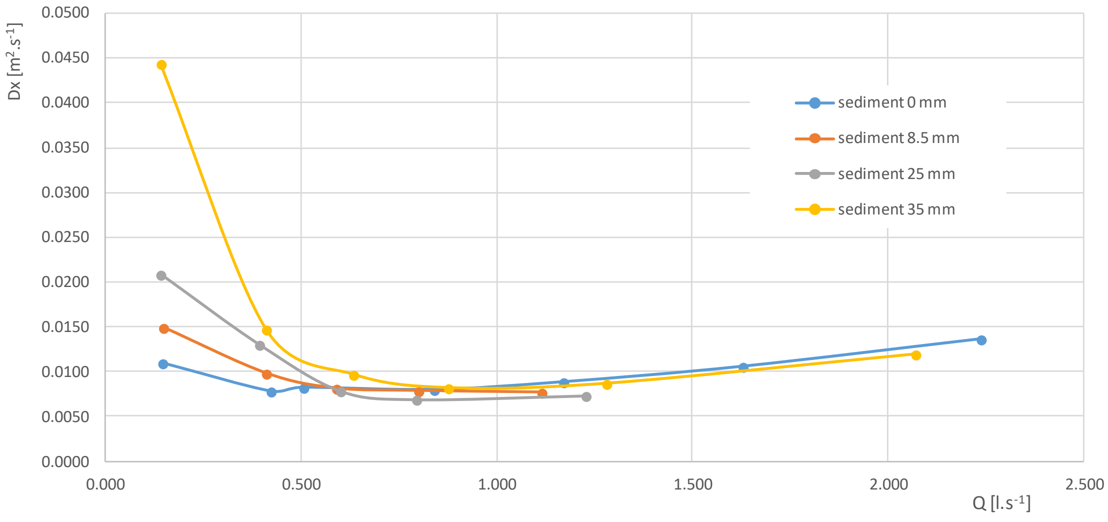

Fig. 3. Results of tracer experiments (D_x vs discharge Q).

From these figures it can be seen that the course of all evaluated dependencies is the same. The only difference is in the values of the dispersion coefficients: the values determined by using the Gaussian distribution are generally smaller than the values of the coefficient according to the distribution by Gumbel.

Interestingly, results of the tracer experiments also show that the value of the dispersion coefficient in the hydraulic conditions of circular sewer pipe with sediment and deposits reaches its minimal value in certain range of velocities (discharges), which are definitely not close to the minimal velocity. We assume that this phenomenon

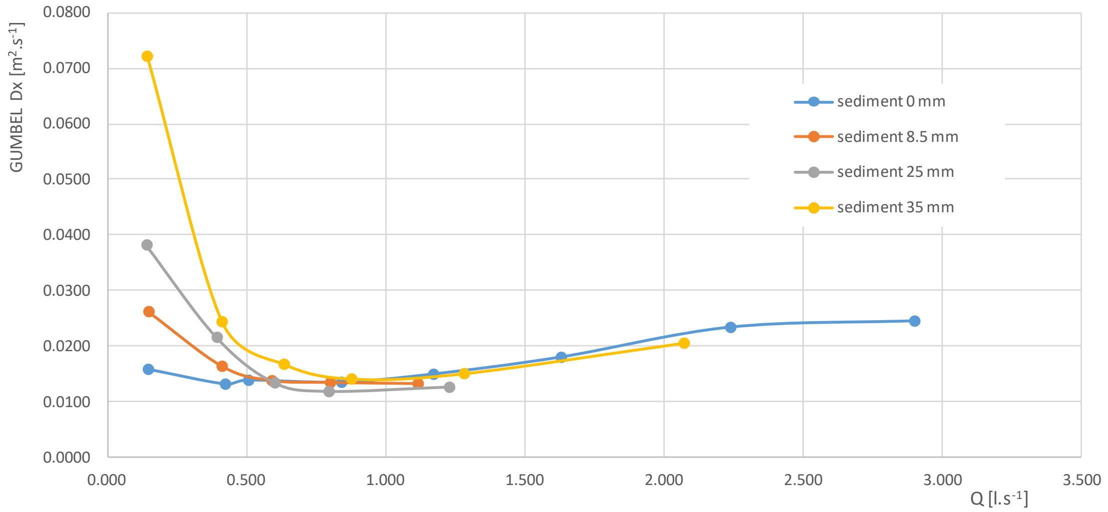

Fig. 4. *Results of tracer experiments ($D_{x,\,G}$ vs discharge Q).*

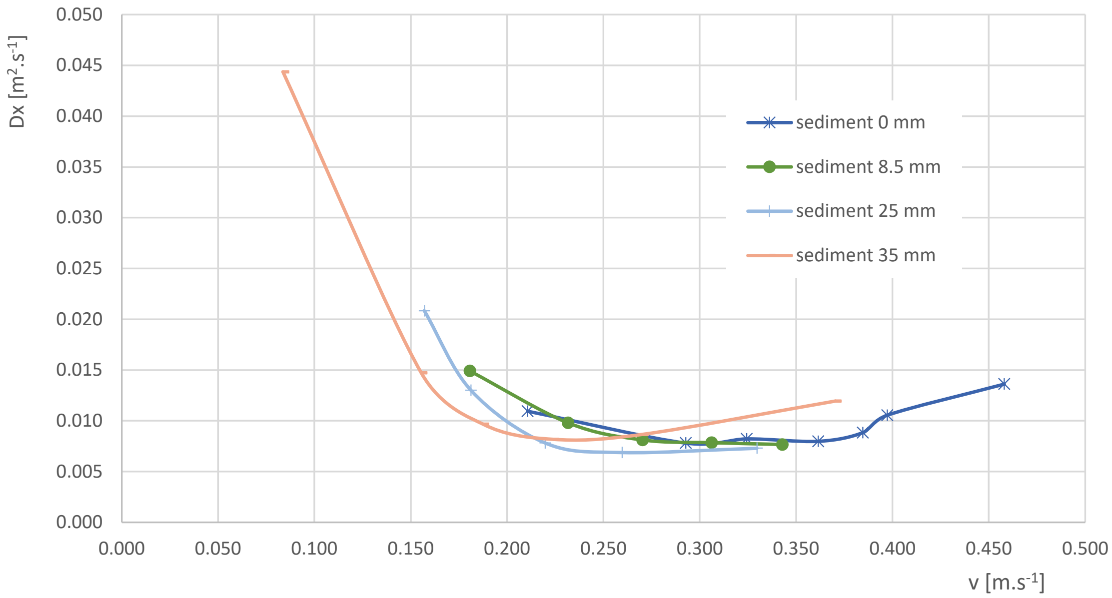

Fig. 5. *Results of tracer experiments (D_x vs velocity).*

can be caused due to specific hydrodynamic condition of the flow, which varies at shallow depths. However, this assumption needs to be further analysed.

In this study, we have tried to define the point with the minimum value of the dispersion coefficient, which has been not easy. One of the possible ways can be definition based on the Reynolds number, eventually based on geometric characteristics of the streambed (e.g. depth / width ratio).

In our case we have observed some dependency between the Reynolds number and the minimal value of the dispersion coefficient: the minimal values of the longitudinal dispersion coefficient occur for both applied distribution in the Reynolds number range from 4500 up to 10000 (Fig. 7 and 8).

Conclusions

The aim of this paper was to present the partial results of the study concerning dispersion processes in water flows with low velocity and occurrence of sediments or deposits. These results were obtained from the analysis of data from experiments in laboratory conditions. In this analysis there were used values of the longitudinal dispersion coefficient as a characteristic of mixing rate of flowing water. There were used two ways of their determination: by using Gaussian and Gumbel statistical distribution. These parameters were compared or put in the dependency with values of discharges and velocities in the various thicknesses of bed sediments conditions. Obtained values of the longitudinal dispersion coefficient have had a similar course of mentioned dependencies in both cases of used distributions, only values determined by using the Gaussian distribution are generally smaller than the values of the coefficient according to the distribution by Gumbel distribution. Results of the tracer experiments also have showed, that the value of the longitudinal dispersion coefficient in the hydraulic conditions of circular sewer pipe with sediment and deposits reaches its minimal value not in or close to the minimal velocity. Trying to define the point with the minimum value of this coefficient, we used the Reynolds number *Re* and analysed dependency of *Re* and D_x, eventually $D_{x,G}$. Results of analysis have showed that minimal values of the longitudinal dispersion coefficient occur in the Reynolds number range (4500–10000).

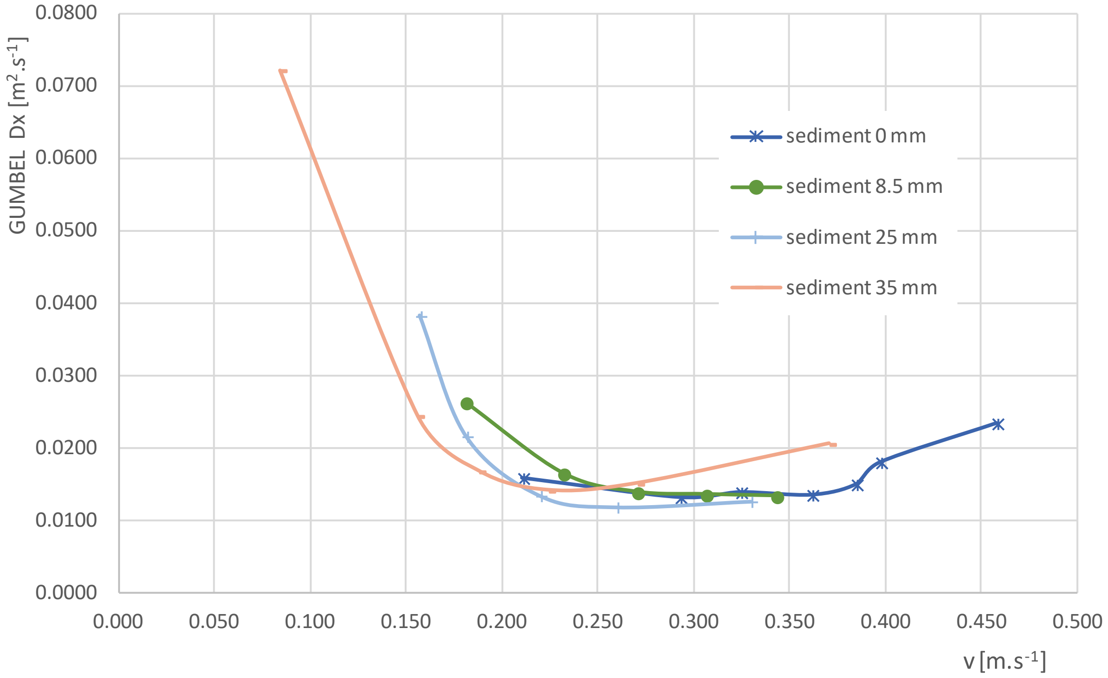

Fig. 6. *Results of tracer experiments ($D_{x,G}$ vs velocity).*

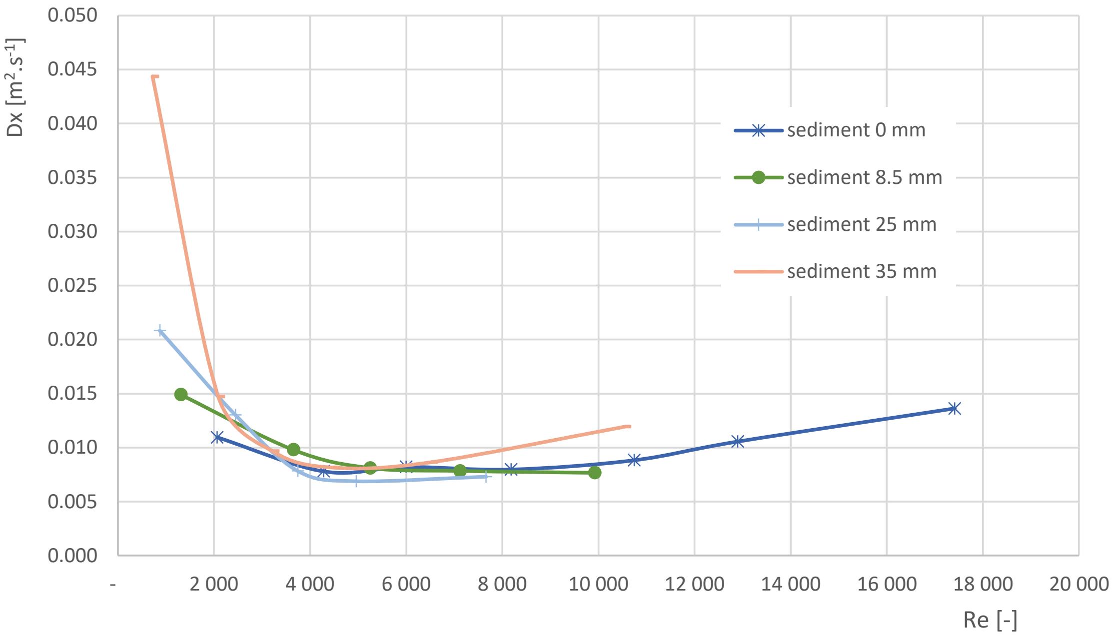

Fig. 7. *Results of tracer experiments (D_x vs Re).*

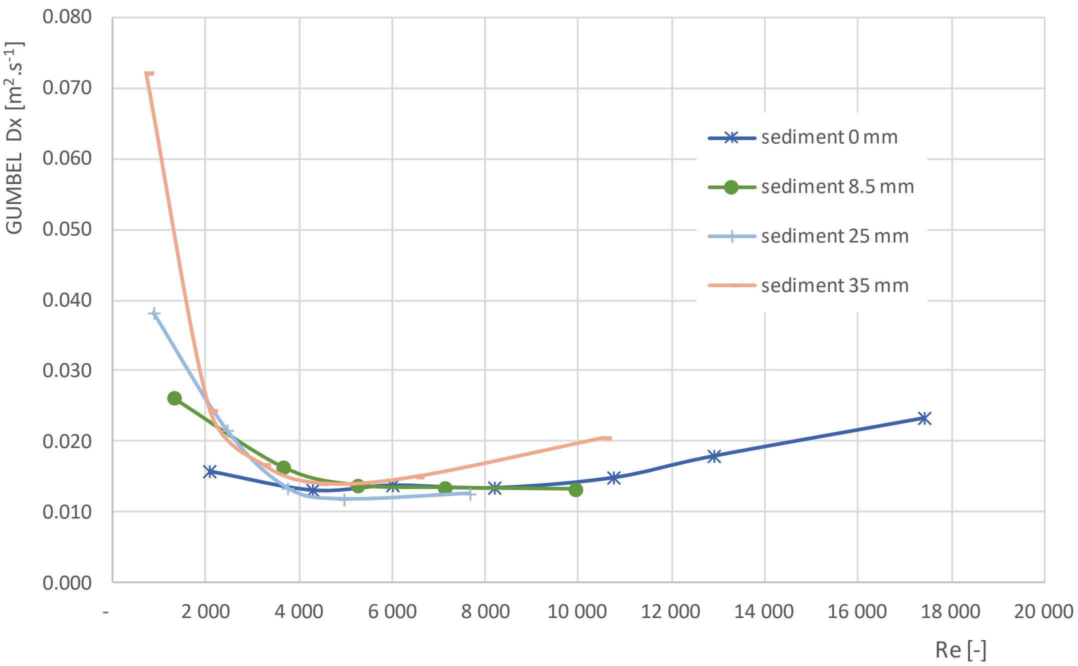

Fig. 8. Results of tracer experiments ($D_{x,G}$ vs Re).

Acknowledgment

This work was supported by the Scientific Grant Agency VEGA–grant number VEGA 2/0085/20, and by the project H2020–"SYSTEM", grant agreement No. 787128.

References

Fischer, H. B., et al. (1979): Mixing in Inland and Coastal Waters. New York: Academic Press.

Graf, W. (1998): Fluvial Hydraulics: Flow and Transport Processes in Channels of Simple Geometry. Hoboken, NJ, USA: Wiley.

Gualtieri, C. (2008): Numerical simulation of flow patterns and mass exchange processes in dead zones. Proceedings of the iEMSs Fourth Biennial Meeting: International Congress on Environmental Modelling and Software (iEMSs 2008), Barcelona, Spain.

Chapra, S. (1997): Surface Water-Quality Modeling. Series in Water Resources and Environmental Engineering ed. New York, NY, USA: McGraw-Hill.

Marsalek, J., Sztruhar, D., Giulianelli, M., Urbonas, B. (2004): Enhancing Urban Environment by Environmental Upgrading and Restoration. Dordrecht, The Netherlands: Kluwer Academic Publishers.

Martin, J. L., McCutcheon, S. C. (1998): Hydrodynamics and Transport for Water Quality Modeling. s.l.: CRC Press, Inc..

Meddah, S., Saidane, A., Hadjel, M., Hireche, O. (2015): Pollutant Dispersion Modeling in Natural Streams Using the Transmission Line Matrix Method. Water, Issue 7, 4932–4950.

Runkel, R., Broshears, R. (1991): One-Dimensional Transport with Inflow and Storage (OTIS)–A Solute Transport Model for Small Streams. Boulder City, CO, USA: University of Colorado.

Rutherford, J. (1994): River Mixing. Chichester, U.K.: John Wiley & Sons.

Socolofsky, S. A., Jirka, G. H. (2005): Mixing and transport processes in the environment. Texas: Texas A&M University.

Sokáč, M., Velísková, Y., Gualtieri, C. (2019): Application of Asymmetrical Statistical Distributions for 1D Simulation of Solute Transport in Streams. Water, 11(10), p. 2145.

Valentine, E. M., Wood, I. R. (1977): Longitudinal dispersion with dead zones. Journal of Hydraulics Division, ASCE, 103(9), 975–990.

Valentine, E., Wood, I. (1979): Experiments in Longitudinal Dispersion with Dead Zones. Journal of Hydraulics Division, ASCE, 105(HY9), 999–1016.

Weitbrecht, V. (2004): Influence of dead-water zones on the dispersive mass-transport in rivers. Dissertationsreihe am Institut fuer Hydromechanik der Universitat Karlsruhe ed. Karlsruhe: Universitatsverlag Karlsruhe.

Doc. Ing. Marek Sokáč, PhD. (*corresponding author, e-mail: sokac@uh.savba.sk)
Ing. Yvetta Velísková, PhD.
Institute of Hydrology SAS
Dúbravská cesta 9
84104 Bratislava
Slovak Republic

DOI: 10.31577/ahs-2020-0021.02.0019

ACTA HYDROLOGICA SLOVACA

Volume 21, No. 2, 2020, 152 – 159

STORAGE CAPACITY OF RAIN TANKS OPTIMIZED FOR THE LOCAL CLIMATE IN TWO METROPOLITAN AREAS OF SLOVAKIA

Milan Onderka*, Jozef Pecho, Pavol Nejedlík

Combating the adverse effects of drought and extensive precipitation in urban areas can be achieved by efficiently designed rain water harvesting systems such as green roofs, rain tanks, infiltration trenches, etc. Their performance, however, is inherently affected by local rainfall patterns. In this paper we focus on the rainfall regime at six locations within two metropolitan areas in Slovakia. Four sites are located in the capital of Bratislava and its environs, and two sites are located in the second largest city Košice. Using event-based statistical characteristics and an analytical probabilistic model, the optimal capacity of rain tanks for the metropolitan areas of Bratislava and Košice were estimated. The presented event rainfall statistics can facilitate the design of green infrastructure (e.g. vegetative roofs, rain gardens, infiltration trenches etc.), optimized irrigation of urban gardens and improvement of storm water management in these two metropolitan areas of Slovakia.

KEY WORDS: rain water harvesting, drought, green city, rain tanks

Introduction

The most recent scientific reports show (including IPCC) that increasing concentrations of greenhouse gasses affect the climate of the Earth, which is manifested by global warming and fast complex changes within the entire climatic system. Global warming has also its consequences in Slovakia and in the investigated regions of Bratislava and Košice. The observed upward trend in Earth's surface temperature is the most readily perceived manifestation of the ongoing climate change especially after the mid-1980s and the early 1990s in Slovakia. Whereas the global average temperature of the boundary -layer atmosphere increased since the start of the 20th century by 1°C (AR5 IPCC, 2013), the region of Central Europe, including Slovakia, witnessed a double increase in temperature (~1.7 to 2.0°C) over the same period. Based on climatic models, in the southern parts of Slovakia, the annual average of air temperature is very likely to increase by 0.8–0.9°C by 2025, and 2.0–2.5°C by 2050, compared to the climatic normal 1961–1990. But climate change is not limited only to increasing global and local air temperature. It brings a host of other manifestations and phenomena (e.g. droughts and extreme rainfall).
Combating the adverse effects of drought and extensive precipitation in urban areas can be achieved by efficiently designed rain water harvesting (RWH) systems such as green roofs, rain tanks, infiltration trenches, etc. Their performance, however, is inherently affected by local rainfall patterns. Rain water harvesting (RWH) systems have been shown to be an alternative source of water in cities (Zhang and Guo, 2014; Cain 2010; Rahman et al., 2014). In general, the goal of introducing RWH systems into urban planning is to collect and store rain water. The most common uses of rainwater in cities include watering of public gardens, parks and to flush public toilets. Apart from the environmental benefits associated with saving water resources, RWS reduce water bills.
In this paper we focus on the rainfall regime at six locations in Slovakia. Four sites are located in the capital of Bratislava and its environs, and two sites are located in the second largest city Košice. Using event-based statistical characteristics and an analytical probabilistic model we estimate the optimal capacity of rain tanks for the metropolitan areas of Bratislava and Kosice. Despite the widespread use of rain tanks in Slovakia, the optimal capacity (volumes) of rain tanks is often anecdotal. The goal of this paper is to describe the local rain regime and climate in the metropolitan areas of Bratislava and Košice, and subsequently to provide a tool to estimate optimal capacity of rain tanks.

Material and methods

Source data and sites description

The rainfall data analysed in this paper were obtained from the internal climatological databases of the Slovak Hydrometeorological Institute. In this study, 14–19 years (1991–2009) of pluviographic records measured at four rain gauges located within the city Bratislava, one gauge at Malý Javorník located some 20 km north from the city center in the Small Carpathians Mts., and two gaugess in Košice, were used. The geographical attributes of the rain gauges are listed in Table 1. The temporal resolution of the time series is one minute. The rainfall data cover the 'warm' part of the year when precipitation falls in liquid form (April–October), hence the cold season (November–February) was not analysed.

Local climate

The climate in the metropolitan area of Bratislava has been estimated for the period 1961–2010. According to the Koncek climate classification the area belongs to the warm (*T*) area which is characterized with an annual incidence of more than 50 warm days in the summertime (a summer day is a day when the maximum diurnal air temperature T_{max} surpassed 25°C), sub-region T1–T6 (warm, moderately humid with mild winters). The average annual temperature in this region is 10.1°C (determined for the climatic normal 1981–2010), the warmest month is July with average monthly temperature 20.5 to 21.6°C, the coolest month is January (average monthly temperature -0.8°C, average annual air temperature between 10.5 and 11.0°C). The annual incidence of summer days is 67.3 ($T_{max} \geq 25$°C), 18.4 tropical days ($T_{max} \geq 30$ °C), and 83.3 frost days (minimum diurnal temperature $T_{min} < 0$°C), 29 ice days ($T_{max} < 0$°C) and 0.4 arctic days ($T_{max} \leq -10$°C). The precipitation regime and its spatial variability in the area of Bratislava is affected by geography (Small Carpathians, Danubian and Morava lowlands). The average annual precipitation total is between 560 to 680 mm, with up to 60% of precipitation falling during the warm part of the year (April–September). Most precipitation falls between June and August, accounting to 170 to 200 mm. The average air temperature in Bratislava increased by almost 2°C since 1951 (the mean decadal increase in air temperature is 0.3°C/10 years). The annual precipitation total increased, on average, by 6–12 mm (comparison of 30-year averages estimated for 1951–1980 and 1981–2010 (16)) which is only a 2% increase. The number of frost days between the periods 1951–1980 and 1981–2010 dropped by 13 days (from 96 days to 83 days); on the other hand, the number of summer days increased by 14 days, and the number of tropical days increased by 9 days (from 10 to 19). The diurnal maximum and minimum air temperature is expected to rise in the upcoming decades. By 2050, the number of summer days is expected to substantially increase by 25 days per year, the number of tropical days with increase by 15 days; while the number of frost days can decrease by 25 days and ice days by 15 days. The most important consequence in terms of the thermal comfort is the increasing incidence of heat waves with an earlier onset (in May) and occurring until mid-September. Due to the elevated water holding capacity of the atmosphere, the number of days with muggy weather will probably increase. The precipitation totals will slightly increase, especially in the cold part of the year. But with the increasing air temperature, evaporation will increase too. This will create conditions for conditions for longer lasting droughts in the investigated region. Torrential and long-lasting rains will become more frequent and more severe (by approximately 7–14% per every °C increase in air temperature). Changing temperature and precipitation regimes in the winter season will affect the snow cover. The number of days with snow cover is expected to decline. More severe and storms are also expected to occur in the future as a response to the increasing air temperature and humidity.

Rain event separation and event characteristics

Knowing the so called „minimum inter-event time“ is essential in order to isolate statistically independent rainfall events. The minimum inter-event time (MIT), as defined by Restrepo and Eagleson (1982), is a rainless period separating two successive rains events. Two successive rains are considered as a single event if the rainless periods between two rains is shorter than the MIT value. The procedure of event selection is based on the premise that the inter-event times are exponentially distributed (Restrepo and Eagleson, 1982), and the arrival of independent events is thought to follow a Poisson process.

Every independent rainfall event can be described by various statistical characteristics such as total event volume, event duration, time between successive events, time-to-peak and maximum intensity (Wang et al., 2019; Dunkerley, 2008; 2015). In this paper, we present the event characteristics that are required for probabilistic analytical models proposed by Guo and Baetz (2007), i.e. mean event duration, mean event depth and mean inter-

Table 1. Basic geographic description of the analysed locations

Station ID	Station Name	Latitude	Longitude	Record length	Altitude [m a.s.l]
17100	Bratislava–Mudroňova	48.15219	17.07034	14	205
17140	Bratislava–Koliba	48.16778	17.10611	15	283
17320	Bratislava–Airport	48.17028	17.2075	15	128
17400	Malý Javorník	48.25583	17.1525	15	575
58220	Košice–Mesto	48.72528	21.265	15	207
60120	Košice–Airport	48.67056	21.23861	19	229

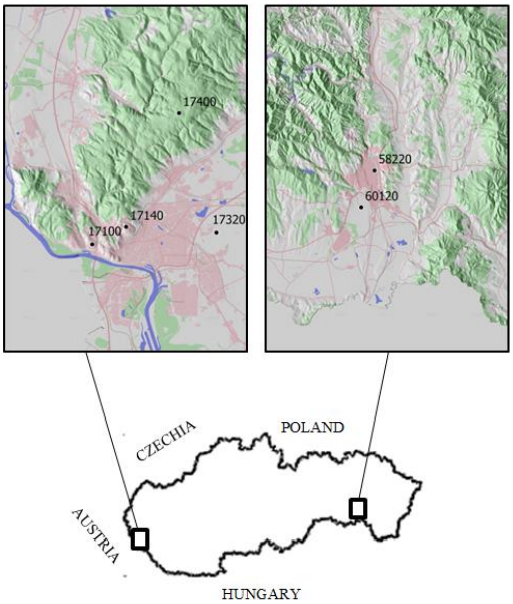

Fig. 1. Location of investigated metropolitan areas and rain gauges (left: Bratislava; right: Košice). The gauge names corresponding to the displayed gauge IDs are indicated in Table 1.

event time. These characteristics were calculated for each location from the series of previously separated rainfall events following the procedure described in Restrepo and Eagleson (1982) and Bedient et al. (2008).

Estimation of tank sizing and maximum water use rate

The local rainfall event characteristics were used as an input in an analytical probabilistic model proposed by Guo and Baetz (2007). Briefly, the capacity of a rain tank (Eq 1) and maximum daily water use rate (Eg 2) are defined as:

$$B = \frac{A\phi G}{\zeta G + A\phi\psi} ln\left[\frac{A\phi\psi\ e^{-\zeta\,\nu_{ff}}}{A\phi\psi\ e^{-\zeta\nu_{ff}} - R(A\phi\psi + \zeta G)}\right] \tag{1}$$

where
A – rooftop catchment area (roof) [m^2];
B – rain tank volume [L];
R – desired reliability of tank in supplying water [-];
G – daily use rate [L day^{-1}];
ζ – distribution parameter of event depth ν [mm^{-1}];
ψ – distribution parameter of inter-event time τ [hour^{-1}]
ϕ – dimensionless runoff coefficient [-];
ν_{ff} – depth of first flush that is diverted from rain tank [mm].

The daily maximum use rate G_{max} [L day^{-1}] is defined as:

$$G_{max} = \frac{A\phi\psi}{\zeta}\left(\frac{e^{-\zeta\,\nu_{ff}}}{R} - 1\right) \tag{2}$$

The ζ and ψ distribution parameters in Eq. 2 were determined as the inverse of the mean of the event depth ν and rainfall inter-event time τ, respectively (Guo and Baetz; 2007). Usually, the first flush may be contaminated with e.g. dust and vegetation debris. The first flush ν_{ff} is the rain water that is diverted from the downspout gutter just before the water enters the tank. To simulate tank sizes for a range of rooftop areas and reliability factors, Eq. 1 and Eq. 2 were applied pre-specified input parameters. The rooftop surface catchment areas was allowed to very between 25 to 250 m^2 in order to cover broad range of rooftop areas. The reliability factor R is here defined as a fraction of time when the desired water use rate (G_{max}) is guaranteed. R was allowed to vary from 0.2 to 0.8. These simulations were conducted for all six locations (Table 1), using the statistics of the mean event depth $\hat{\nu}$ and the mean inter-event time $\widehat{IET}$ (Tables 2). In the examples presented in Fig. 3, the reliability factor R was set to 0.4 and the rooftop catchment area A to 190 m^2, which are arbitrarily chosen design parameters.

Results and discussion

The analysed rainfall records were separated into statistically independent rainfall events that were later used to derive event-based statistical characteristics such as mean rainfall duration, mean event depth and mean inter-event time for each location. The empirical estimates of mean event depth and mean inter-event time are listed in Table 2. As rainfall is a highly spatially variable phenomenon, it is essential to investigate how the average rain event duration, total rain event volume and inter-event time vary in space. For example, the MIT values across the analysed locations range from 11 hours at Malý Javorník and 23.5 hours in the city of Košice (Table 2). The average event volume is a highly variable characteristics within the area of Bratislava (ranging from 6.3 to 9.3 mm). In the case of Kosice, the average event volume ranges from 10.5 to 17.8. The other event characteristics show also a large spatial variability within and between the two metropolitan areas.

To show the applicability of the presented analytical probabilistic approach, a real-world situation is simulated for a hypothetical homeowner living in the vicinity of the Bratislava Airport wants to collect rain water and use it for irrigating a small backyard. Let us suppose that the house has a roof with surface area 190 m^2 and the expected daily use rate is 320 L day^{-1}. In all simulations, the runoff coefficient ϕ was set to 0.95. As shown in Fig. 3a, this will require a tank (or several smallest tanks) of almost 3 m^3. Note, that this particular location does not allow the homeowner to use more than 320 litres per day, supposing the reliability is set to 40%. i.e. 40% of time the requirements will be satisfied. If the house was located in Bratislava–Koliba, the same tank volume would allow the homeowner exploit 430 L per day. Similar comparisons can be readily made for other situations and locations (Fig. 2a–b).

The maximum daily use rates were also simulated for a range of reliabilities and rooftop catchment areas estimated for stations located in the Bratislava area (Fig. 3) and in Košice (Fig. 4). In general, the maximum daily use rate decreases exponentially with increasing reliability. Fig. 3 and Fig. 4 show that increasing the rooftop catchment areas does not lead to a substantial increase in the maximum daily use rate when the reliabilities are expected to be too high. Considering that a reliability of 0.8 means that water can be abstracted from the rain tank almost every day, the rain tank can provide very small amounts of water.

Apart from the application presented in this paper, the tabulated statistical properties of rainfall (Table 2) can be used in the design of water detention reservoirs (Bacchi et al., 2008), bioretention systems and infiltration systems (Guo and Hughes, 2001), vegetative roofs (Guo, 2016), sewer tanks (Balistrocchi et al., 2009), or to conduct hydrologic analysis of rainfall-runoff relationships in catchments (Guo and Adams, 1998). Although only the mean inter-event time and mean event depth were used in the estimation of proper sizing for rain tanks, the values of mean event duration and the mean number of events (Table 2) as presented as well, as these statistical properties of rain are essential for the design of drought mitigation measures mentioned earlier.

Fig. 5 is important in respect to the actual choice of rain tank volumes. The sizing of rain tanks was simulated an hypothetical house with a rooftop catchment of 190 m^2 (a typical urban family house in the investigated region), reliabilities from 0.1 to 0.8 (or 10 to 80%), daily water use rates 10 to 500 L day^{-1} (with 10-liter increments). Choosing the optimal size of a rain barrel is a trade-off between the desired use rate G and reliability R. For example, a reliability of 10% actually means that, on average, the tank volume will be completely depleted once in every 10 days. Increasing the reliability to 30 and 40%, the largest tank sizes will reach 1.5 and 4 m^2, respectively; depending on the location. Note that above the reliabilities of 40% the tank volumes are determined only to a certain limit.

This limit is displayed in Fig. 4 as white spots. These white spots indicate that the tank volume cannot be mathematically determined because the denominator in the logarithm of Eq. 1 becomes negative for high values of reliability. Thus, additionally increasing the tank volume would not guarantee more water in the tank, as rain-fall becomes the limiting factor. An extreme situation happens when the reliabilities are set to 80%. In this case, the rain tanks cannot provide more water than 10 liters of water from a 0.5 m^3 rain tank at Bratislava–Aiport and not more than 50 liters of water from a 1 m^3 rain tank in Košice–Mesto.

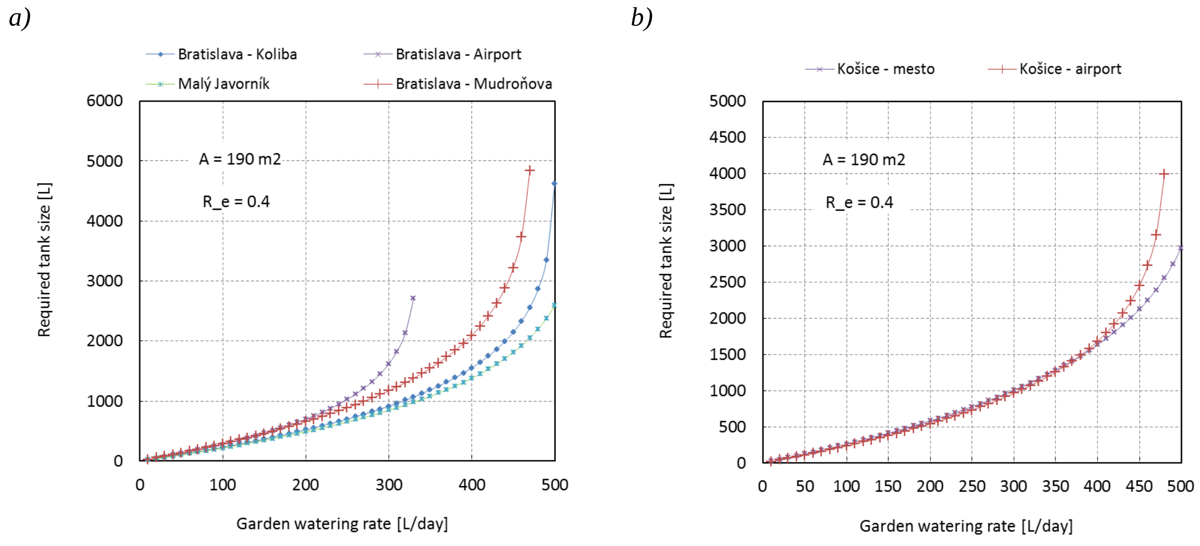

Fig. 2. Required tank sizes calculated by Eq. 1 for four stations in the capital city Bratislava and Malý Javorník a); and b) for two stations at the second most-populated city (Košice).

Table 2. **Spatial variability of event characteristics (annual mean values): event depth $\hat{\nu}$, event duration $\hat{\tau}$, inter-event time $\widehat{IET}$, and number (incidence) of rainfall events $\widehat{N}$**

Station ID	Station Name	$\hat{\nu}$ [mm]	$\hat{\tau}$ [hrs]	$\widehat{IET}$ [hrs]	$\widehat{N}$ [-]	MIT [hrs]
17100	Bratislava–Mudroňova	9.3	14.1	105.5	27.5	20.0
17140	Bratislava–Koliba	8.0	10.3	83.3	30.1	14.5
17320	Bratislava–Airport	6.3	8.9	91.1	29.9	14.5
17400	Malý Javorník	8.1	8.6	79.8	25.8	11.0
58220	Košice–Mesto	9.8	17.8	245.8	29.7	23.5
60120	Košice–Airport	8.0	10.5	215.1	31.2	16.5

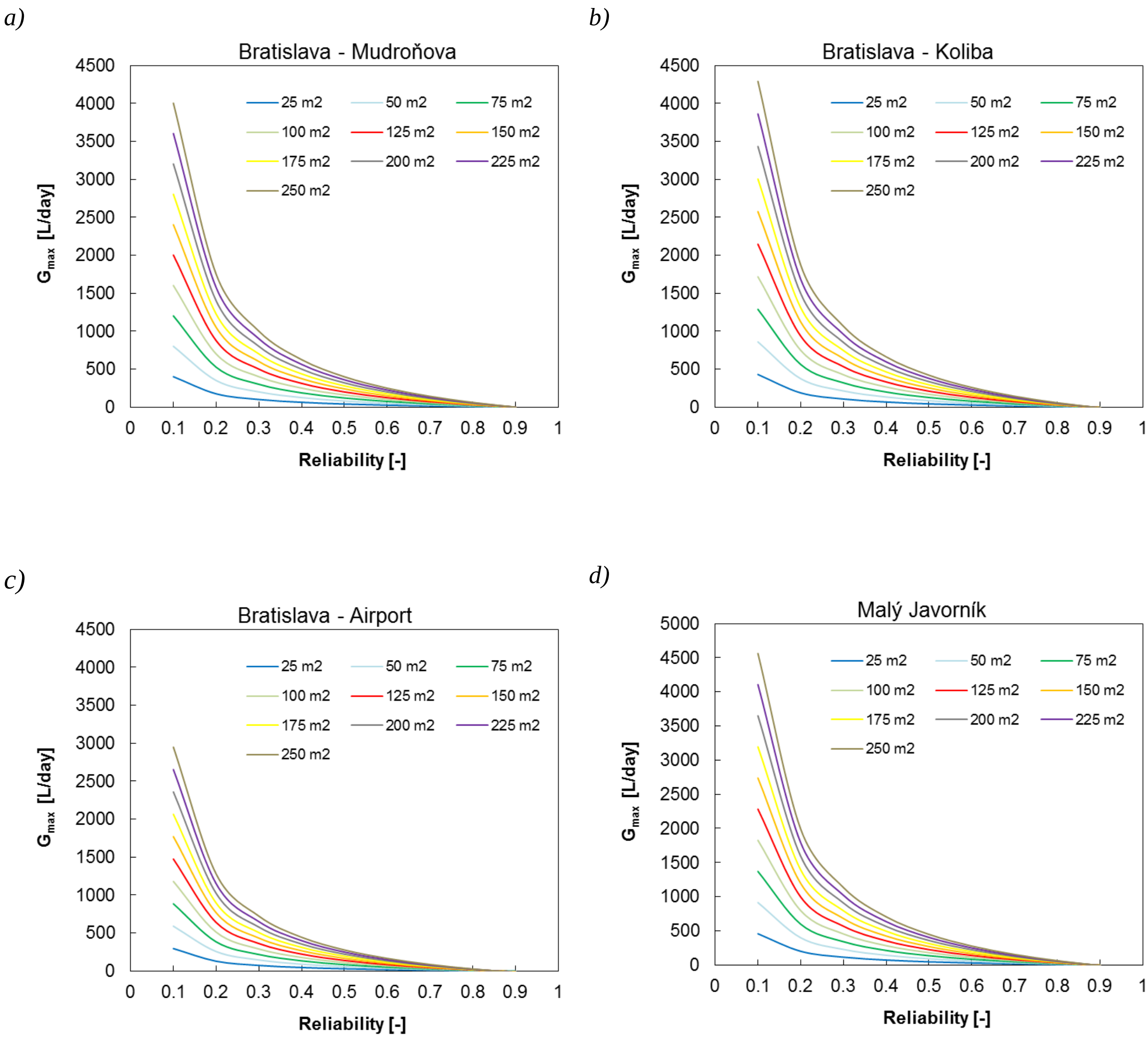

Fig. 3. Maximum daily use rates calculated by Eq. 2 for a range of reliabilities R ∈ (0.1–0.9) estimated for: a) Bratislava–Mudroňova; b) Bratislava–Koliba; c) Bratislava–Airport; d) Malý Javorník.

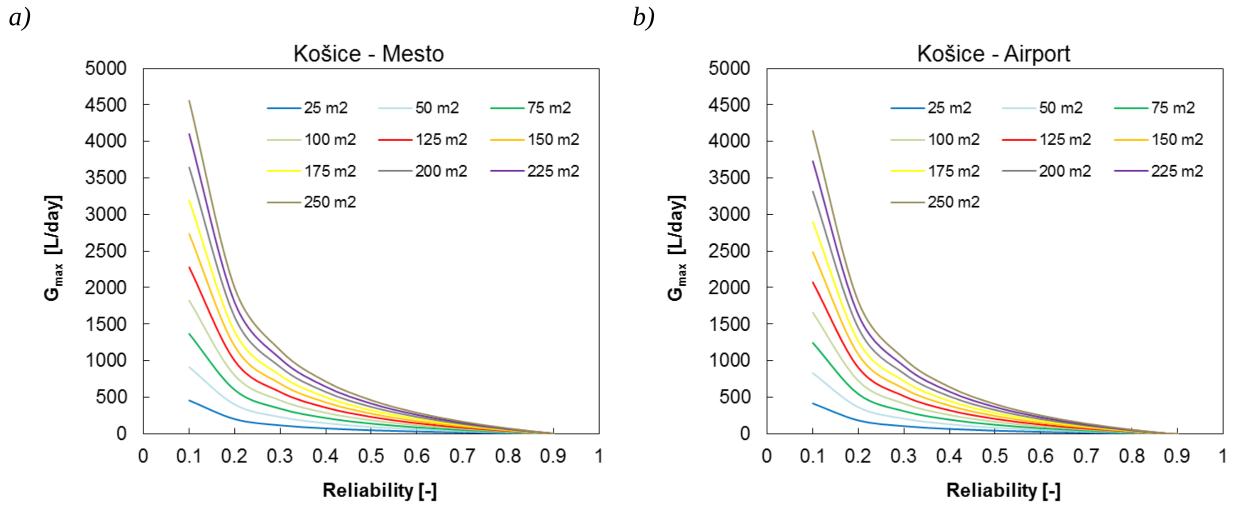

Fig. 4. Maximum daily use rates (Eq. 2) simulated for a range of reliabilities R (0.1– 0.8), rooftop catchment area 190 m², and first flush 1mm, estimated for: a) Košice – mesto; b) Košice – Airport.

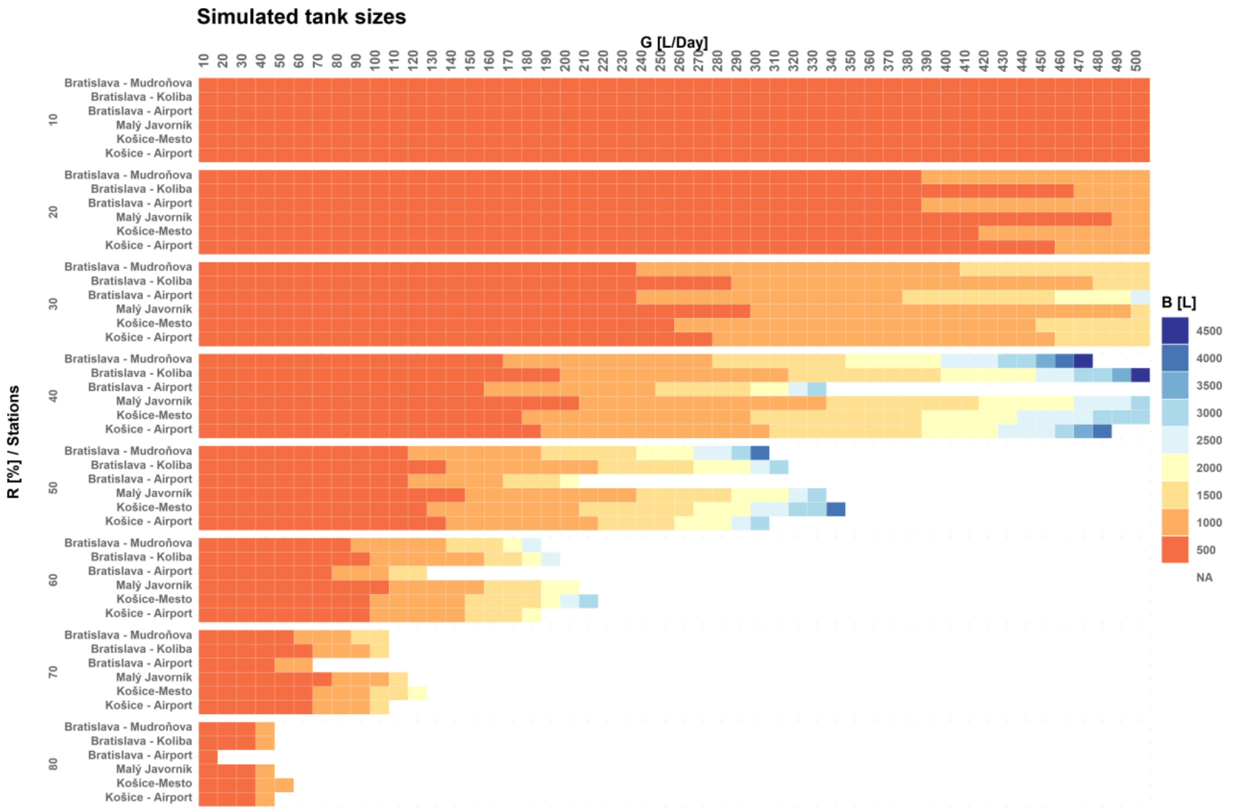

Fig. 5. Simulation results for a hypothetical rooftop area A=190 m², reliabilities range from 10 to 80 %. The daily use rate G [L day^{-1}] are indicated in increments of 10 L day^{-1}.

Conclusions

By 2050 the number of days with extreme air temperatures is expected to substantially increase. On the local and national levels, there are several initiatives supported by the EU to combat the manifestations of drought in cities. The most important measures are green infrastructure and improvement of water retention structures in the urban environment as part of the urban green agriculture. The use of rooftop inexpensive rainwater harvesting systems increases the quantity of water for urban green architecture. In this study, six rainfall records were analysed in two major metropolitan areas in Slovakia to show local rainfall characteristics are detrimental in the design of rainfall harvesting systems. As a practical example, the analytical probabilistic approach was deployed to estimate optimal rain tank capacity for three sites in Bratislava, one site in the Small Carpathians and two stations in Košice. The model is parameterized on locally estimated event-based rainfall statistics: rainfall volume and inter-event time and rainfall. The rainfall records were separated into statistically independent rainfall events to derive the event-based rainfall statistics. The presented rainfall statistics can be used as design values directly by homeowners or municipalities that may assist homeowners in selecting the proper sizing of rain tanks without having to laboriously acquiring local statistics of rainfall. As analytical probabilistic models are gaining in popularity in the hydro-meteorological community, we are convinced that the presented statistical properties of rainfall can used also in the design of bio-retention systems, infiltration systems, vegetated roofs, and hydrologic analysis of rainfall-runoff relationships in catchments.

Acknowledgement

These research outcomes presented in this paper could not be accomplished without the support of the project „Scientific support of climate change adaptation in agriculture and mitigation of soil degradation" (ITMS 2014+ 313011W580), supported by the Integrated Infrastructure Operational Programme funded by the ERDF, and the VEGA grant No. 2/0015/18 „Meso- and micro-meteorological exploration of the occurrence of hydrometeors in boundary layer of troposphere based on passive evaluation of changes of electromagnetic radiation from anthropogenic sources".

References

Bacchi, B., Balistrocchi, M., Grossi, G. (2008): Proposal of a semi-probabilistic approach for storage facility design. Urban Water Journal, 5(3), 195–208

Balistrocchi, M., Grossi, G., Bacchi, B. (2009): An analytical probabilistic model of the quality efficiency of a sewer tank.

Bedient, P. B., Huber, W. C., Vieux, B. E. (2008): Hydrology and floodplain analysis. Published by Prentice Hall, ISBN 13>0-13-242285-7, p 373.

Cain, N. L. (2010): A different path: the global water crisis and rainwater harvesting. Consilience: The Journal of Sustainable Development. 3(1): 187–196.

Dunkerley, D. (2008): Rain event properties in nature and in rainfall simulation experiments: a comparative review with recommendations for increasingly systematic study and reporting. Hydrol. Process., 22, 4415–4435

Dunkerley, D. (2015): Intra-event intermittency of rainfall: an analysis of the metrics of rain and no-rain periods. Hydrol. Process. 29, 3294–3305

Guo, Y., Adams, B. J. (1998): Hydrologic analysis of urban catchments with event-based probabilistic models 1. Runoff volume. Water Resources Research, 34(12), 3421–3431

Guo, Y., Hughes, W. (2001): Storage volume and overflow risk for infiltration basin design. Journal of Irrigation and Drainage engineering. 170–175

Guo, Y., Baetz, B. (2007): Sizing of Rainwater Storage Units for Green Building Applications. J Hydrol Eng, 12, 10.1061/(ASCE)1084-0699(2007)12:2(197).

Guo, Y. (2016): Stochastic analysis of hydrologic operation of green roofs. J. Hydrol. Eng. 21(7), 04016016

Rahman, S., Khan, M. T. R., Akib, S. (2014): Sustainability of rainwater harvesting system in terms of water quality. The Scientific World Journal. 2014: 721357.

Restrepo, P., Eagleson, P. (1982). Identification of Independent Rainstorms. Journal of Hydrology. 55. 303–319. 10.1016/0022-1694(82)90136-6.

Wang, W., Yin, S., Xie, Y., Nearing, M. A. (2019): Minimum inter-event times for rainfall in the eastern monsoon region of China. American Society of Agricultural and Biological engineers. ISSN 2151-0032, Vol. 62(1), 9–18.

Zhang, S., Guo, Y. (2014): Stormwater capture efficiency of bioretention systems. Water Resour Manage., 28, 149–168

Mgr. Milan Onderka, PhD. (*corresponding author, e-mail: milan.onderka@savba.sk)
Earth Science Institute, SAS
Dúbravská cesta 9,
840 05 Bratislava,

Slovak Hydrometeorological Institute
Jeséniova 17,
83315 Bratislava,
Slovak Republic

RNDr. Pavol Nejedlík, CSc.
Earth Science Institute, SAS
Dúbravská cesta 9,
840 05Bratislava,
Slovak Republic

Mgr. Jozef Pecho
Slovak Hydrometeorological Institute
Jeséniova 17,
83315 Bratislava
Comenius University,
Faculty of Mathematics, Physics, and Informatics
Mlynská dolina F1,
842 48 Bratislava,
Slovak Republic

DOI: 10.31577/ahs-2020-0021.02.0020

ACTA HYDROLOGICA SLOVACA

Volume 21, No. 2, 2020, 160 – 171

CLIMATE CHANGE IMPACT STUDY ON 100-YEAR FLOODS OF SELECTED SLOVAK CATCHMENTS

Eva Kopáčiková, Hana Hlaváčiková*, Danica Lešková

During the ongoing climate change, this work provides an analysis of the modelled expected change in floods (100-year) for 11 Slovak river basins. It also analyses the possibilities of using data from the latest climate projections of global and regional models from the EURO-CORDEX initiative, as well as outputs from two hydrological models from the SWICCA database (Service for Water Indicators in Climate Change Adaptation) within the Copernicus service, for regional conditions in Slovakia. To estimate the 100-year flood, a frequency analysis was applied to each member of the climate and hydrological model output ensemble. The statistical distribution of generalized extreme values (GEV) was used. In case the data showed a significant trend, the non-stationarity of the environment was also taken into account. The bias of hydrological models outputs were corrected by the variance scaling method. The results indicate an increase in Q_{100} for seven gauges, a decrease for three gauges and for one station no change in Q_{100} (change more than ± 5%). Based on the results, we recommend applying hydrological data from the SWICCA database, preferably for large to medium-sized river basins.

KEY WORDS: Copernicus, climate change, hydrological models, 100-year flood

Introduction

In-depth studies of historical climate change confirm that the climate is changing over the last decades to centuries, mainly due to the growing anthropogenic impact. Several studies show that we are already feeling the impact of this change in various areas of life (Huntington, 2006; IPCC, 2014; Duethmann et al., 2020). Impact of climate change is already partially measurable and identifiable on: average annual flows (Nijssen et al., 2001; Krajewski et al., 2019), increase of peak flows and shift of their occurrence (Hirabayashi et al., 2013; Blöschl et al. 2017; Blöschl et al., 2019), changes in long-term flow duration curves (Arora and Boer, 2001), changes in the length of the period with low flows (Stahl et al., 2010; Fendeková et al., 2017) and changes in the elements of the hydrological balance (Pekárová et al., 2018).

It is not easy to estimate the impact of climate change in water management as well as in other fields of study. Climate change is manifested differently in different geographical areas. The great variability of natural processes, not to mention anthropogenic influences, are a natural part of the climate.

The expected climate change brings with it a number of scientific issues and uncertainties that are the subject of studies and discussions. Analysed are mainly: the increase in the extremity of hydrological phenomena (increase in extreme values, but also the frequency of their occurrence) in form of droughts or floods, but also a change in the hydrological regime of watercourses themselves and the impact of these phenomena on society as a whole. The modification of the period with the highest or the lowest expected water bearing of streams in a year, their frequency, but also the values of absolute maximum and minimum discharges, the time shift of snow accumulation and snow melting and the total water balance in river basins are not entirely clear.

Floods occur regularly in Europe. Their incidence is well documented in a recent study by Blöschl et al. (2020) focusing on several flood-rich periods over the last 500 years. Reliable information on the potential change of future hydrological conditions in the field of water management is the basis for long-term strategies and adaptation plans. Solving these tasks is even more urgent given the fact that most Slovak streams originate in Slovakia.

A hundred year flood is an important design variable needed for the planning and operation of water management structures. Generaly, it is determined from a series of measured peak annual flows (or flows exceeding a selected threshold value) by the method of frequency analysis, applying the most suitable theoretical exceedance curve (in Slovakia according to the norm OTN ŽP 3112-1: 03). The measured data can also be supplemented by historical data, which complements and extends the sample of observations with rare data having a long return period (as extreme floods in the past) (Pekárová et al., 2018). The second way one could determine the direction of change in flows is to analyse the trend from measured time series, especially in recent decades, as shown in Bertola et al. (2020). Although such analyses are necessary and important, their disadvantage may be the absence of sufficiently long series of observed data needed for analyses of flood flows with long return periods. Also, from these analyses it is not possible to predict the development of the climate in the future, which seems to be greatly influenced by the development of anthropogenic activity.

An interesting way to quantify the expected impact of climate change on flood flows, but also on the changing hydrological regime of river basins is a method based on analysis of climate change predictions in form of the latest outputs from climate models, climate projections (so-called impact studies) (Hakala et al., 2019). This approach, in contrast to the analysis of long-term historical data and assumption that conditions remain unchanged, makes it possible to obtain the latest forecastted time series of climate characteristics from the future for a sufficiently long period of approximately 90–100 years and apply the frequency analysis on a relatively large and thus more reliable sample of data.

The Copernicus Climate Change Service (C3S) is one of the 6 products of the Copernicus Earth Observation Programme. Copernicus is an EU operational program based on the existing European scientific infrastructure and available European scientific knowledge. The C3S project is, besides its own research, also based on the climate research addressed within the World Climate Research Program (WCRP). C3S provides information on the historical, current and projected future climate of Europe and the world (https://climate.copernicus.eu/, available on 18.02.2020) such as climate observation data, climate reanalysis, seasonal forecasts and future climate projections. By offering consistent information on climate change, the service was set up to support the elaboration of adaptation plans and climate change mitigation policies for the EU. C3S provides specific information for different fields. The water management was served by the SWICCA portal (Service for Water Indicators in Climate Change Adaptation) (http://swicca.climate. copernicus.eu/, available on 15.5.2019) operated by the Swedish Meteorological and Hydrological Institute (SMHI).

In this work, data from the SWICCA database were used to estimate the change in Q_{100}, namely climate data from five global circulation models (GCM), four regional climate models (RCM), three climate scenarios (RCP 2.6; 4.5; 8, 5) and two hydrological models E-HYPE and LISFLOOD.

The aim of this work was to answer the following questions: 1/ whether it is possible to expect a change in 100-year floods on selected Slovak streams due to expected climate change and with what degree of uncertainty, 2/ whether it is possible to find some regional similarities in identified changes, 3/ whether significant growth trends of peak flows will be identified and on which rivers? The methodology of estimating Q_{100} based on the outputs of climate models from the SWICCA database was used for the first time in Slovakia in the project C3S_441_ Lot1_SMHI contract (SWICCA project) (http://swicca. eu/about/, available on 18.12.2018). The first results of the local case study "Flood warnings in a changing climate", which was addressed in the period 2015 to 2017 within the SWICCA project in cooperation between MicroStep-MIS and the Slovak Hydrometeorological Institute, were published in Gaál (2018) and Gaál et al. (2017) for the Bratislava (Danube) water gauging station. Therefore, our next goal was to test the database and methodology for several river basins in Slovakia. In no case does this work provide data on the official change of existing design variables. However, it may point to indications of an expected change that need to be further examined.

Material and methods

The SWICCA portal and database

The first version of the SWICCA portal was created under contract C3S_441_Lot1_SMHI of the C3S service, operated by the ECMWF on behalf of the European Commission. In the period 2015–2018, the portal was operated with the help of SMHI together with ten other partners from all over Europe.

The aim of the SWICCA portal is to provide users with the necessary data to assess climate change and its impact in various areas of water management (for case studies) across Europe in order to subsequently quantify the impact of projected climate change in the field of water resources.

The interconnection of information between experts from different fields (climatologists, water managers, hydrologists, numerical mathematicians), but also competent decision-makers should serve this goal. Case studies serve as basis for the design of adaptation plans, which is also one of the main goals of SWICCA. SWICCA data is currently available through the Climate Data Store (https://cds. climate.copernicus.eu/cdsapp#!/dataset/sis-water-quantity-swicca?tab=overview, available 20.02. 2020) within the portal Copernicus Climate Change Service one can find various simulated impact indicators, e.g. data on water quantity and quality, air temperature, precipitation, cloud cover, air humidity and many others, on which it is possible to analyse the impact of climate change in terms of trends and variability of a particular indicator.

For the purpose of this impact study, two types of time series of average daily flows were downloaded from the SWICCA portal (as of 01.02.2019) as outputs of eleven mutual combinations of five global circulation models (GCM), four regional climate models (RCM), three climate scenarios (RCP) and two hydrological models: 1 / hydrological model E-HYPE and 2 / hydrological model LISFLOOD (Table 1). Table 1 lists the names of GCM and RCM, along with the name of the institute that develops these models.

Representative concentration pathway RCP (Emission scenarios)

Different climate datasets are based on different climate

Table 1. Summary of climate model runs used in SWICCA database. RCP–indicates the representative concentration pathway and its development direction, GCM–global circulation model, RCM–regional circulation model. *missing data in years 2095–2100. The period 1.1.1971–31.12.2000 was taken as the reference period and 1.1.2011–31.12.2100 was considered as future

No.	RCP	GCM	RCM	Time period	Institute
1	2.6	EC-EARTH	RCA4	1970–2100	SMHI
2		MPI-ESM-LR	REMO2009	1970–2100	CSC
3	4.5	EC-EARTH	RCA4	1970–2100	SMHI
4		EC-EARTH	RACMO22E	1970–2100	KNMI
5		HadGEM2-ES	RCA4	1970–2098	SMHI
6		MPI-ESM-LR	REMO2009	1970–2100	CSC
7*		CM5A	WRF33	1970–2100*	IPSL
8	8.5	EC-EARTH	RCA4	1970–2100	SMHI
9		EC-EARTH	RACMO22E	1970–2100	KNMI
10		HadGEM2-ES	RCA4	1970–2098	SMHI
11		MPI-ESM-LR	REMO2009	1970–2100	CSC

models, as well as three different emission scenarios, which represent the scenarios of climate development. The Intergovernmental Panel on Climate Change (IPCC) lists them in a recent report in the form of representative concentration pathways (RCPs) (van Vuuren et al., 2012). SWICCA works with three basic scenarios, defining them as follows: 1/ RCP2.6 assumes that CO_2 emissions will be constant at the beginning of the century, then start to decrease and reach negative values at the end of the century, 2/ RCP4.5 assumes that CO_2 emissions will increase by the middle of the century and then begin to decline, 3/ RCP8.5 assumes that CO_2 emissions will triple by the end of the century and methane emissions as well as the use of energy and fossil fuels will also increase. The most pessimistic scenario further assumes that understanding the concept of renewables will be very limited and the implementation of the climate strategy will be missing. More information on emission scenarios can be found at: http://swicca.climate.copernicus.eu/wp-content/uploads/2016/02/How-to-use-different-RCPs.pdf (available 5.2.2019).

Estimation of the 100-year flood

The following procedure was chosen for estimating Q_{100}: 1/ download time series of average daily flows from all available climatic outputs and from two hydrological models HYPE and LISFLOOD from the SWICCA portal for selected gauges in Slovakia, 2/ data check and bias-correction for the reference period 1971–2000, 3/ selection of annual maxima, 4/ conversion of annual maxima of average daily flows into annual peak flows according to the methodology of Hlaváčiková et al. (2019), 5/ trend analysis by non-parametric Mann-Kendall test, 6/ frequency analysis (stationary or non-stationary).
Due to the low quality of raw data for the stations Banská Bystrica (Hron), Liptovský Mikuláš (Váh), Janík (Bodva) and Spišské Vlachy (Hornád) found by data check at the reference period, flow outputs from the SWICCA database (from hydrological models Lisflood and HYPE) were not used in this case. Instead the following procedure was adopted: 1/ download of time series of precipitation and temperatures from all available climatic outputs from the SWICCA portal, 2/ calibration of hydrological model HBV for daily step, 3/ model run for different sets of input data from climate models. The next procedure was the same as in the previous one starting at point 2.

Hydrological models used for climate change impact modelling

All hydrological models, the outputs of which were used in this work, are conceptual rainfall-runoff models. The HYPE model (**E-HYPE** v. 3.1.2) is a semi-distributed successfully used model in the short-term and seasonal forecasting, as well as in the hydrological warning operational service at the SMHI. The model was calibrated and validated in a daily step for more than 35,000 sub-basins in Europe with an average river basin size of 215 km^2. For these sub-basins, it has also been assessed for its suitability for application to climate change (Hundecha et al., 2016).
The **LISFLOOD** hydrological model was developed as part of the Natural Hazard Project by the Joint Research Centre (JRC) of the European Commission. LISFLOOD is used for daily forecasts within the EFAS and GLOFAS operational alert systems. More information about the model can be found in the report by Burek et al. (2013).
The application of both models for climate change analyses has also been tested on 46 major European river

basins (Greuell et al., 2015). Further details on the hydrological models used in the climate change impact studies and the data obtained from these models are given in Hundecha et al. (2016) (E-HYPE model v.3.1.2) and Greuell et al. (2015), Roudier et al. (2016) and Burek et al. (2013) (LISFLOOD model). The spatial resolution of hydrological models for the SWICCA database is as follows: 0.5 degrees x 0.5 degrees (approx. 50 x 50 km) in the LISFLOOD model, irregular polygons of river basins with a median area of 215 km^2 in the E-HYPE model.

The **HBV** model (IHMS 6.4) is used daily for approximately 60 Slovak river basins in the Department of Hydrological Forecasts and Warnings of the SHMU (Slovak Hydrometeorological Institute). It is also commonly used worldwide in a modified form such as HBV-Light. The model was calibrated in a daily time step for four Slovak river basins, for which it was used to estimate the impact of climate change.

Regional climate models outputs correction

The outputs from the GCM have a coarse resolution. Therefore, a first step of adjusting the climate data is rescaling GCM outputs into a resolution usable by RCM. The next step is to eliminate RCMs structural defects (bias correction) that needs to be applied before using the data in impact studies (Wilcke et al., 2013). The climatic data from the SWICCA database used in this work (outputs from RCM in the spatial resolution of 12 x 12 km obtained within the EURO-CORDEX initiative) were corrected by the "quantile-mapping" method (Wilcke et al., 2013).

Bias correction of hydrological data

Hydrological simulations of future will mostly improve if their inputs are bias corrected (Hakala et al., 2019). The parameters of the hydrological models, which were calibrated on the current climate conditions, are then used for simulations of the period of the assumed changed climate with the bias corrected forecasted meteorological data. Despite great efforts to adjust the outputs of RCM models by bias correction and downscaling, several meteorological variables from RCM models are still not suitable for their use in hydrological impact studies (Teutschbein and Seibert, 2012; Dakhlaoui et al., 2019; Gao et al., 2020). This can be resolved using e.g. a multi-ensemble approach, which uses an ensemble of climatic outputs from RCM models (precipitation and temperatures), downscaled so that when used in the hydrological model they correspond to the measured hydrological data as much as possible (usually comparing average monthly flows or peak flow exceedance curves according to the type of analysis) (Teutschbein and Seibert, 2010; Hakala et al., 2019; Gao et al., 2020). Another solution is to use an ensemble of climate and hydrological models (Donnelly et al., 2017; Hakala et al., 2019) without further correction of previously corrected climate data (IMPACT2C, 2015). Some authors also performed the bias correction directly on hydrological data (González-Zeas et al., 2012; Gaál et al., 2017). The reason may be that homogeneous data of historical meteorological characteristics (precipitation and temperature) and measured flows necessary for the calibration of the own hydrological model are not available, or a suitable hydrological model is missing.

The bias correction was performed in this work directly on hydrological data, because the statistical characteristics of hydrological simulations from the SWICCA database sometimes showed a greater or lesser deviation compared to the characteristics of the measured average daily flows.

Because of a high number of analysed data (in the first phase, 572 time series for 26 stations were processed, all listed in Hlaváčiková et al., 2019) it was decided to apply a uniform method of bias correction on hydrological data called the variance scaling method (according to Teutschbein, 2013). The analysis was performed on a control period 1971–2000 for which both outputs from the SWICCA database and observations were available. Four basic criteria were applied to compare the characteristics of hydrological model outputs with measured data: 1/ coefficients Nash-Sutcliffe (NSE) (Nash-Sutcliffe, 1970) and Kling-Gupta (KGE) (Gupta et al., 2009), 2/ visual assessment of box plots with emphasis on capturing extremes, 3/ Mann-Whitney test to assess whether data from models come from the same population as observations, and 4/ visual comparison of time series in the daily time step, monthly averages, and annual maxima. Based on the above criteria, better results (fits) were obtained by data corrected by the above-mentioned variance scaling method than by the linear scaling or raw data.

In this way, the selection of stations for further analysis was also considerably narrowed down. Seven stations were selected for further analysis: Bratislava, Moravský Svätý Ján, Ipeľský Sokolec, Chmeľnica, Vlkyňa, Streda nad Bodrogom and Veľké Kapušany.

However, the intention was to analyse the impact of climate change on the whole territory of the Slovak Republic and the current selection of stations did not cover all large Slovak river basins. Thus, it was decided to supplement the missing river basins with simulations from the HBV model which is used in SHMU operationally in an hourly time step. The model had to be recalibrated to a daily step and then mathematical simulation with inputs from the SWICCA database (daily precipitation and temperature) had to be run. For completion, following stations were tested: Kysucké Nové Mesto, Liptovský Mikuláš, Chalmová, Banská Bystrica, Spišské Vlachy and Janík. All gauges were assessed during the overlapping control period. Four stations met the criteria of good fit: Banská Bystrica, Liptovský Mikuláš, Janík and Spišské Vlachy. Demonstration of raw (unadjusted) data and corrected average daily flows by linear scaling and variance scaling for Moravský Sv. Ján is in Figure 1.

Frequency analysis

The 100-year flood is generally estimated by the method of frequency analysis. It is a statistical method of estimating the frequency of occurrence of rare events

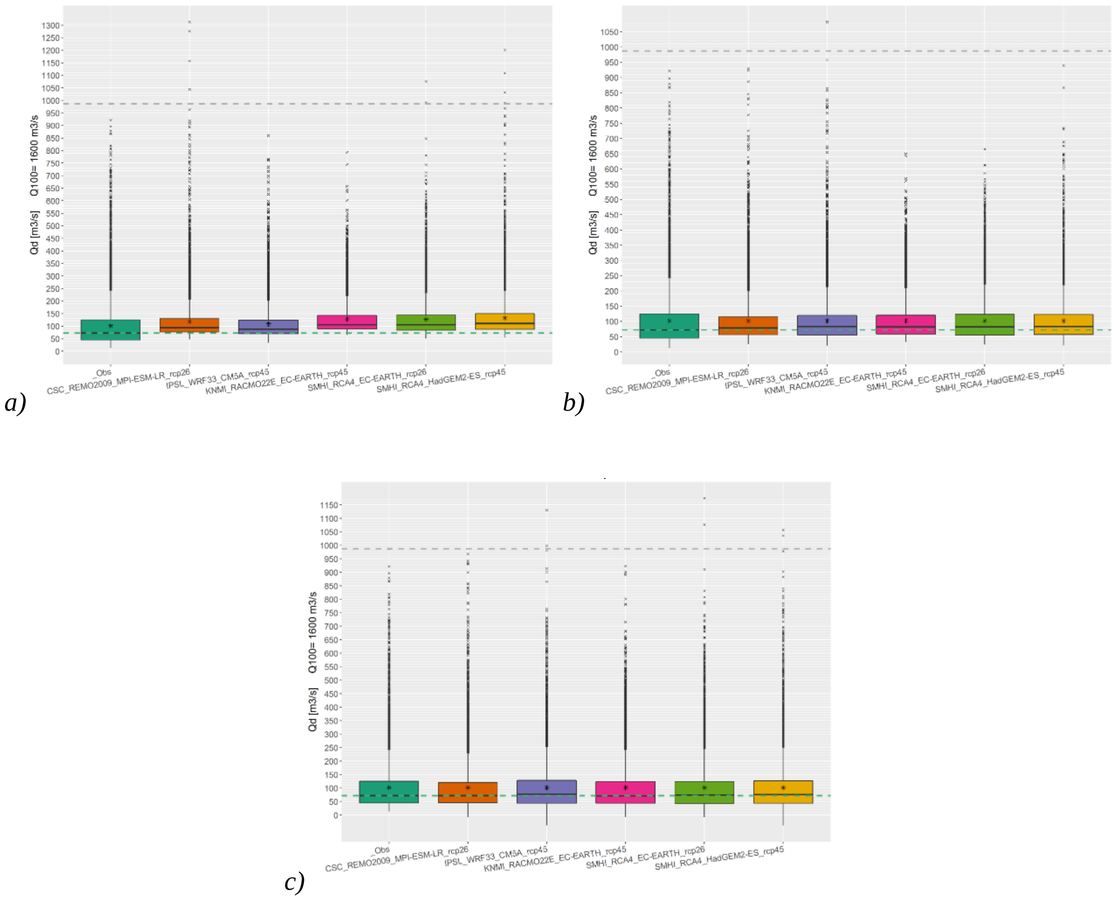

Fig. 1. Boxplots of average daily flows at Moravský Sv. Ján a) uncorrected (raw) data, b) bias correction by linear scaling , c) bias correction by variance scaling. The first box from the left shows the observed flows, other boxes indicate the outputs from climate models for the hydrological model LISFLOOD. The upper dashed line marks the value of the currently valid Q_{100}, the lower one indicates the value of median from observations.

using probability distributions. First of all, for the application of frequency analysis it is necessary to verify whether its assumptions apply: randomness of occurrence, homogeneity and independence of the analysed data. Subsequently, it is necessary to select the distribution function, determine its parameters, and evaluate the goodness of the fit. According to Gilleland and Katz (2016), the distribution of generalized extreme values (GEV) has a theoretical basis for application to the data of block maxima characterizing floods. GEV is a family of continuous 3-parametric probability distributions, which can be divided into three types of distributions according to the shape parameter ξ: Gumbel, Weibull and Fréchet (Pareto). The GEV function is a function that generalizes all three of the above distributions and can therefore be used for the first estimate. Based on its diagnostics, it is also possible to select the most appropriate function, and thus cover the data with a more accurate distribution. Such an approach is recommended especially when estimating long return periods, as this greatly reduces the variance of their confidence interval.

Non-stationarity of future time series

In analyses of the future, it is necessary to take into account the non-stationarity of the environment and to consider the possibility that probabilities of the occurrence of extreme phenomena in hydrology will shift (Milly et al., 2008). The change in extreme events over time can be characterized by expressing one or more parameters of the distribution function as time-dependent. In order to take into account the non-stationarity in the frequency analysis of the maximum annual flows, it is first necessary to determine the trajectory and the significance of the change in the time series. Subsequently, it is decided whether and to which parameter of the distribution function, the non-stationarity will be taken into account. The choice of model should be as simple as possible and at the same time it should be able to take into account variations of the dataset as much as possible. The model of non-stationarity is applied to describe the process of data creation, not the data itself, so if the trend is not particularly significant, a simpler model should be chosen (Coles, 2001).

Trend analysis

For annual maxima series, a linear trend is being used most frequently in the literature. In this analysis, a non-parametric Mann-Kendall test was applied for identification of a significant trend.

Expression of climate change impact for the estimation of Q_{100}

The climate change impact for Q_{100} (CCQ_{100}) was expressed as the percentage change in Q_{100} in the future compared to the present as follows:

$$CCQ_{100}=100*(Q_{100,fut}-Q_{100})/Q_{100} \quad [\%] \tag{1}$$

where

$Q_{100,fut}$ – is the estimated 100-year flood for the period 2011–2100;

Q_{100} – is the current 100-year flood at the relevant water gauging station.

The final average values of future Q_{100} were obtained from the whole ensemble of climatic and hydrological models available for a given station (i.e. for 11 outputs from climate models and 2 outputs from two hydrological models, i.e. 22 members of the ensemble). Uncertainties in estimating the change in Q_{100} were quantified from the interquartile range of average climatic impact factors of the entire CCQ_{100} ensemble for a particular station. This method expresses uncertainty by giving the range where 50% of the average CCQ_{100} values for a given station were estimated.

Uncertainties in estimation of Q_{100}

Several uncertainties need to be considered in climate change impact studies. These uncertainties cover all aspects of the lack of knowledge of the future climate (IMPACT2C, 2014). The main sources of uncertainty can be divided into several groups, namely the uncertainties associated with:

1 – selection of used climate models (global or regional) and their parameterization and conceptualization (i.e. by way of mathematical description of physical processes in the atmosphere),

2 – selection of climate scenario, but also with the way these scenarios are determined (scenario uncertainty),

3 – by climate model outputs correction using downscaling techniques and bias correction.

In the case of impact studies in the field of water management, it is necessary to take into account the uncertainties arising from the selection of hydrological models and, similarly to climate models, their parameterization and conceptualization.

Models always represent a simplified version of natural processes. All climatic models are based on more or less the same physical principles, but differ in their mathematical expression. Model uncertainties arise from incomplete knowledge of the climate system and from the unlikelihood to include all processes and characteristics of the climate system in models. The same applies to hydrological models, reflecting hydrological processes in river basins. To reduce the degree of uncertainty, climatologists use multi-model ensemble simulations. Different combinations of GCM and RCM are used in regional climate projections resulting in a multi-global/regional-model-ensemble dataset. An example for Europe is the results of the EURO-CORDEX project. Ensemble experiments are a common method of assessing the uncertainties arising from climate change projections (Knutti and Sedlacek, 2013).

We have tried to eliminate uncertainties related to the choice of hydrological models in several ways: First of all, we have tried to use hydrological models that have been and are tested on many river basins in Europe and provide good results. The second method of eliminating the uncertainties was a comparison of statistical characteristics of time series from HYPE and LISFLOOD models for selected Slovak water gauging stations with characteristics from measured time series on an overlapping reference period of 30 years and bias correction of model outputs by variance scaling method. If the results were not satisfactory even after the application of the bias correction, we excluded the models and stations from further analysis, or replaced them with the results from the calibrated HBV model, if these were satisfactory for the reference period.

Other uncertainties may be related to the appropriate choice of the distribution function for the frequency analysis and to the uncertainties of the estimation of the peak flows from the average daily flows (Hlaváčiková et al., 2019).

Results and discussion

The final selection of river basins with the results of the climate change impact on Q_{100}, expressed by the climate change impact CCQ_{100}, which is the percentage change of Q_{100} in the future compared to the present, is shown in Fig. 2 and in Table 2. The results show an increase in Q_{100} for seven stations: Bratislava (Danube), Moravský Sv. Ján (Morava), Liptovský Mikuláš (Váh), Vlkyňa (Slaná), Ipeľský Sokolec (Ipeľ), Streda n. Bodrogom (Bodrog) and Veľké Kapušany (Latorica), in the range of values 5.48–34.12%. A decrease in Q_{100} is indicated for stations Chmeľnica (Poprad), Banská Bystrica (Hron) and Janík (Ida, Bodva river basin) in the range of -17.99 to -47.03%. No significant change in Q_{100} (change of more than ±5%) was found for the Spišské Vlachy (Hornád) station. The most significant increase is indicated for the Liptovský Mikuláš station, where the average impact of climate change CCQ_{100} is +34%, half of the values are in the range of 17–53% (Fig. 3). On the contrary, the most significant decrease is expected in the Bodva river basin (Janík–Ida station), where the impact of climate change CCQ_{100} ranged from -67 to -23% with an average value of -47%.

Uncertainties in estimating the change in Q_{100} can be seen from the interquartile range of average climate change impact factors of the entire CCQ_{100} ensemble for a particular station (Fig. 3). Fig. 3 shows a relatively wide interquartile range of CCQ_{100} for the stations Veľké Kapušany, Ipeľský Sokolec and Chmeľnica, which indicates a greater uncertainty in the estimation of the future Q_{100}. Based on the CCQ_{100} interquartile range (range of values from the 25th to the 75th percentile), it is possible to divide stations into three categories: stations with the least estimation uncertainty in the range of 18–25% (Bratislava, Moravský Sv. Ján, Banská Bystrica, Vlkyňa, Janík), stations with a medium estimation uncertainty in the range of 34–39% (Streda n. Bodrogom, Liptovský Mikuláš, Spišské Vlachy) and stations with the highest estimation uncertainty in the range of 59–91% (Chmeľnica, Ipeľský Sokolec, Veľké Kapušany).

Table 3 shows the number of increases or decreases of CCQ_{100} for individual hydrological models as well as for the whole ensemble. Balanced results for Bratislava and Moravský Sv. Ján are indicated by the similar number of increases, decreases or no change for both hydrological models. Conversely, for Ipeľský Sokolec, Chmeľnica and Veľké Kapušany, one model indicates more increases, while the other indicates more decreases in CCQ_{100}.

Peak flows and their development over time represent important information for changes in high flows. Based on trends, possible future changes in Q_{100} can be expected. It was possible to identify several significant trends in future peak flows from model analyses. An upward trend was identified for one model at Bratislava station, and 3 (4) models at Moravský Sv. Ján and Ipeľský Sokolec, whereby the climate model from the IPSL institute indicated an increase for both hydrological models. No significant trends were identified for the Vlkyňa and Liptovský Mikuláš stations. One or two upward trends were identified at other stations. For Janík and Banská Bystrica stations, upward trends were identified despite the fact that the estimate of the future Q_{100} was lower than the current value. These model outputs suggest that although the peak flows at these stations should be lower in the future, it is possible to expect their increasing trend. Only four downward trends were identified among the ensembles (at the stations Moravský Sv. Ján, Ipeľský Sokolec, Streda n. Bodrogom and Spišské Vlachy). Although several significant trends have been identified, their number within the whole ensemble for a particular station is still relatively small.

More detailed results of climate change impact hydrological modeling for the Banská Bystrica station can be found in the literature Kopáčiková et al. (2019).

With increasing global atmospheric temperature, intense precipitation is expected to strengthen due to the greater capacity of the warmer atmosphere to absorb water vapor. This fact is a common argument used for the automatic assumption that the incidence of floods and high flows will globally increase. Recent European studies suggest that the occurrence of floods and changes in their periodicity and magnitude depend primarily on the geo-

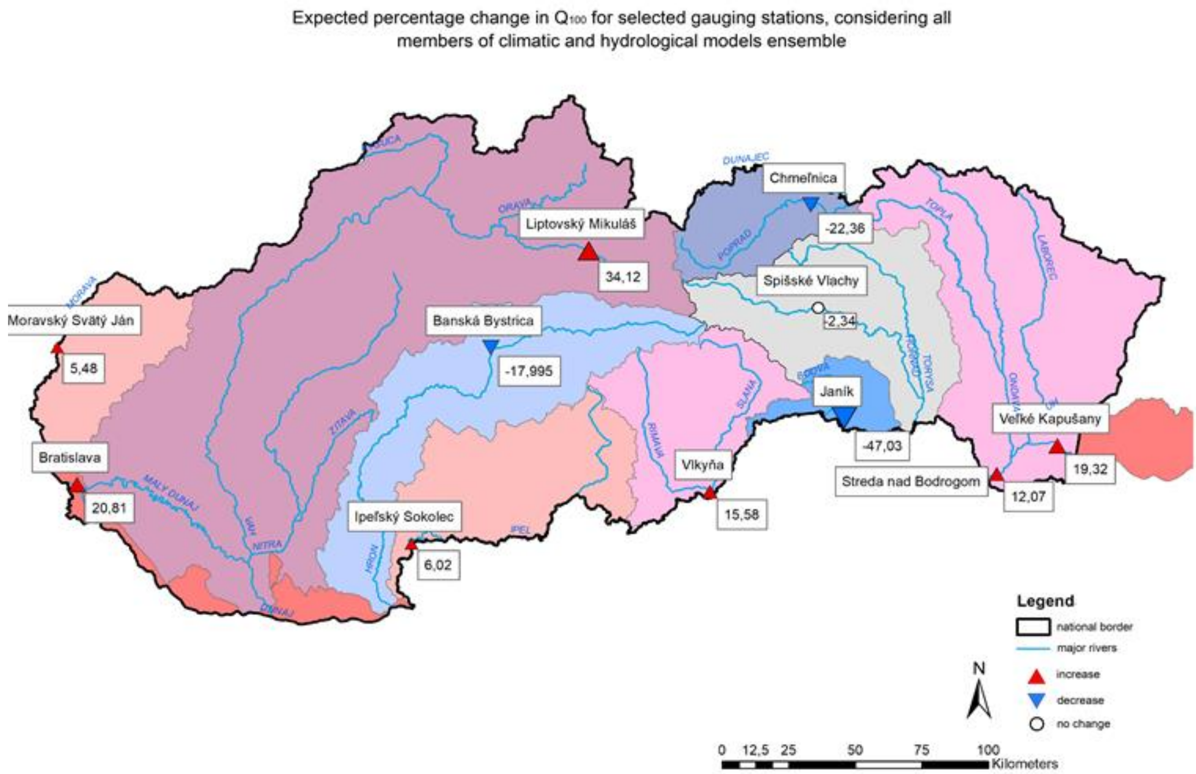

Fig. 2. Location of gauging stations within the territory of Slovakia along with the expected change in Q_{100} expressed by the impact of climate change for Q_{100} (CCQ_{100}) in percent.

Table 2. Data on gauging stations, current and estimated Q_{100} along with the change in Q_{100} expressed by the average climate change impact for Q_{100} (CCQ_{100}). The applied hydrological model for the respective gauge is given in parentheses; the Hype and Lisflood model were used in the other stations

Gauging station	River	Catchment	Catchment area [km^2]	Q_{100} current [$m^3 s^{-1}$]	Q_{100} future [$m^3 s^{-1}$]	CCQ_{100} [%]
Bratislava	Dunaj	Dunaj	131331	11000	13290	20,32
Moravský Sv. Ján	Morava	Morava	24129	1600	1690	5,48
Streda n. Bodrogom	Bodrog	Bodrog	11474	1400	1570	12,07
Ipeľský Sokolec	Ipeľ	Ipeľ	4838	670	710	6,02
Veľké Kapušany	Latorica	Bodrog	2915	736	880	19,32
Banská Bystrica (HBV)	Hron	Hron	1766	540	440	-18,00
Vlkyňa (Lisflood)	Rimava	Slaná	1377	190	220	15,58
Chmeľnica	Poprad	Poprad	1262	820	640	-22,36
Liptovský Mikuláš (HBV)	Váh	Váh	1107	500	670	34,12
Spišské Vlachy (HBV)	Hornád	Hornád	775	400	390	-2,34
Janík (HBV)	Ida	Bodva	378	95	50	-47,03

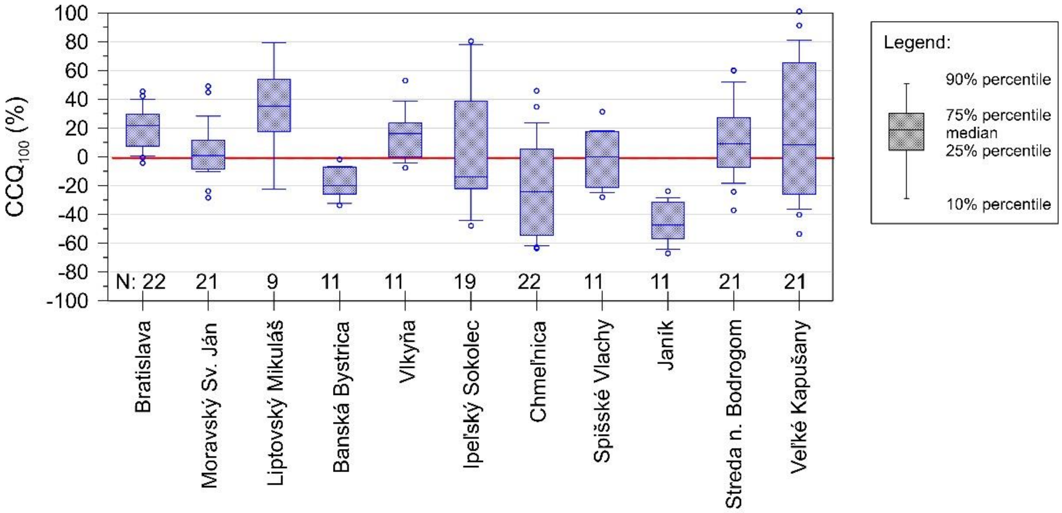

Fig. 3. Box plots showing the variability and extent of the climate change impact for Q_{100} (CCQ_{100}) obtained from ensembles of climate and hydrological models. N is the number of ensemble members used for analysis.

graphical location, the size of the river basin and the conditions under which floods occur (Blöschl et al., 2019). In small river basins, short-term convective precipitation with high intensities is especially important for flood generation. Conversely, in medium-sized and large river basins, longer-lasting synoptic frontal precipitation covering a larger area is crucial. From this point of view, the size of the river basin is a vital information. Also important are changes in water reserves in the snow cover and the period of snow melting, which in combination with liquid precipitation is in the spring period in many river basins a major factor for the occurrence of floods.

This work showed increases in Q_{100} at most stations. Decreases are estimated only at Chmeľnica, Banská Bystrica and Janík stations. The Danube basin (to the gauge in Bratislava) and the Morava river basin (to the gauge Moravský Sv. Ján) are the largest river basins in this study. An increase in Q_{100} is indicated in both stations, although in Moravský Sv. Ján only mild. The estimates of Q_{100} from the members of the ensembles are relatively consistent for both stations, i.e. the variability of the average Q_{100} is satisfactory and the hydrolo-

Table 3. Evaluation of the number of increases, decreases or no change in average CCQ_{100} for individual hydrological models and the whole ensemble of models (highlighted in grey)

	No. of increase (>5%)			No. of decrease (<-5%)			without change (-5% < x <5%)		
gauging station	**HYPE**	**LISFLOOD**	**ansambel**	**HYPE**	**LISFLOOD**	**ansambel**	**HYPE**	**LISFLOOD**	**ansambel**
Bratislava	8	9	17	0	0	0	3	2	5
Moravský sv. Ján	5	5	10	2	5	7	4	1	5
Vlkyňa	-	7	7	-	1	1	-	3	3
Ipeľský Sokolec	8	0	8	0	11	11	3	0	3
Chmeľnica	0	7	7	11	3	14	0	1	1
Streda nad Bodrogom	10	4	14	0	6	6	1	1	2
Veľké Kapušany	10	2	12	0	9	9	1	0	1
	No. of increase (>5%)			**No. of decrease (<-5%)**			**without change (-5% < x <5%)**		
gauging station	**HBV**			**HBV**			**HBV**		
Liptovský Mikuláš	7	-	-	1	-	-	3	-	-
Banská Bystrica	0	-	-	10	-	-	1	-	-
Spišské Vlachy	4	-	-	5	-	-	2	-	-
Janík	0	-	-	11	-	-	0	-	-

gical models give comparable outputs for individual climatic ensembles in terms of the number of increases or decreases. The third largest catchment is the Bodrog catchment (to the gauge Streda n. Bodrogom), where an increase in Q_{100} is also indicated, but data from hydrological models are not completely consistent (HYPE model estimates increases from all 11 members of the ensemble, LISFLOOD model indicates 6 decreases out of 11).

A decrease in Q_{100} was indicated at Banská Bystrica (Hron), Janík (Bodva) and Chmeľnica (Poprad) stations. The uncertainty of the Q_{100} estimation for the Banská Bystrica and Janík stations may be increased due to the fact that only one hydrological model was available for these stations.

Stations with high uncertainty of Q_{100} estimation according to the CCQ_{100} interquartile range 59–91% are Veľké Kapušany (Latorica), Ipeľský Sokolec (Ipeľ) and Chmeľnica (Poprad). A closer analysis of the results from these stations shows that this uncertainty results from the inconsistency of outputs from hydrological models. At the Veľké Kapušany and Ipeľský Sokolec stations, the HYPE model indicates more increases, while LISFLOOD indicates decreases. At the Chmeľnica station, the situation is the opposite, with declines from the HYPE model and increases from the LISFLOOD model prevailing. The choice of hydrological model and the uncertainty associated with it is probably higher in this case than the uncertainty arising from climate models.

Furthermore, another uncertainty in the Q_{100} estimation may be the narrowed ensemble of hydrological models at some stations (Banská Bystrica, Janík, Liptovský Mikuláš, Spišské Vlachy and Vlkyňa). As the outputs from the SWICCA database of hydrological models for the mentioned stations did not meet the required criteria for the reference period, it was necessary to look for an alternative solution in form of the HBV hydrological model. Here, arises a need to verify the estimated Q_{100} by other hydrological models in terms of the ensemble predictions philosophy as it is commonly used in climate models or by another suitable method, e.g. by correcting climatic ensemble data for hydrological data (Hakala et al., 2019).

The catchments with the smallest area are Spišské Vlachy (Hornád) and Janík (Ida, Bodva basin). Depending on the size of the river basin, it would seem that these river basins should provide data with the highest degree of uncertainty. It is true that hydrological data from the SWICCA database (outputs from the LISFLOOD and HYPE models) were not applicable for these river basins, probably also due to the coarse resolution of hydrological models to a small area of these river basins (775 and 378 km^2). However, the calibrated HBV model provided relatively consistent results for the individual climatic ensembles, and according to the CCQ_{100} interquartile range, these two stations are among the stations with the least and medium uncertainty of the Q_{100} estimate.

No significant differences between individual climate scenarios (RCPs) were identified in this work. Probably these were masked by uncertainties related to climatic and hydrological models. This may also be due to the fact that the data period was analysed as a whole (2011–2100) for the purposes of the Q_{100} estimation as opposed to the more typical 30 years sections.

Conclusions

This impact study provides the results of estimating the impact of climate change on Q_{100} for 11 gauging stations in Slovakia. In the first phase of the work, at least 572 time series of average daily flows for 26 stations were analysed. Relationships between peak and maximum average daily flows were derived (Hlaváčiková et al., 2019). For 242 time series, trends were analysed and frequency analysis was performed fitting the GEV distribution function. Data from climate projections as well as from hydrological models available in the SWICCA database were used to analyse the impact of climate change. Such an extensive analysis of data from the C3S database has probably not yet been implemented in Slovakia, despite the fact that some reputable organizations, such as the International Association of Hydrological Sciences (IAHS) recommended it. The results of this work can lead to a discussion regarding the usability of climate data from the C3S database for Slovak river basins, their limits, but also other perspectives.

The results of the whole work can be summarized in several points:

1 – The results indicate an increase in Q_{100} for seven gauging stations: Bratislava (Dunaj), Moravský Sv. Ján (Morava), Liptovský Mikuláš (Váh), Vlkyňa (Slaná), Ipeľský Sokolec (Ipeľ), Streda n. Bodrogom (Bodrog), Veľké Kapušany (Latorica), in the range of percentage change of Q_{100} (CCQ_{100}) 5.48–34.12%. A decrease in Q_{100} is indicated for stations Chmeľnica (Poprad), Banská Bystrica (Hron) and Janík (Ida, Bodva river basin) in the range of -17.99 to -47.03%. For the station Spišské Vlachy (Hornád) no significant change in Q_{100} was indicated (change more than ± 5%),

2 – the largest river basins in the analysis (Danube upto the Bratislava station and Morava upto Moravský Sv. Ján) provided results that fell into the group with the least degree of uncertainty in terms of CCQ_{100} impact variability and had the most consistent results for the two hydrological models used,

3 – the higher estimate uncertainty at stations Veľké Kapušany (Latorica), Ipeľský Sokolec (Ipeľ) and Chmeľnica (Poprad) resulted from conflicting outputs of hydrological models HYPE and LISFLOOD. Here, the use of a larger ensemble of hydrological models should be considered,

4 – the impact of climate change on the smallest river basins Janík (Bodva) and Spišské Vlachy (Hornád) could not be satisfactorily estimated with the hydrological outputs from the SWICCA database probably due to the rough resolution of models in relation to these river basins. The impact of climate change for these river basins was modeled by a calibrated HBV model using climate inputs from the SWICCA database. The impact of climate change for the Hron (Banská Bystrica) and Váh (Liptovský Mikuláš) river basins was estimated in a similar way. We assume that the complex orography and runoff formation in these river basins needs a finer resolution of climatic and hydrological models,

5 – in this work, it was not possible to clearly identify significant differences between individual climate scenarios (RCP) and their impact on Q_{100}. We assume that these were masked by uncertainties carried by climatic and hydrological models themselves.

The advantage of the SWICCA database is the availability of a large number of climatic and hydrological model outputs for a number of European river basins, as well as the latest knowledge on the state of the climate and modelled estimates of its development in one place. Not every user of a hydrological model has all the relevant meteorological data needed to calibrate the hydrological model and climatic data on the future climate. Another advantage is the time saved having ready to use calibrated data from the hydrological model that has been run for individual climatic inputs. The SWICCA database is constantly evolving and supplemented by necessary data. Its ambition is to provide users with a finer resolution of the outputs from the RCM models and to extend the reference period from 30 years to the longest possible period in the past. To achieve this, the necessary climatic and hydrological data in a sufficiently dense network of measurements provided by individual European countries are also indispensable.

The climate change is ongoing and its impacts are visible already. Therefore, an effort is made to best understand the ongoing processes and to use different methods to estimate the final impact of these changes in the field of water management. From this point of view, this work offers possibilities for a promising way in which it is possible to estimate the impact of climate change on extreme flows on the basis of currently available data. There is a strong presumption that the future will require more frequent and in-depth analyses of the impacts of climate change on design high flows, which will need to be taken into account in individual EU countries. That is why we consider this work to be an initial step towards solving this urgent and serious task in Slovakia.

The EU Working Group on Floods (WGF) is currently calling on the professional institutions of all Member States to be involved in addressing the effects of climate change on the occurrence of floods. Interdepartmental, interdisciplinary communication and data exchange is an essential part of mastering this task at both domestic and international levels.

Acknowledgement

We would like to thank several of our colleagues, without whose help this work would not have been completed in the form in which it is presented. For the provision and preparation of historical data needed for analyses we thank to our colleagues from the Department of Quantity of Surface Water at SHMU. We are also grateful to Dr. Kateřina Hrušková and Dr. Marcel Zvolenský for their help at the HBV model calibration and running. We highly appreciate valuable comments of Dr. Oľga Majerčáková. This work was supported by the Slovak Research and Development Agency under the Contract no. APVV-19-0340.

References

Arora, V. K., Boer, G. J. (2001): Effects of simulated climate change on the hydrology of major river basins, Journal of Geophysical research, 106, 3335–3348.

Bertola, M., et al. (2020): Flood trends in Europe: are changes in small and big floods different? Hydrology and Earth

System Sciences, 24, 1806–1822.
Blöschl, G., Kiss, A., Viglione, A. et al. (2020): Current European flood-rich period exceptional compared with past 500 years. Nature, 583, 560–566.
Blöschl, G. et al. (2019): Changing climate both increases and decreases European river floods, Nature, doi.org/10.1038/s41586-019-1495-6.
Blöschl, G. et al. (2017): Changing climate shifts timing of European floods. Science, 357, 588–590.
Burek, P., van der Knojff, J., de Roo, A. (2013): LISFLOOD, Distributed Water Balance Simulation Model. JRC technical report JRC78917, EUR 26162 EN, Revised User Manual, Luxembourg, p. 150.
Coles, S. (2001): An introduction to statistical modelling of extreme values. Springer London. doi: 10.1007%2F978-1-4471-3675-0. ISBN: 9781447136750.
Dakhlaoui, H., Seibert, J., Hakala, K. (2019): Hydrological Impacts of Climate Change in Northern Tunisia, Chaminé, H. I., et al. (eds.), Advances in Sustainable and Environmental Hydrology, Hydrogeology, Hydrochemistry and Water Resources, Advances in Science, Technology & Innovation, Springer Nature Switzerland AG, 301–303.
Donnelly, C., et al. (2017): Impacts of climate change on European hydrology at 1.5, 2 and 3 degrees mean global warming above preindustrial level, Climatic Change, 143, 13–26.
Duethmann, D., Blöschl, G., Parajka, J. (2020): Why does a conceptual hydrological model fail to predict discharge changes in response to climate change? Hydrology and Earth System Sciences, 24, 3493–3511.
Fendeková, M., Poórová, J., Slivová, V., (Eds.) (2017): Hydrologické sucho na Slovensku a prognóza jeho vývoja. Vydavateľstvo Univ. Komenského v Bratislave, ISBN 978-80-223-4398-5 (in Slovak with English summary).
Gaál, L. (2018): Flood Warnings in a Changing Climate. Full Technical Report, Copernicus Climate Change Servis, p. 19. Available at (7-12-2018): http://swicca.climate.copernicus.eu/wp-content/uploads/Full-Technical-Report-SWICCA-MicroStep-MIS_checked.pdf
Gaál, L., Lešková, D., Kopáčiková, E. (2017): Changes in the 100-year flood at the Danube River in Bratislava due to the expected climate change. Acta Hydrologica Slovaca, 18(2), 154–164 (in Slovak with English abstract and summary).
Gao, Ch., Booij, M. J., Xu, Y. P. (2020): Assessment of extreme flows and uncertainty under climate change: disentangling the contribution of RCPs, GCMs and internal climate variability, Hydrology and Earth System Sciences, doi.org/10.5194/hess-2020-25.
Gilleland E., Katz R. W. (2016): extRemes 2.0: An Extreme Value Analysis Package in R. Journal of Statistical Software, 72(8), 1–3.
Gonzáles-Zeas, D. et al. (2012): Improving runoff estimates from regional climate models: a performance analysis in Spain, Hydrology and Earth System Sciences, 16, 1709–1723.
Greuell, W. et al. (2015): Evaluation of five hydrological models across Europe. Hydrology and Earth System Sciences, 12, 10289–10330.
Gupta, H. V. et al. (2009): Decomposition of the mean squared error and NSE performance criteria Implications for improving hydrological modelling. Journal of Hydrology, 377, 80–91.
Hakala, K. et al. (2019): Hydrological modeling of Climate Change Impacts. Encyclopedia of Water: Science, Technology, and Society, Maurice, P. A. (ed.), Wiley & Sons, DOI: 10.1002/9781119300762.wsts0062
Hirabayashi, Y. et al. (2013): Global flood risk under climate change, Nature Climate Change, 3, 816–821.
Hlaváčiková, H., Bírová, M., Kopáčiková, E. (2019): Estimation of instantaneous peak flows from mean daily flows. Acta Hydrologica Slovaca, 20(1), 3–9 (in Slovak with English abstract and summary).
Hundecha, Y. et al. (2016): A regional parameter estimation scheme for a pan-European multi-basin model. Journal of Hydrology: Regional Studies, vol. 6, 90–111.
Huntington, T. G. (2006): Evidence for intensification of the global water cycle: Review and synthesis, Journal of Hydrology, 319 (1–4), 83–95.
IMPACT2C (2015): Quantifying projected impacts under 2°C warming, D6.1 Maps showing the climate change impacts, at 1.5 and 2°C For the Water, Energy, and Tourism each sector and for coastal impacts, FP7-ENV.2011.1.1.6-1, Wageningen University.
IMPACT2C (2014): Quantifying projected impacts under 2°C warming, Deliverable D4.1, Report on requested meteorological data and climate change indicators, Project FP7-ENV.2011.1.1.6-1, KNMI.
IPCC Climate Change (2014): Synthesis Report. Contribution of Working Groups I, II and III to the Fifth Assessment Report of the Intergovernmental Panel on Climate Change, IPCC, Geneva, Switzerland, doi: 10.1017/CBO9781107415324.
Knutti, R., Sedlacek, J. (2013): Robustness and uncertainties in the new CMIP5 coordinated climate model projections. Nature Climate Change, 3, 369–373.
Kopáčiková, E., Hlaváčiková, H., Lešková, D., Hrušková, K., (2019): Copernicus Climate Change Service a jej využitie pre odhad vplyvu klimatickej zmeny na návrhové storočné prietoky. In Zborník s príspevkami z konferencie Manažment povodí a extrémne hydrologické javy 2019, Vyhne 8.-9.10.2019. Združenie zamestnávateľov vo vodnom hospodárstve na Slovensku (in Slovak with English abstract)
Krajewski, A., Sikorska-Senoner, A., Ranzi, R., and Banasik, K. (2019): Long-term changes of hydrological variables in a small lowland watershed in central Poland. Water 11(3), 564, doi:10.3390/w11030564.
Milly, P. C. D et al. (2008): Stationarity is dead: Whither water management? Science, 319(5863), 573–574, doi:10.1126/science.1151915.
Nash, J. E., Sutcliffe, J. V. (1970): River flow forecasting through conceptual models: Part 1. A discussion of principles. Journal of Hydrology, 10(3), 282–290.
Nijssen, B. et al. (2001): Hydrologic Sensitivity of Global Rivers to Climate Change, Climate Change, 50, 143–175.
OTN ŽP 3112-1:03 (2003): Hydrologické údaje povrchových vôd. Kvantifikácia povodňového režimu. Časť 1: Stanovenie N-ročných prietokov a N-ročných prietokových vĺn na väčších tokoch (in Slovak)
Pekárová, P., Garaj, M., Pekár, J., Miklánek, P. (2018): Long-term development of hydrological balance In the Topľa basin in 1961–2015. Acta Hydrologica Slovaca, 19(1), 17–26 (in Slovak with English abstract and summary).
Roudier, P. et al. (2016): Projections of future floods and hydrological droughts in Europe under a +2°C global warming. Climatic Change, 135(2), 341–355.
Stahl, K. et al. (2010): Streamflow trends in Europe: evidence from a dataset of near-natural catchments, Hydrological Earth System Sciences, 14, 2367–2382.
Teutschbein, C. (2013): Hydrological Modeling for Climate Change Impact Assessment: Transferring Large-Scale Information from Global Climate Models to the Catchment Scale. Doctoral Dissertation, Stockholm University, Faculty of Science, Department of Physical Geography and Quaternary Geology, p. 44, ISBN: 978-91-7447-622-4.
Teutschbein, C., Seibert, J. (2012): Bias correction of regional

climate model simulations for hydrological climate-change impact studies: Review and evaluation of different methods. Journal of Hydrology, 456–457, 12–29.
Teutschbein, C., Seibert, J. (2010): Regional Climate Models for Hydrological Impact Studies at the Catchment Scale: A Review of Recent Modelling Strategies. Geography Compass, 4(7), 834–860.
Van Vuuren, D.P. et. al. (2012): A proposal for a new scenario framework to support research and assessment in different climate research communities. Global Environmental Change 22 (1), 2135.
Wilcke, R.A.I. et al. (2013): Multi-Variable Error Correction of Regional Climate Models. Climatic Change, 120 (4), 871–887.

Ing. Eva Kopáčiková
Ing. Hana Hlaváčiková, PhD. (*corresponding author: hana.hlavacikova@shmu.sk)
Ing. Danica Lešková, PhD.
Slovenský hydrometeorologický ústav
Jeséniova 17
833 15 Bratislava 37
Slovak Republic

DOI: 10.31577/ahs-2020-0021.02.0021

ACTA HYDROLOGICA SLOVACA

Volume 21, No. 2, 2020, 172 – 177

COMPARISON OF THE VARIANCES OF A LUMPED AND SEMI-DISTRIBUTED MODEL PARAMETERS

Adam Brziak*, Martin Kubáň, Silvia Kohnová, Ján Szolgay

The accurate modelling of discharges in catchments plays an important role in solving a large variety of water management tasks. Three basic errors may affect the outputs modelled: the quality of the input data, uncertainities about the parameters, and the structure of the model. This paper is focused on a comparison of the performances of the lumped and semi-distributed versions of the conceptual TUW rainfall-runoff model, which represents two different model structures. The comparison took place on 180 Austrian catchments, which have variable morphologies, altitudes, land uses, etc. We focused on the variability of the efficiencies and parameters of both types of HBV models, which were calibrated based on discharges in the period from 1991 to 2000. Whether the morphology and mean elevation of the catchment affect the calibration results was also take in account. Finally, we realized that the semi-distributed version of the TUW model gave better results as to the calibration efficiencies, when we calibrated the model for discharges; at the same time, the variations in the model parameters also gave better results in the semi-distributed version of the TUW model.

KEY WORDS: HBV model, model parameters, model efficiency, Austrian catchments

Introduction

Hydrological models are a useful tool for estimating various hydrological phenomena. Due to the continuing development of computer technologies in recent decades, models have become an important tool in hydrology and water management practice (Jeníček, 2012). However, with the increasing number of hydrological models, there is an ongoing problem concerning the right choice of the type of the model. Many authors have discussed this problem, see (e.g. Jeníček, 2005; Beven and Freer, 2001; Buchtele, 2002; Kulhavý and Kovař, 2002; Bergström, 1995, etc.).
Hydrological modelling involves multiple steps, each of which can be associated with uncertainties in the calibration of the model. There are three main errors, i.e., the model´s structure, uncertainties about the parameters, and uncertainties about the input data, that influence the correct selection and operation of the model. In our study, we compared two types of HBV models with different structures to determine which model structure better fits the selected region. We have also focused on the hypsometric characteristics of the catchments and how they affect the calibration of lumped and semi-distributed rainfall-runoff models.
In this paper, we calibrated the conceptual lumped version of the "Technische Universität Wien" (TUW model) and the dual-layer semi-distributed TUW model. We calibrated the models for the instrumental period of 1991–2000. We have compared the efficiencies between the lumped and semi-distributed versions of the TUW model, and we also observed the variances in the parameters and how the hypsometric characteristics of the catchments affect the results of the calibration.

Methods

In the study, we applied the two types of HBV model, i.e., the lumped TUW model and the semi-distributed TUW model (Parajka et al., 2007; 2009). The main difference between the lumped and semi-distributed versions is that the inputs in the semi-distributed version are divided into 200-meter hypsometric zones (1. Zone 0–200 m a.s.l., 2. Zone 200–400, etc.). In Fig. 1 we can observe the structure of the TUW model.
The TUW rainfall-runoff model is frequently used for solving many hydrological problems (e.g., flood predictions, estimations of droughts, or duration of floods). Input data for rain, the air temperature, and potential evapotranspiration were used to calibrate both models. The model consists of three submodels: a snow submodel, a soil submodel, and a runoff formation submodel. The snow submodel simulates the accumulation of water from melted snow and contains the following parameters: snow correction factor-(SCF), degree day factor-(DDF), and threshold temperature limits for rain-(Tr), snow-(Ts), and melting snow-(Tm). The soil submodel simulated the processes in the soil part of

the catchment. This submodel contains the following parameters: limit of potential evaporation-(Lprat), field capacity-(FC), and (BETA)-non-linear parameter for the formation of runoff (Table 1).
The runoff formation submodel simulated the surface and underground runoff. This submodel contains the following parameters: (K0, K1, and K2): parameters for the surface, underground and base runoff; (Bmax)-maximum base at low flows; (Lsuz)-threshold for the storage state, i.e., the very fast response start if the Lsuz is exceeded; and the (Croute)-free scaling parameter. The Deoptim differential evolution algorithm (Sleziak et. al., 2017), was used for the calibrations in this work. The range of the model for the parameters was estimated by Merz (Merz et al., 2011) using a daily time step.

Input data

The calibration was run on the 180 catchments selected for the whole territory of Austria. The catchment areas varied from 14.2 km^2 to 6214 km^2. The runoff in these catchments is not affected by dams, canals, or any other transformations from another catchment. For the lumped TUW model version we used input data (rainfall, runoff, potential evaporation, air temperature) in daily time steps from the period 1.1.1991 to 31.12.2000. These data were interpolated from measurement stations across Austria (Sleziak et al., 2017). The rainfall data were interpolated from 1091 stations by the method of external drift kriging. The runoff data were from 180 gauged stations (Austrian Hydrographical Service). The potential evapo-

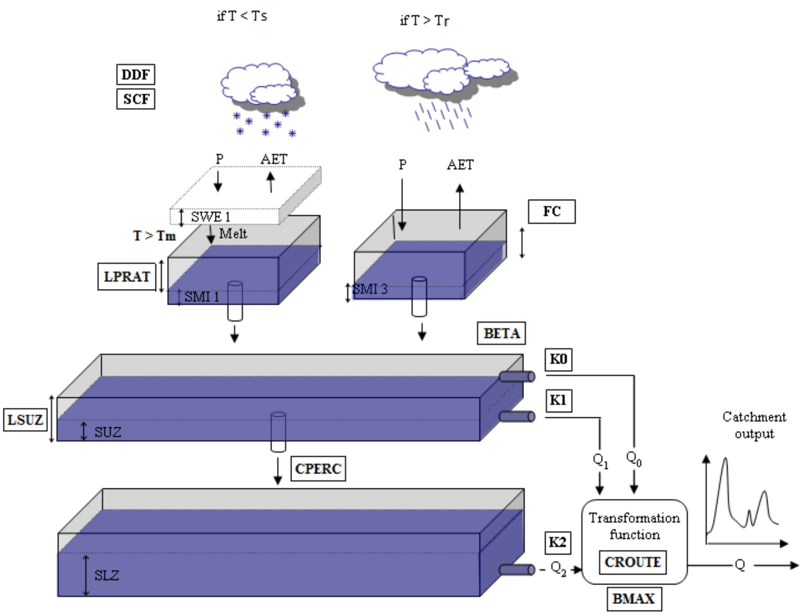

Fig. 1. Schematic description of the TUW model (Sleziak, 2017).

Table 1. TUW model parameters (Merz et al. 2011)

Abbreviations	Description of the model parameters	Range
1. SCF	snow correction factor	0.9–1.5 [-]
2. DDF	degree day factor	0.0–5.0 [mm degC^{-1} day^{-1}]
3. Tr	threshold temperature above which precipitation is rain	1.0–3.0 [degC]
4. Ts	threshold temperature below which precipitation is snow	-3.0–1.0 [degC]
5. Tm	threshold temperature above which melting starts	-2.0–2.0 [degC]
6. Lprat	parameter related to the limit for potential evaporation	0.0–1.0 [-]
7. FC	field capacity, i.e., max soil moisture storage	0–600 [mm]
8. BETA	the non-linear parameter for runoff production	0.0–20.0 [-]
9. K0	storage coefficient for a very fast response	0.0–2.0 [days]
10. K1	storage coefficient for a fast response	2.0–30.0 [days]
11. K2	storage coefficient for a slow response	30.0–250 [days]
12. lsuz	threshold storage state, i.e., start of the very fast response if exceeded	1.0–100 [mm]
13. cperc	constant percolation rate	0.0–8.0 [mm day^{-1}]
14. bmax	maximum base at low flows	0.0–30.0 [days]
15. croute	free scaling parameter	0.0–50.0 [days^2 mm^{-1}]

ration data were calculated with the Blaney-Criddle method (Parajka, 2009).
The rainfall and air temperature input data for the semi-distributed TUW model version were from the Spartacus database (Hiebl et al., 2016) and were interpolated into the hypsometric zones by 200 vertical meters, also potential evaporation was calculated with the Blaney-Criddle method in hypsometric zones by 200 m. The runoff data were the same as the input data for the lumped TUW model version; we used the discharge data from the 180 gauged stations, which were provided by the Austrian Hydrographical Service. The calibration period was set for the period 1991–2000 because of a data overlap.
For a better comparison of the results, we finally divided the catchments into two groups (Sleziak, 2017). The first group includes catchments where the major contributor to the runoff is water from rain; this group we called the "Lowland" type. The second group includes catchments where there is a significant part of runoff from water from melted snow or glaciers; we called it the "Alpine type". In Fig. 2 we can observe selected catchments, divided by hypsometric characteristics.

Results and discussion

One of the major difficulties of calibrating rainfall-runoff models is that these models generally have a large number of parameters that cannot be directly obtained from measurable quantities of catchment characteristics; this is especially true when we have a large area of interest or want to calibrate more catchments at the same time. This is why we focused on comparing the variability in parameters between both the lumped and semi-distributed versions of the TUW model. We compared all 15 model parameters. In Fig. 3 we can see the variance in the parameters that affect the snow submodel of the TUW model. As can be seen, the semi-distributed version of the model gives us better results with regard to the parameter variances.
Fig. 4 represents the variance in parameters that affect the soil submodel of the TUW model. We can again observe that the variance of the semi-distributed model is smaller and that the model gives us better results than the lumped version of the TUW model.
In Fig. 5 we can observe the differences in the values of the parameter variances of the flow submodel. However, we can observe that parameters K1 (the storage coefficient for a fast response) and croute (free-scaling parameter) give us better results in the lumped version of the TUW model. The other five parameters showed less variance in the semi-distributed version of the TUW model as in the snow and soil submodels.
The objective function was used to select the best set of the parameters. Nash-Sutcliffe efficiency (NSE) and Nash-Sutcliffe efficiency logarithm (logNSE) criteria were used to determine the runoff model efficiency (RME) of the model´s performance. NSE is sensitive to high peaks, log NSE for lower discharges, and the RME represents the average of NSE and log NSE.
In Table 2, we can see the RME results, which show that the semi-distributed version of the TUW model gives us better results for the calibration efficiencies, due to the hypso-metric characteristics of the catchments. We can observe that the average improvement in RME is 0.137 in the Alpine catchments and 0.119 in the lowland catchments.
Fig. 6 represents the spatial distribution of the catchments; the circles represent catchments with lowland characteristics, and the triangles represent catchments with Alpine characteristics. As can be seen, the red colour points are catchments with a RME value lower or equal to 0.60, and the green points are catchments with a RME value higher than 0.60.

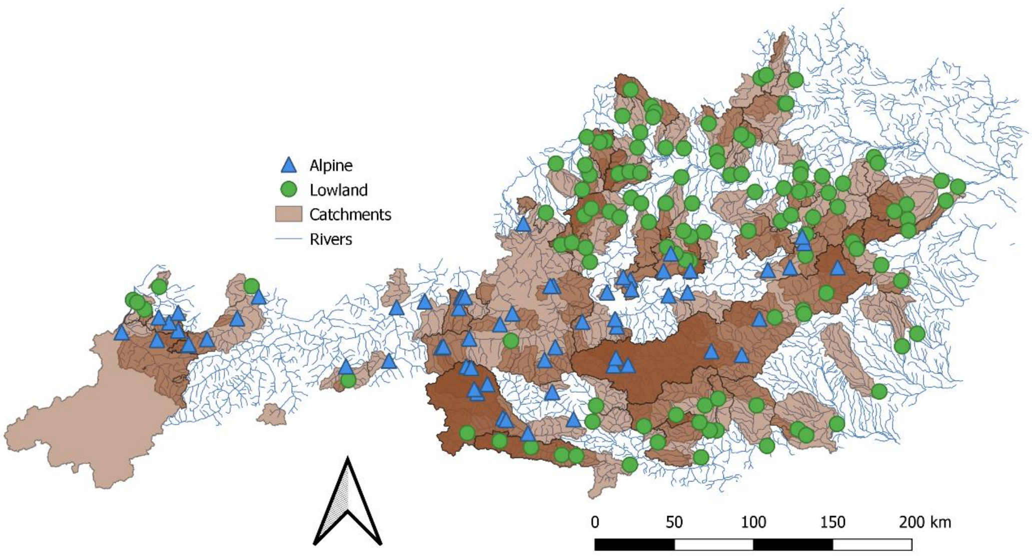

Fig. 2. Selected Austrian catchments, Blue – alpine, and green – lowland catchments.

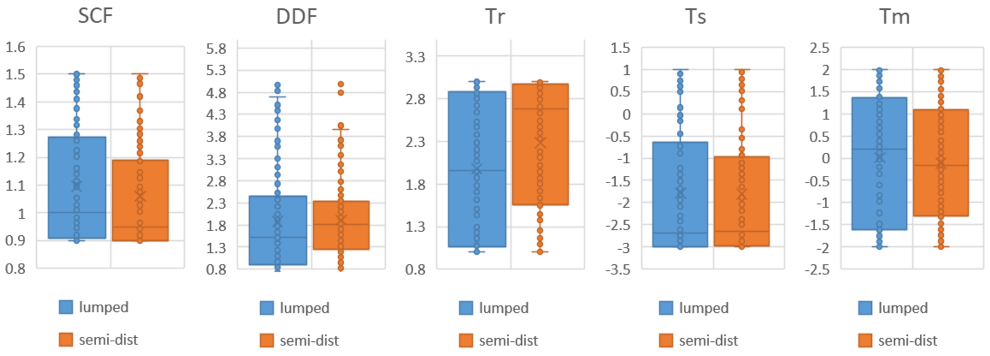

Fig. 3. The variance in parameters belonging to the snow submodel.

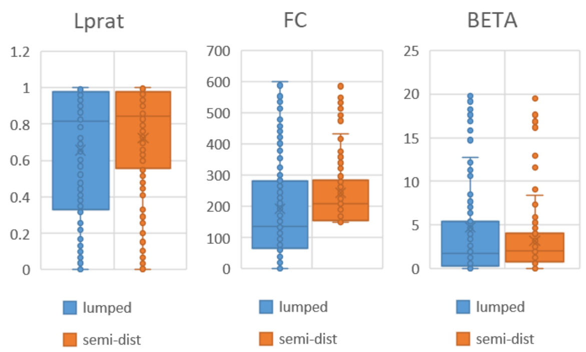

Fig. 4. The variance in parameters belonging to the soil submodel.

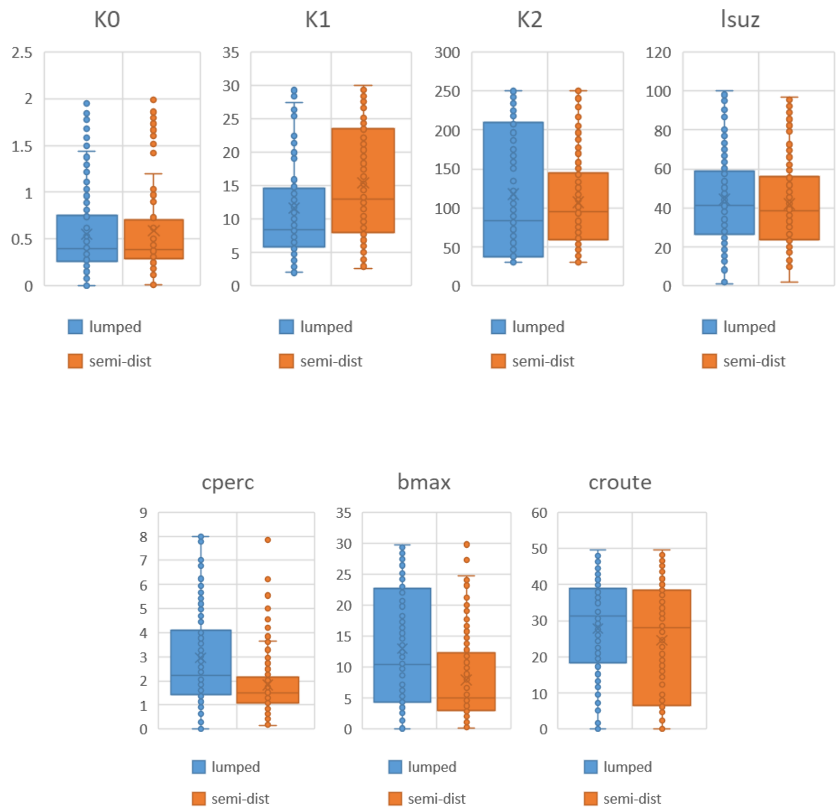

Fig. 5. The variance in parameters belonging to the flow submodel.

Table 2. **Results of the calibration efficiencies**

180 catchments (1991-2000)	Lumped	Semi-distributed
RME median	0.650	0.787
RME median Alpine	0.673	0.833
RME median Lowland	0.642	0.761

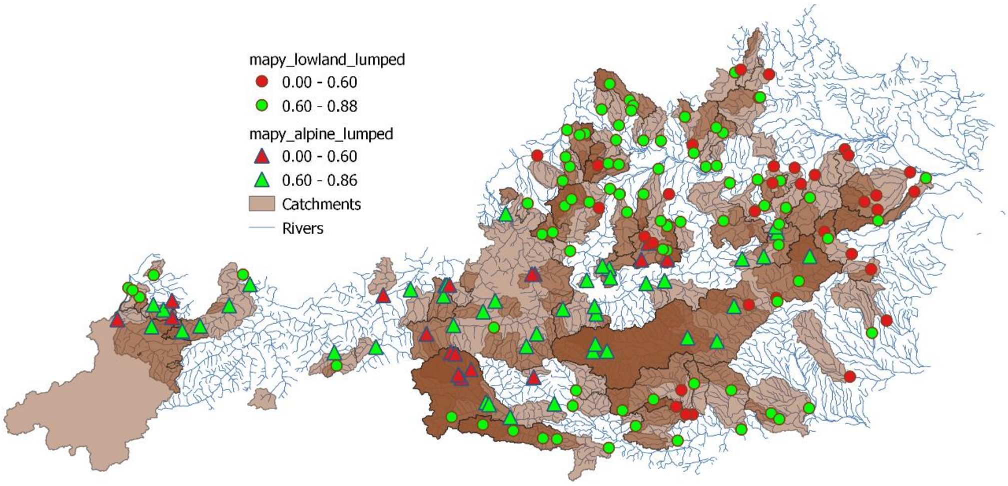

Fig. 6. Results of the calibration efficiencies, circles – lowland catchments, triangles – alpine catchments, RME ≤ 60 => red, RME > 60 => green colour

Conclusion

In this study, we focused on the calibration of two versions of the TUW model. We tested the performance of both models on 180 Austrian catchments in which discharges are not affected by hydraulic structures or other anthropogenic impacts. After the calibration of the model, we compared three indicators of the model´s performance:

- Model efficiencies
- Parameter ranges
- Differences in model efficiencies due to hypsometric characteristics.

We determined that the semi-distributed version of the TUW model gave better results for all the criteria tested. We achieved better results in the model efficiencies and parameter resolutions, and we also determined that the semi-distributed version provided better modelling results in the Alpine (79%) catchments rather than the lowlands (65%). The main reason could be in the spatial distribution by elevation zones of the semi-distributed model, which provided a better and more detailed resolution of the input data than the input data in the lumped version of the model.
Due to the results achieved, we recommend the use of the semi-distributed version of the TUW model in this geographical area. In the future we plan to focus on the performance of the model in the validation period.

Acknowledgment

This work was supported by the Slovak Research and Development Agency under Contract No. APVV-19-034 and the VEGA Grant Agency No. 1/0632/19. This work has been supported in the frame of the AlpCarp Project No. 2019-10-15-002 under the bilateral program "Action Austria–Slovakia, Cooperation in Science and Education". The authors thank the agency for its research support.

References

Beven, K. J., Freer, J. (2001): "A dynamic TOPMODEL", Hydrol. Process. 15, 1993-2011, DOI: 10.1002/hyp.252.

Bergström, S. (1995) The HBV model. In: Singh V.P. (ed.), Computer Models in Watershed Hydrology. Water Resources Publications, Highland Ranch, CO, USA, 443–476. ISBN 0-918334-91-8.

Buchtele, J. (2002): Okolnosti ovlivňující využití modelů a tendence v uplatňování různých přístupů. In Patera, A. et al.: Povodně: prognózy, vodní toky a krajina ČVUT, Praha. 51–55.

Hiebl, J., Frei, C. (2016): Daily precipitation grids for Austria since 1961, development and evaluation of spatial dataset for hydroclimatic monitoring and modelling. Theoretical and Applied Climatology 124, 161–178, doi:10.1007/s00704-015-1411-4

Jeníček, M. (2012): Klasifikace hydrologických modelů. Accessed on: 16.2.2012, Available at: https://is.muni.cz/

el/1431/podzim2014/Z0059/um/hydromodelovani_cleneni_modelu.pdf
Jeníček, M. (2005): Možnosti využití srážkovo-odtokových modelů na malých a středně velkých povodích. In Langhammer, J (ed.): Vliv změn přírodního prostředí povodí a údolní nivy na povodňové riziko. PřF UK, Prague, 112–126.
Kulhavý, Z., Kovář, R. (2002): Využití modelů hydrologické bilance pro malá povodí, VÚMOP, Prague, p. 123.
Merz, R., Parajka, J., Blöschl, G., (2011): Time stability of catchment model parameters: Implications for climate impact analyses, Water Resour. Res., 47, W02531, doi: 10.1029/2010WR009505.,
Parajka, J., Merz, R., Blöschl, G. (2007): Uncertainty and multiple calibration in regional water balance modelling case study in 20 Austrian catchments (Neistota a viacnásobná kalibrácia v modelovaní regionálnej vodnej bilancie v 320 rakúskych povodiach. Hydrol. Process., 21, 423–446. Doi: 10.1002/hyp.6253.
Parajka, J., Naiemi, V., Blöschl, G., Komma, J., (2009): Matching ERS scatterometer based soil moisture patterns with simulation of a conceptual dual layer hydrologic model over Austria Hydrol.Earth Syst. Sci. 13, 259–271.
Sleziak, P., Hlavčová, K., Szolgay, J., Parajka, J., (2017): Dependence of the quality of runoff-simulation by a rainfall-runoff model on the differences in hydroclimatic conditions of calibration and validation period. Acta Hydrologica Slovaca. 18, 1, 23–30.
Sleziak, P., Hlavčová, K., Szolgay, J., Parajka, J., (2017): Závislosť kvality simulácie odtoku pomocou zrážkovo-odtokového modelu od rozdielnosti hydro-klimatických podmienok kalibračného a validačného obdobia. [Dependence of the quality of runoff-simulation by a rainfall-runoff model on the differences in hydroclimatic conditions of calibration and validation period] Acta Hydrologica Slovaca. 18, 1, 23–30.

Ing. Adam Brziak (* corresponding author, e-mail: adam.brziak@stuba.sk)
Ing. Martin Kubáň
Prof. Ing. Silvia Kohnová, PhD.
Prof. Ing. Ján Szolgay PhD.
Department of Land and Water Resources Management
Faculty of Civil Engineering
Slovak University of Technology
Radlinského 11
810 05 Bratislava
Slovak Republic

DOI: 10.31577/ahs-2020-0021.02.0022

ACTA HYDROLOGICA SLOVACA

Volume 21, No. 2, 2020, 178 – 187

DIFFERENCES IN THE LONG-TERM REGIME OF EXTREME FLOODS USING SEASONALITY INDICES AT SLOVAK DANUBE RIVER TRIBUTARIES

Dana Halmová*, Pavla Pekárová

The issue of seasonality occurrence of hydrological, hydrogeological or meteorological phenomena and their regional expression has recently devoted increasing attention. The results of some analyses suggest that the seasonality of the selected hydrological characteristics is an important indicator of flood processes, but varies considerably in space. The seasonality of extreme flood events and, hence flood processes, tends to change with the flood magnitude. Investigation of changes in the rainfall-runoff regimes of rivers and its extremes has become more important especially in the context of ongoing and future climate changes.

This paper deals with a statistical analysis of changes in the hydrological regime of Slovak tributaries of the Danube River at 11 stations and the main objective of this study is to find the seasonality indices. Monthly seasonality indices are analysed to interpret the long-term climatic behaviour, while the seasonality of extremes is analysed to understand flood occurrence. For the extreme events seasonality analyses we used the Burn index (1997), which shows the mean date and variability of occurrence of the extreme events.

KEY WORDS: intra-annual flow regime, seasonality, variability, Burn index, daily and monthly discharge, Slovak Danube River tributaries

Introduction

The term seasonality in hydrology, but also hydrogeology means a regular cyclical change of the evaluated element during one hydrological year; in hydrology we mean, for example, water level or flow. In hydrology, several domestic and foreign authors have addressed the issue of seasonal flows (minimum or maximum), (e.g. Parajka et al., 2008; Burn, 1997; Laaha and Blöschl, 2006; Villarini, 2016; Villarini et al., 2011).

The seasonality of hydrological characteristics is one of the key factors controlling the development and stability of natural ecosystems. From a hydrological perspective, seasonality analysis of runoff and precipitation is an appealing method for inferring flood generation mechanisms, which, in turn, supports other hydrological applications, such as hydrological regionalisation. Recently, the assessment of hydrological seasonality and regime stability has attracted a renewed interest, especially in connection with water resources management, engineering design and land cover and climate change assessment studies (e.g. Krasovskaia and Gottschalk, 2002; Bower et al., 2004; García and Mechoso, 2005; Blahušiaková, Matoušková, 2012; 2015; 2016; Milano et al., 2015).

The seasonality of the hydrologic characteristics is characterised by two indices. The first one describes the seasonality of mean monthly precipitation and runoff and is quantified by the Pardé coefficient, as an index defined for each month of the year (Halmová and Pekárová, 2020). The second index describes the seasonality of the maximum annual floods and annual maxima of daily precipitation, respectively. It is based on Burn's index (1997), which indicates the mean date and variability of occurrence of the extreme events. The mean date of occurrence (D) at a given site is obtained following a transformation of the dates of the occurrence – D_i of the event in the i-th year of observation to the directional statistics, where D_i is expressed as Julian date (D_i=1 for January 1st, and D_i=365 for December 31st). The dates of occurrence D_i are represented in polar coordinates as vectors of unit lengths and of direction given by (4).

- The average direction Θ is calculated as the average of the projections of the individual vectors D_i to the x and y axis, respectively.
- The length of the mean vector r represents the variability of the date of occurrence (5). It ranges from r=0 (uniform distribution around the year) to r=1 (all extreme events of precipitation or floods occur on the same day).

The main objective of this study is to analyse the changes in seasonality of the maximum annual floods of the selected Slovak rivers in the Danube Basin and its changes during the time period 1956–2015. We based the analysis on data of average daily flows from selected stations for the period 1931–2015.

Material and Methods

For studying of the natural runoff variability in any of the river gauging stations, existence of the long term reliable river discharge observations is inevitable. Detailed daily discharges are available at Slovak water gauging stations, but the size of the river basins is different. Selected Slovak water gauging stations (T13–T23; Table 1) at Danube tributaries are described in more details in Halmová and Pekárová (2020) and describe on Fig. 1.

Maximum annual flood seasonality analysis according to Burn index

The seasonality-index according to Burn (Burn, 1997; Parajka et al., 2009) allows to estimate the date and probability of the occurrence of a (flood or low-flow) extreme in the calendar year. The result is the most probable date of the occurrence of an extreme event along with the stability-index $\bar{r}$ (expressing the probability, which the event will actually occur on this day).

For the purposes of the calculation D_i is defined as the date of the occurrence of the *i*-th event in the Julian calendar, with D=1 standing for 1 January and D=366 for 31 December. D is to be understood as polar coordinates on the unit circle with the angle θ. The direction of the mean vector of all events gives the mean date of the occurrence *MD*, and the length r of the mean vectors is a measure of the variability of the date of the occurrence. Values of $\bar{r}$ range between 0 (events occur with equal probability on all days of the year) and 1 (all events occur on one single day in the year).

MD and $\bar{r}$ are calculated with the following formulas:

$$\theta_i = D_i\left(\frac{2\pi}{366}\right), i = 1, n \tag{1}$$

$$\bar{x} = \frac{1}{n}\sum_{i=1}^{n}\cos(\theta_i),\ \ \bar{y} = \frac{1}{n}\sum_{i=1}^{n}\sin(\theta_i) \tag{2}$$

$$\bar{\theta} = \tan^{-1}\left(\frac{\bar{y}}{\bar{x}}\right) \tag{3}$$

$$MD = \bar{\theta}\,\frac{366}{2\pi} \tag{4}$$

$$\bar{r} = \sqrt{\bar{x}^2 + \bar{y}^2} \tag{5}$$

The mean date of occurrence D is then obtained using the inverse form of (4).

It should be noted that the exact-to-the-day dates that result from the Burn test have a more orientation character against the background of a probability statement and should not be misinterpreted as a true or exact predicted value/prediction.

Results

Flood seasonality along the Danube River and its tributaries

To understand the reasons for the spatial and temporal patterns of flood seasonality, it is helpful to apply the concept of disposition: The flood favouring conditions can be classified into two dispositions: The basis disposition, and the variable disposition. The basic disposition represents literally invariable conditions like catchment shape, location in a climate zone, or river morphology. In contrast, the variable disposition comprises of changeable conditions like sum

Table 1. List of selected stations on the Danube River, *Qa* – mean annual discharge, *V* – annual runoff volume, *R* – runoff depth, period 1931–2005

	RIVER	PROFILE	COUNTRY	AREA [km^2]	LAT	LONG	ALTITUDE [m a.s.l.]	Q_a [m^3 s^{-1}]	V 10^9 [m^3 y^{-1}]	R [mm y^{-1}]
T13	Morava	Mor.Sv.Ján	SK	24129	48.60	16.94	146.0	107.6	3.39	141
T14	Belá	Podbanské	SK	93	49.14	19.90	922.7	3.0	0.09	1017
T15	Váh	L. Mikuláš	SK	1107	49.09	19.61	568.0	20.6	0.65	586
T16	Váh	Šaľa	SK	11218	48.16	17.88	109.0	145.7	4.60	410
T17	Hron	B. Bystrica	SK	1766	48.73	19.13	334.0	24.5	0.77	437
T18	Hron	Brehy	SK	3821	48.41	18.65	195.0	47.2	1.49	390
T19	Kysuca	Kysucké N. Mesto	SK	955	49.30	18.79	346.0	16.4	0.52	542
T20	Topľa	Hanušovce	SK	1050	49.03	21.50	160.4	8.0	0.25	239
T21	Krupinica	Plášťovce	SK	303	48.16	18.96	139.5	2.0	0.06	208
T22	Ipeľ	Holiša	SK	686	48.30	19.74	172.0	3.1	0.10	144
T23	Nitra	Nitrianska Streda	SK	2094	48.30	18.10	158.3	14.7	0.46	221

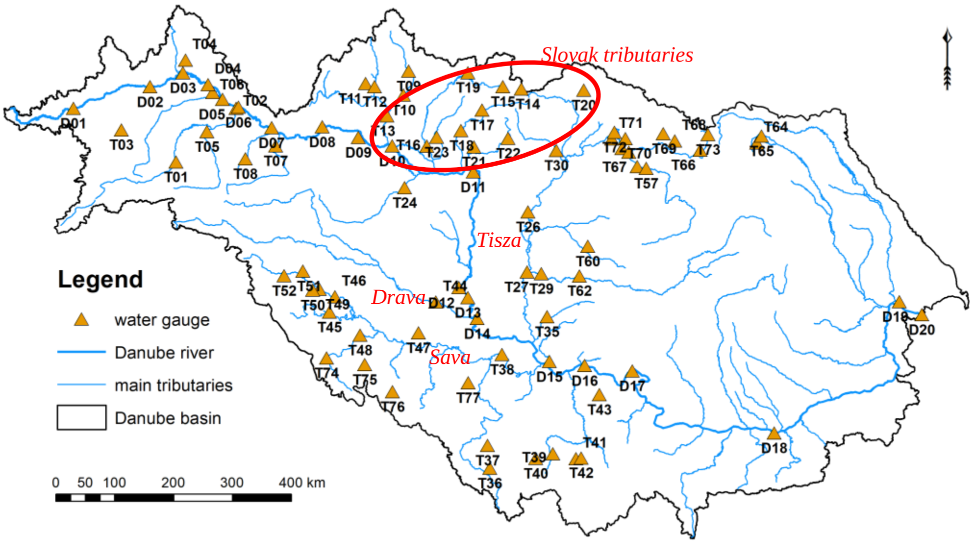

Fig. 1. Water gauges on the Danube River and on the Danube tributaries. (The Slovak tributaries are indicated graphically: T13–Morava, Moravský sv. Ján, T14–Belá, Podbanské, T15–Váh, Liptovský Mikuláš, T16–Váh, Šaľa, T17–Hron, Banská Bystrica, T18–Hron, Brehy, T19–Kysuca, Kysucké N. Mesto, T20–Topľa, Hanušovce, T21–Krupinica, Plášťovce, T22–Ipeľ, Holiša, T23–Nitra, Nitrianska Streda).

or time distribution of precipitation, or storage level. The higher the total disposition level rises, the likelier a triggering event (rainfall) can cause an extreme event like a flood. In the case of Danube River basin, different climate zones and mountain areas contribute to the basic disposition, and glaciermelt, snowmelt, or regular rainfalls contribute to an increase of the variable disposition. That is the reason for floods to occur typically during months with high runoff, hence high river water levels and likely filled water storages within the landscape.

For calculation of the Burn indexes, the mean daily discharge time series were used. Figure 2 depicts the Burn vectors for all selected gauges on Danube River basin and its tributaries, time periods 1956–1980 and 1981–2005. Slovak tributaries are indicated graphically in red. The arrows thereby mark the calculated day of average flood occurrence (*MD*), indicated by the direction of the arrow, and the severity of the seasonality, indicated by the scale of the arrow.

The Middle Danube at its beginning is characterized by a shift to summer floods (July/ Julian Date ~180) and later on – from the inflow of the Morava to the gauge of Bogojevo – to early summer (June/Julian Date ~90) (Fig. 2). With the inflow of Drava and Sava, the flood regime of the Danube alters again and regains more pronounced flood seasonality with an occurrence day in spring. This type of regime persists from here on down-stream to the Lower Danube. As on this section of the Danube the stream shares its seasonality pattern with the Tisza and the Velika Morava, the influence of these two major tributaries is not detectable within the regime characteristics.

Flood seasonality of the Danube tributaries is a function of catchment characteristics, namely topography and climate zone, that is to say runoff regime. Alpine rivers like Isar, Inn, Enns, and Drava show a typical summer flood season. The nivo-pluvial rivers Morava, Váh, Hron, Ipeľ originating from the Carpathian and Tatra Mountains, and the right-sided Raba too, experience mainly flood events in spring (March or April).

Furthermore, Figure 3 summarizes the average flood day and the *r*-value, the seasonality index, nicely in 3 double charts, for the whole period 1931–2015 and for three 30-years periods 1931–1960, 1961–1990, 1991–2015 and three 20-years periods 1956–1975, 1976–1995 and 1996–2015.

Despite the general similarity between flood season maximum and monthly runoff peak, it needs to be highlighted that the flood seasonality along the Danube River is not very pronounced. In terms of tributaries and their change in seasonality and flood dates, revealed rather unchanged characteristics for most of the rivers. The alpine rivers, the rivers discharging the Carpathian Mountains and the Tatra Mountains, as well as lower Sava, Drava, and upper Tisza showed almost unchanged flood dates and seasonality values. The *r*-value exceeds the value 0.7 (i.e. 70% probability) only at the Belá-Podbanské gauge T14 (Fig. 3). The *r*-values approximately 0.6 (i.e. 60% probability) is in gauge stations T13, T15, and T20–T23. Lower values are recorded at gauges T16–T19 in all monitored periods. For the tributaries the seasonality *r*-values lie in general higher than those of the Danube.

Figure 4 provides a more detailed look into the Burn statistics and its change over time for Slovak Danube

River tributaries gauges. For each gauge a unit circle lines marking flood events and related magnitudes. Furthermore, the annual maximum time series and the related day of the year are given, allowing for a temporal framing of the date of occurrence and the flood magnitude. We will first explore the unit circle and come back later to the temporal framing.

At the gauges T13 (Morava–Moravský sv. Ján), T14 (Belá–Podbanské), T15 (Váh–Liptovský Mikuláš), T20 (Topľa–Hanušovce) and T22 (Ipeľ–Holiša) a concentration of high flood is recorded during the one, approximately half-yearly, period. Due to the location of stations in the river basin, this period is in different seasons. In addition, a second phase of the year is depicted with floods of smaller magnitudes. At the gauge T19 (Kysuca–Kysucké N. Mesto) is the concentration of floods is evenly distributed over two half-yearly periods. In other gauges, floods are evenly distributed throughout the year, such as at a station T16 (Váh–Šaľa) and T21 (Krupinica–Plášťovce).

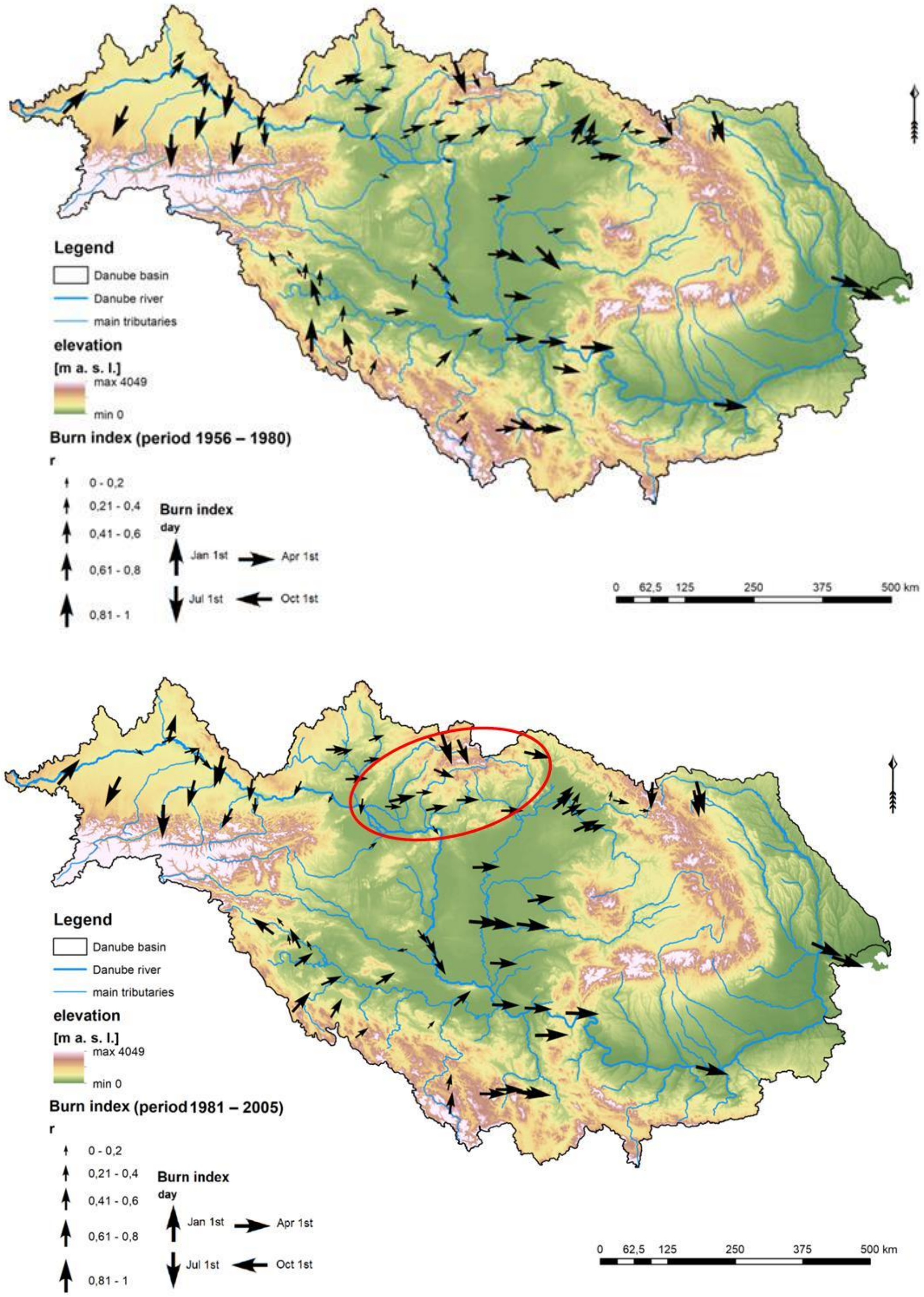

Fig. 2. The Burn r-value as an indication of the seasonality strength and its change over time for 65 gauges of the Danube tributary rivers, period 1956–1980 vs. 1981–2005.

Long term trends of the 25th moving averages of the time series of the Burn indexes

Finally, we have used the time series of the Burn index (period 1931–2015) to analyse the significance of the long-term trends of the Burn index. We computed 25-moving averages of all given time series. We obtained time series for period 1956–2015. For detecting and estimating trend in time series of the Burn indexes we used the non-parametric Mann-Kendall test. In Figure 5 there are plotted the selected gauges series.

In Table 2 there are presented the results of trend significance analysis for selected 11 stations on the Slovak Danube (T13–T23) tributaries, with the longest daily discharge series.

The analysis of trend significance of the Burn index shows different results. The trends in different stations were decreasing, stable or increasing. The stable trend is only in T14 (Belá–Podbanské) and two decreasing trends are in T13 (Morava–Moravský sv. Ján) and T16 (Váh–Šaľa). In the remaining gauges the increasing trend of the Burn index is recorded.

Very interesting are the results from the gauge T23 (Nitra–Nitrianska Streda). In this station is strong varia-

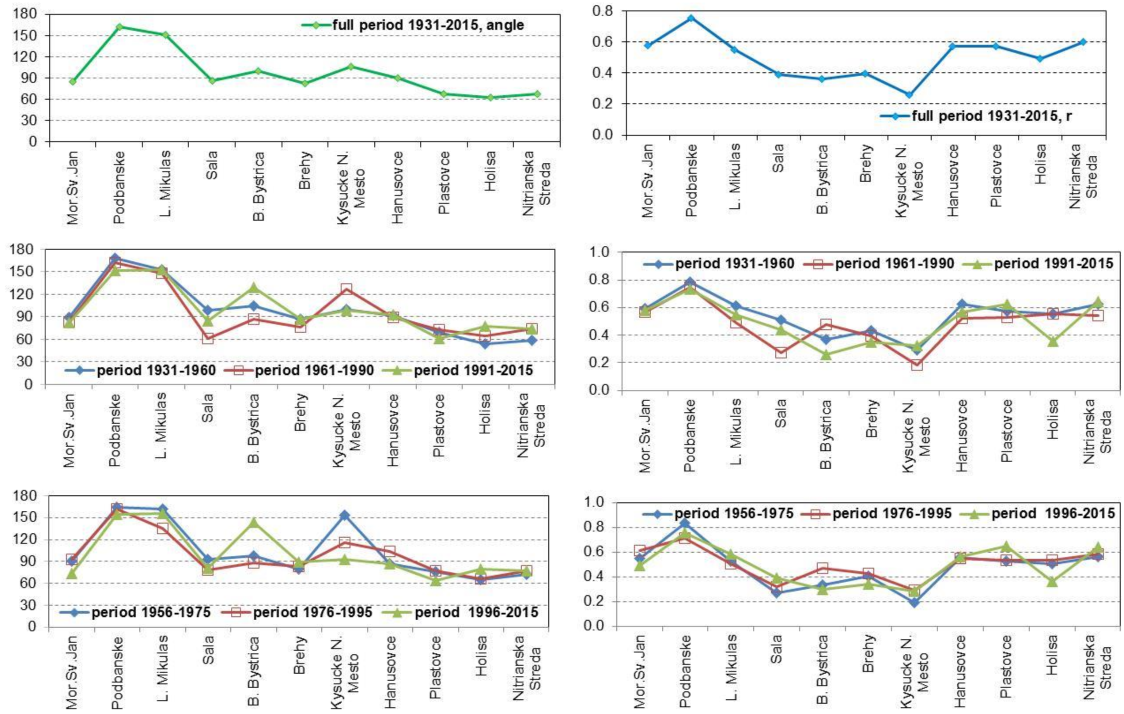

Fig. 3. Average flood day (left charts) and the Burn r-value as an indication of the seasonality strength (right charts) and their change over time for 11 gauges on Slovak tributaries (the whole period 1931–2015 vs. three 30-years periods and three 20-years periods).

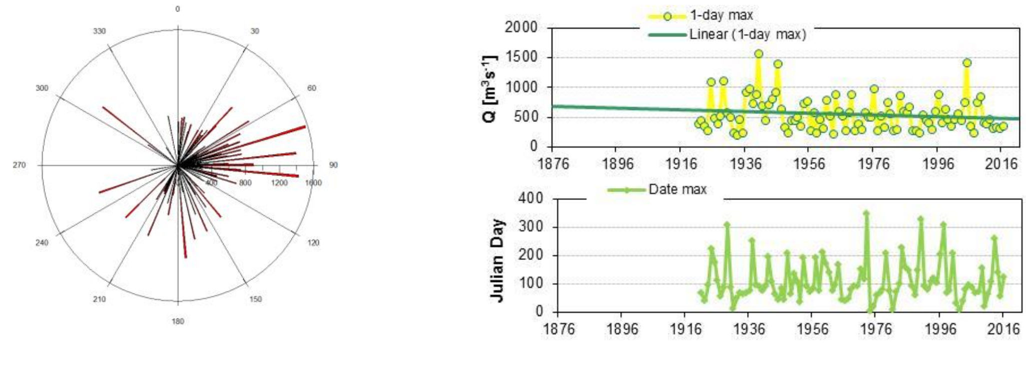

T13 Morava–Moravský sv. Ján 1921–2016

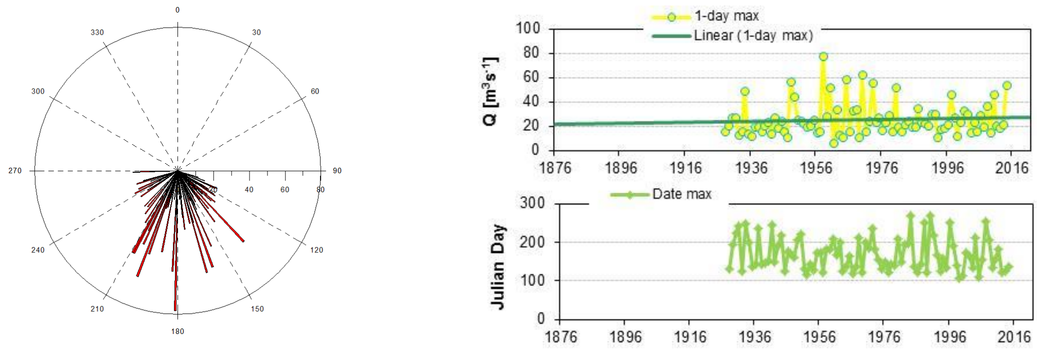

T14 Belá–Podbanské 1928–2014

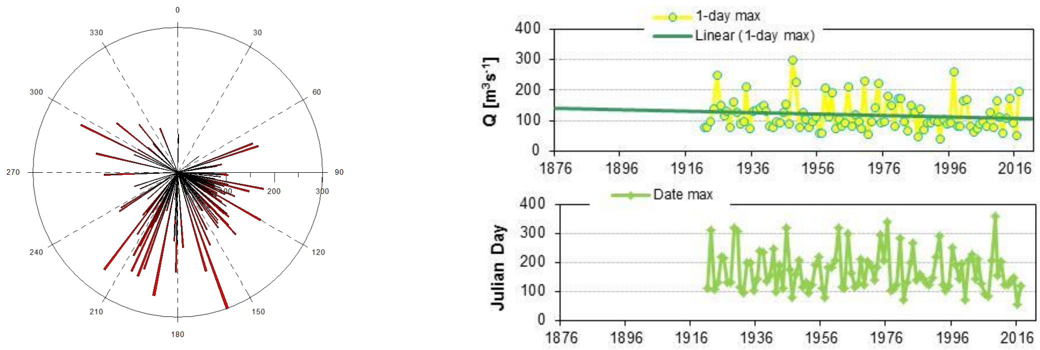

T15 Váh–Liptovský Mikuláš 1921–2017

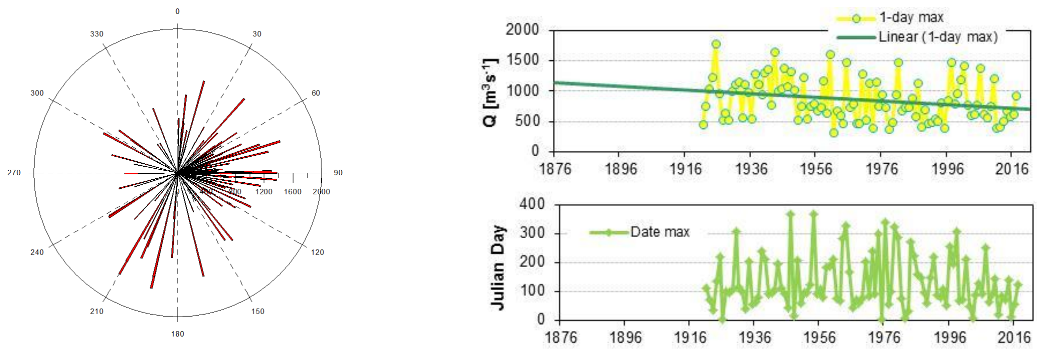

T16 Váh–Šaľa 1921–2017

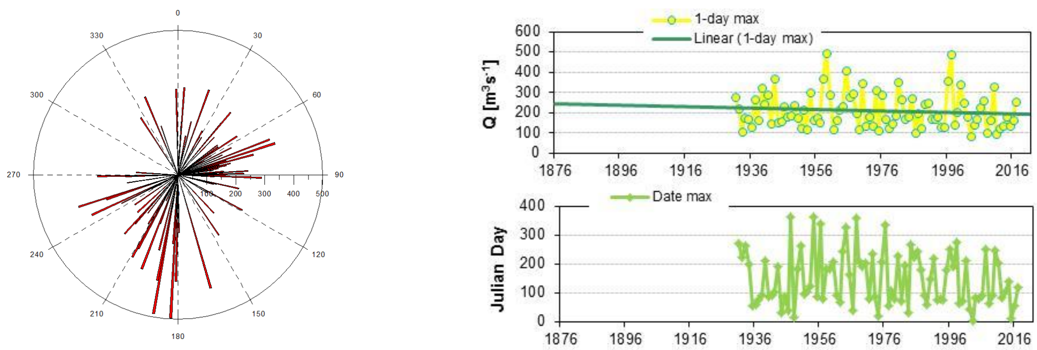

T19 Kysuca–Kysucké n. Mesto 1931–2017

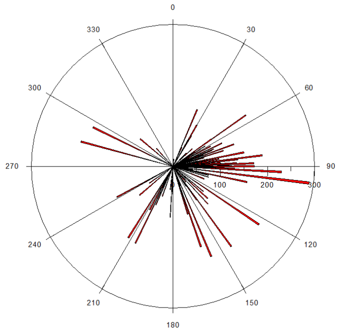

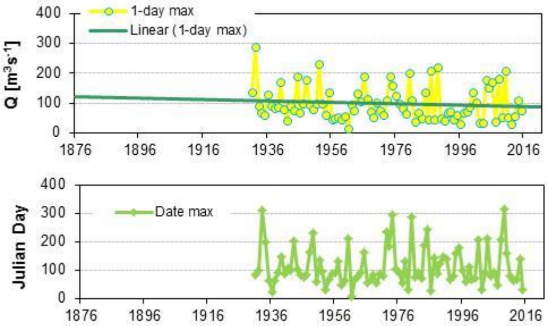

T20 Topľa–Hanušovce 1931–2015

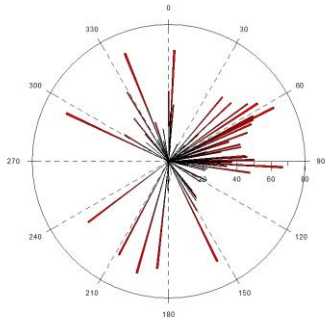

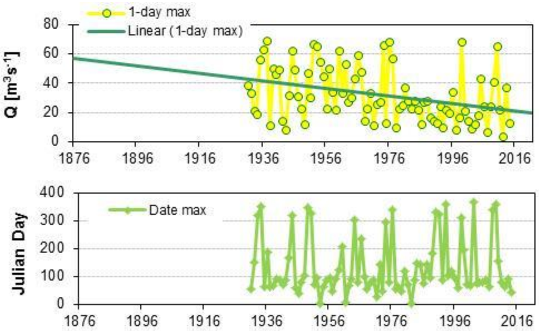

T21 Krupinica–Plášťovce 1931–2014

Fig. 4. Changes in the flow regime shown by the inner-annual variations of streamflow along the Slovak Danube River tributaries.

Table 2. Trend significance analysis for selected stations with the longest series

	Mann-Kendall trend					Sen's slope estimate	
Time series *Burn index, Julian day*	**First year**	**Last Year**	***n***	**Test Z**	**Signific.**	**A**	**B**
T13 (Morava–Moravský sv. Ján)	1956	2015	60	-3.44	***	-0.186	109.38
T14 (Belá–Podbanské)	1956	2014	59	0.00		0.000	162.66
T15 (Váh–Liptovský Mikuláš)	1956	2015	60	1.60		0.062	146.32
T16 (Váh–Šaľa)	1956	2015	60	-0.68		-0.077	94.64
T17 (Hron–Banská Bystrica)	1956	2015	60	1.63		0.120	79.82
T18 (Hron–Brehy)	1956	2015	60	3.03	**	0.223	54.15
T19 (Kysuca–Kysucké N. Mesto)	1956	2015	60	3.60	***	0.647	39.76
T20 (Topľa–Hanušovce)	1956	2015	60	4.03	***	0.271	63.31
T21 (Krupinica–Plášťovce)	1956	2014	59	4.81	***	0.221	45.41
T22 (Ipeľ–Holiša)	1956	2015	60	8.12	***	0.653	-10.77
T23 (Nitra–Nitrianska Streda)	1956	2015	60	6.84	***	0.527	7.79

For the four tested significance levels the following symbols are used
**** if trend at α = 0.001 level of significance; ** if trend at α = 0.01 level of significance*
** if trend at α = 0.05 level of significance; + if trend at α = 0.1 level of significance*

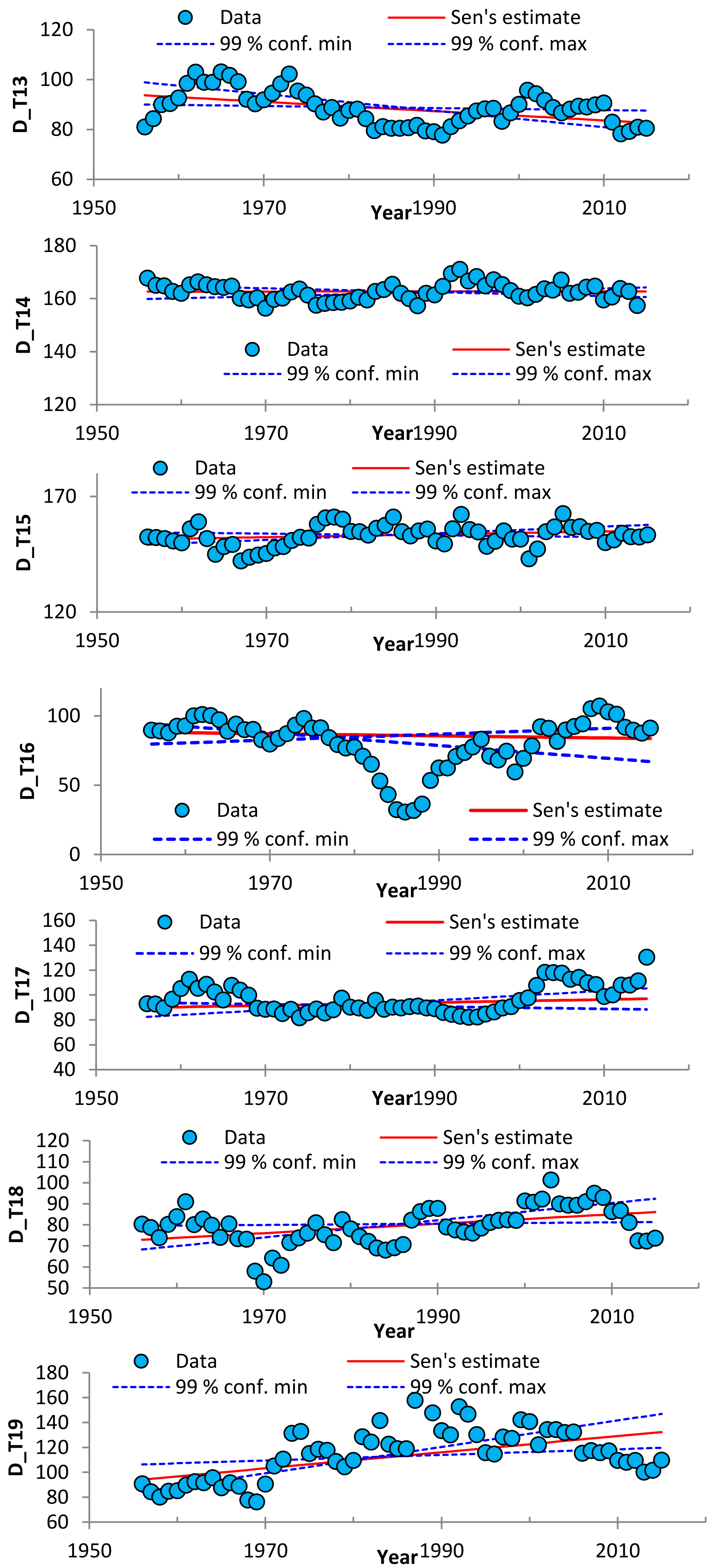
D_T13
Data
Sen's estimate
99 % conf. min
99 % conf. max
Year
D_T14
Data
Sen's estimate
99 % conf. min
99 % conf. max
Year
D_T15
Data
Sen's estimate
99 % conf. min
99 % conf. max
Year
D_T16
Data
Sen's estimate
99 % conf. min
99 % conf. max
Year
D_T17
Data
Sen's estimate
99 % conf. min
99 % conf. max
Year
D_T18
Data
Sen's estimate
99 % conf. min
99 % conf. max
Year
D_T19
Data
Sen's estimate
99 % conf. min
99 % conf. max
Year

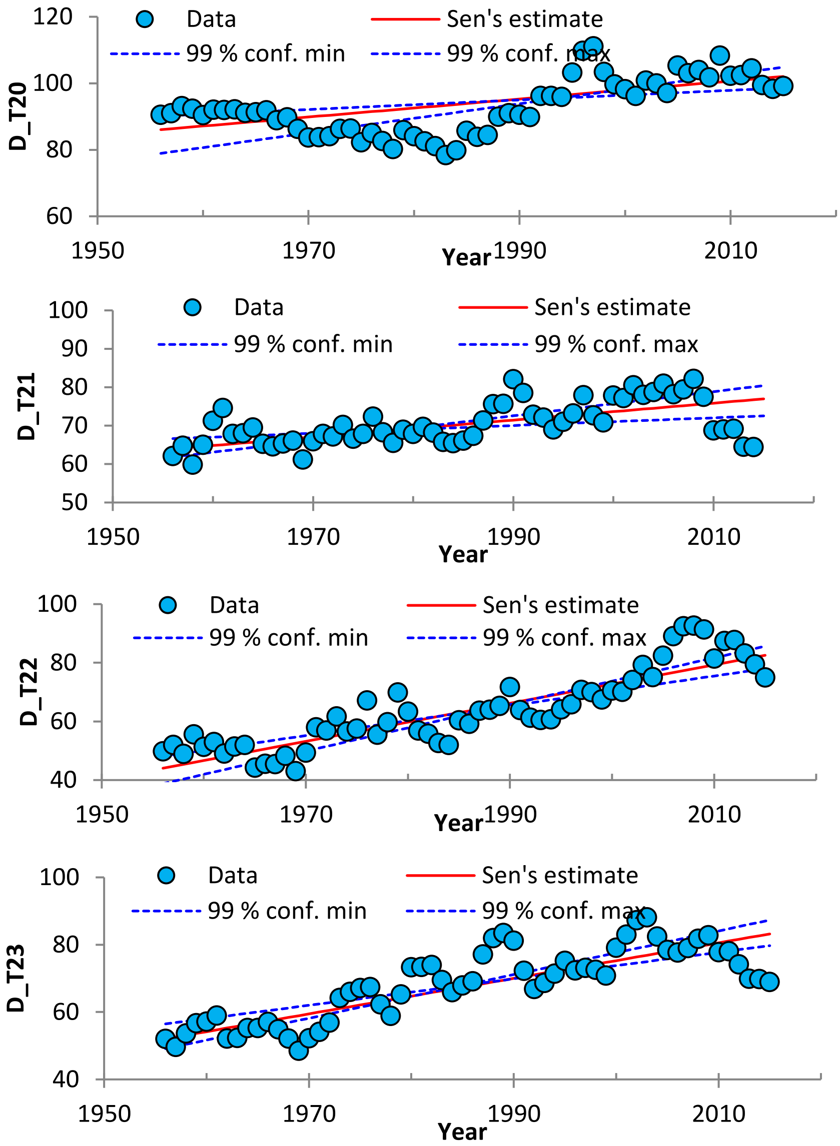

Fig. 5. Long term trends of the Burn index time series calculated for 25-year periods for selected gauges along the Danube River.

bility and increasing of the Burn index time series. The Burn indexes vary from 45 to 90. The similar variability we can see from the results for T21 (Krupinica–Plášťovce) but the wave amplitude is two times longer. Very low variability is in gauges T14 Belá–Podbanské, T15 (Váh–Lipt. Mikuláš) and T16 (Váh–Šaľa).

Conclusions

The Danube River changes its runoff character repeatedly and tributaries, as well as biggest Slovak ones, play a superior role in understanding the Danube River characteristics. That is because they represent the regional water balance and hydrometeorological conditions.

The seasonality of the hydrologic characteristics is characterised by two indices. The first one is quantified by the Pardé coefficient, and the second index describes the seasonality of the maximum annual floods and annual maxima of daily precipitation, respectively. It is based on Burn's index, which indicates the mean date and variability of occurrence of the extreme events. The result is the most probable date of the occurrence of an extreme event along with the stability-index $\bar{r}$ (expressing the probability, which the event will actually occur on this day).

Flood seasonality of the Danube tributaries is a function of catchment characteristics, namely topography and climate zone, that is to say runoff regime. Alpine rivers like Isar, Inn, Enns, and Drava show a typical summer flood season. The nivo-pluvial rivers Morava, Váh, Hron, Ipeľ originating from the Carpathian and Tatra Mountains, and the right-sided Raba too, experience mainly flood events in spring (March or April) (Rössler et al., 2019).

In terms of Slovak Danube tributaries and their change in seasonality and flood dates, revealed rather unchanged characteristics for most of the rivers. The alpine rivers, the rivers discharging the Carpathian Mountains and the Tatra Mountains, as well as lower Sava, Drava, and upper Tisza showed almost unchanged flood dates and seasonality values. The *r*-value exceeds the value 0.7 (i.e. 70% probability) only at the Belá-Podbanské gauge (Fig. 2).

The analysis of trend significance of the Burn index shows variable results. The trends in different stations were decreasing, stable or increasing. The stable trend is only in Belá–Podbanské and two increasing trends are in Morava–Moravský sv. Ján and Váh–Šaľa. In the remaining gauges the increasing trend of the Burn index is recorded.

Defining temporal change in river discharge is a fundamental part of establishing hydrological variability, and crucially important for identifying climate–streamflow linkages, water resource planning, flood and drought management and for assessing geomorphological and hydro-ecological responses.

The detection of trends in hydrological data is a complex issue. The results have shown that the trend analysis is dependent on the chosen period: in particular, it can have significant influence on both trend magnitude and the direction. The implications of analytical decisions on the interpretations of hydrological change are important and impact on planning and development in many fields including water resources, flood defence, hydro-ecology and climate-flow analysis.

Acknowledgements

This work was supported by the project VEGA No. 2/0004/19 "Analysis of changes in surface water balance and harmonization of design discharge calculations for estimation of flood and drought risks in the Carpathian region".

References:

Blahušiaková, A., Matoušková, M. (2012): Analýza povodní na hornom toku Hrona v rokoch 1930–2010. Geografie, 117, 4, 415–433.

Blahušiaková, A., Matoušková, M. (2015): Rainfall and runoff regime trends in mountain catchments (Case study area: the upper Hron River basin, Slovakia). J. Hydrol. Hydromech., 63, 3, 183–192. DOI: 10.1515/johh-2015-0030.

Blahušiaková, A., Matoušková, M. (2016): Evaluation of the hydroclimatic extremes in the upper Hron River basin, Slovakia. AUC Geographica, 51, 2, 189–204. DOI: 10.14712/23361980.2016.16.

Burn, D.H. (1997): Catchments Similarity for Regional Flood Frequency Analysis Using Seasonality Measures. Article in Journal of Hydrology, 202(1): 212–230. Doi: 10.1016/S0022-1694(97)00068-1.

Bower, D., Hannah, D. M., McGregor, G. R. (2004): Techniques for assessing the climatic sensitivity of river flow regimes. Hydrol. Processes 18, 2515–2543.

Garcíja, N. O., Mechoso, C. R. (2005) Variability in the discharge of South American rivers and in climate. Hydrol. Sci. J. 50(3), 459–478.

Halmová, D., Pekárová, P. (2020): Runoff regime changes in the Slovak Danube River tributaries. Acta Hydrologica Slovaca, Volume 21, No. 1, 2020, 3–12. DOI: 10.31577/ahs-2020-0021.01.0001.

Krasovskaia, I., Gottschalk, L. (2002): River flow regimes in a changing climate. Hydrol. Sci. J. 47(4), 597–609.

Milano, M., Reynard, E., Bosshard, N., Weingartner, R. (2015): Simulating future trends in hydrological regimes in Western Switzerland. Journal of Hydrology: Regional Studies, 4, 748–761.

Laaha and Blöschl, (2006): Seasonality indices for regionalizing low flows. Hydrological Processes, 20, 3851–3878.

Parajka, J., Merz, R., Szolgay, J., Blöschl, G., Kohnová, S., Hlavčová, K. (2008): A comparison of precipitation and runoff seasonality in Slovakia and Austria. Meteorologický časopis, 11, 2008, 9–14.

Parajka, J. Kohnová, S., Merz, R., Szolgay, J., Hlavčová, K. Blöschl, G. (2009): Comparative analysis of the seasonality of hydrological characteristics in Slovakia and Austria. Hydrological Sciences–Journal–des Sciences Hydrologiques, 54, 3, 456–473.

Rössler, O., Belz, J., U., Mürlebach, M., Larina-Pooth, M., Halmová, D., Garaj, M., Pekárová, P. (2019): Analysis of the intra-annual regime of flood flow and its changes in the Danube basin. In: Pekárová, P., Miklánek, P. (eds.) Flood regime of rivers in the Danube River basin. Follow-up volume IX of the Regional Co-operation of the Danube Countries in IHP UNESCO. IH SAS, Bratislava, p. 101–122. DOI: https://doi.org/10.31577/2019.9788089139460.

Villarini, G. (2016): On the seasonality of flooding across the continental United States. Advances in Water Resources 87, 80–91.

Villarini, G., Smith, J. A., Serinaldi, F., Ntelekos, A. A. (2011): Analyses of seasonal and annual maximum daily discharge records for central Europe. J. Hydrol., 399, 3–4, 299–312. DOI: 10.1016/j.jhydrol.2011.01.007.

Ing. Dana Halmová, PhD. (*corresponding author, e-mail: halmova@uh.savba.sk)
RNDr. Pavla Pekárová, DrSc.
Institute of Hydrology SAS
Dúbravská cesta 9
84104 Bratislava
Slovak Republic

DOI: 10.31577/ahs-2020-0021.02.0023

ACTA HYDROLOGICA SLOVACA

Volume 21, No. 2, 2020, 188 – 196

ANALYSIS OF THE RUNOFF VOLUMES OF THE WAVE BELONGS TO MAXIMUM ANNUAL DISCHARGES

Veronika Bačová Mitková*, Dana Halmová

Several hypothesis claim that more extremes in climatic in hydrological phenomena are anticipated. In order to verify such hypotheses we described the annual flood risk volume analysis carried out in the Váh River in Slovakia. In the present study, the annual maximum runoff volumes with *t*-day durations (*t*=2-, 5-, 10- and 20-days) were calculated for an 85-year series (1931–2015) of mean daily discharges and maximum annual discharges of Váh River: Liptovský Mikuláš gauge. In the next section, we estimated the total volumes of the wave belongs to maximum annual discharges. The *T*-year volume values were calculated using Log-Pearson type III distribution. Statistical method was used to clarify how the maximum and total volumes of the Váh River changed over the selected period (1931–2015).

KEY WORDS: Váh River, wave volume, Log-Pearson III probability distribution, *T*-year volume

Introduction

The basic need for dimensioning of flood protection structures are designed values of hydrological characteristics which could have disaster effect. Determination of design values for extreme floods with very low probability of occurrence, it means with a long return period (once every 1000 years) is a very difficult and complex process, coupled with great uncertainty. When developing plans and maps of flood threats, it is desirable to use various methods – starting with historical hydrology (mapping historical records), through statistical methods of calculating design values, to using mathematical modelling of extreme hydrological situations and regionalization methods. Solution of some water management tasks requires knowing not only maximum discharge but also the shape of the flood wave or at least its volume. The damage of the protective dam may not occur as a result of high water levels or discharges, but also, as a result of long-time high volumes – wetting, overspill e.g. connection of two flood waves at the confluence. The significance of the flood wave volume as an important hydrological characteristic was evident, e.g. during the flood in 1965 on the Danube River, when the protective dams ruptured due to the long occurrence of high water level, not because of its extreme value (Zatkalík, 1970; Hladný et al., 1970). The similar situation was in the spring of 1941 on the Morava River when the flood lasted more than 3 months and volume was almost 2 times larger than the volume of the flood wave in 1997 with almost identical culmination. Analyzing temporal changes in maximum runoff volume series of the Danube River was investigated in Halmova et. al., (2008). Szolgay et al. (2012) dealt with the estimation of the flood wave volume, which corresponds to the maximum design discharge with an return period of *T*=10 000 years. From foreign authors, e.g. Beard (1956) dealt with determining maximum volumes. Author used theoretical exceedance curves to calculate annual maximum volumes of varying exceedance probability considering the duration of the flow wave *t*.

In assessment of the climate change impacts on the river runoff regime (extremes, flood hydrographs and drought periods), it is expected that the increase of air temperature may cause (or already has caused) the increase of extreme discharges and flood volumes. It is necessary regularly to check the validity of the assumptions in order to have correct statistical results (IACWD, 1982). Significant changes in the river basins (as urbanization or construction of the flood protection structures) may have influence on the hydrological extremes and can corrupt the frequency analysis application. It is well known that in some small streams were floods with atypical ratio of the extreme flood wave volume to its culmination, and belonged to the phenomena, the occurrence of which no one expected. Therefore, for the engineering praxis is necessary to study the flood wave volumes in time. In applied hydrology the problem is the assignment of flood wave volumes with a certain probability of occurrence to the corresponding *T*-year discharges.

The aim of this study is:

- assess the maximum annual runoff volumes V_{maxt}

lasting 2-, 5-, 10-, 20-days and total runoff volumes V of the wave belongs to annual maximum discharges of the Váh River: Liptovský Mikuláš (1931–2015);

- determine the theoretical exceedance probability curves;
- estimate the T-year annual maximum runoff volumes with t-day durations and total runoff volumes of the wave belongs to annual maximum discharge;
- analyze changes in the discharge wave volumes of the Váh River: Liptovský Mikuláš (1931–2015).

Case study area

The Váh River and Input data

The Váh River is an important and the longest Slovak river with a length of 403 km and a basin area of 19 696 km^2. It rises in the Tatra Mountains by the confluence of the White Váh and Black Váh (Fig. 1). The Váh River flows over northern and western Slovakia and finally feeds into the Danube near Komárno. The Váh River basin accounts for about 37% of water bearing of Slovakia. The Váh has a large number of tributaries, many of which are mountain streams from the Tatra Mountains and Carpathians (e.g. Belá, Orava, Kysuca, Rajčianka, Turiec, Malý Dunaj,…). Long-term daily discharges of the Váh River during the period of 1931–2015 reached value about of 20.4 m^3 s^{-1} at Liptovský Mikuláš gauge (basin drainage depth is 582.4 mm) and the maximum discharge reached value 540 m^3 s^{-1} (29th June 1958).

The course of annual peak discharges, long-term linear trend and 5-year moving trend are illustrated on the Figure 1. The annual peak discharges of the Váh River at Liptovský Mikuláš show decreasing long-term linear trend during the selected period of 1931–2015. The deviation of mean long-term annual discharge showed the driest period of 1986–1999 (Fig. 1). There were also occurred some extreme floods in 1934, 1948, 1958 or 1997 and relatively longer wet period in 1973–1981 (Fig. 1). The scenarios of changes of selected elements of the hydrosphere and biosphere in the Váh basin are reported in monography of Pekárová and Szolgay (2005) and in Jeneiova et al. (2014).

Methodology

To define the volumes of individual waves, we introduced the parameter t – runoff duration in days. In this way, we determined maximum runoff volumes of t=2-, 5-, 10- and 20 days. The series of mean daily discharges were used to determine the annual maximum runoff volume V_{maxt} lasting 2-, 5-, 10- and 20- days. If the wave duration was less than 20 days, the steady discharges were included into the analysis. Figure 2 presents an example of the determination of maximum volumes with a given runoff duration.

For determination of the total duration and total volume of the wave, it was necessary to identify the beginning and end of the wave. It is quite difficult to identify the beginning and end of the discharge wave, in some cases. In our analysis, the beginning and end of the wave was determined approximately at the level of the long-term average daily discharge $\overline{Q}_d$=21 m^3 s^{-1} (1931–2015). We also assumed that there were no others significant atmospheric events.

In the world literature, there is a number of scientific papers dealing with the selection and testing of the suitability of theoretical probability distributions in estimating maximum values of hydrological characteristics (Cunnane 1989; Helsel and Hirsch, 2002; Langat et al., 2019). The type of statistical methods, especially selection of the theoretical probability distribution, which is used to estimate the extreme values, also influences the estimation of their return periods. Based on our knowledge, we propose to use only one type of distribution, namely the Log-Pearson distribution III. type (LPIII distribution). Log-Pearson distribution III. type is used to

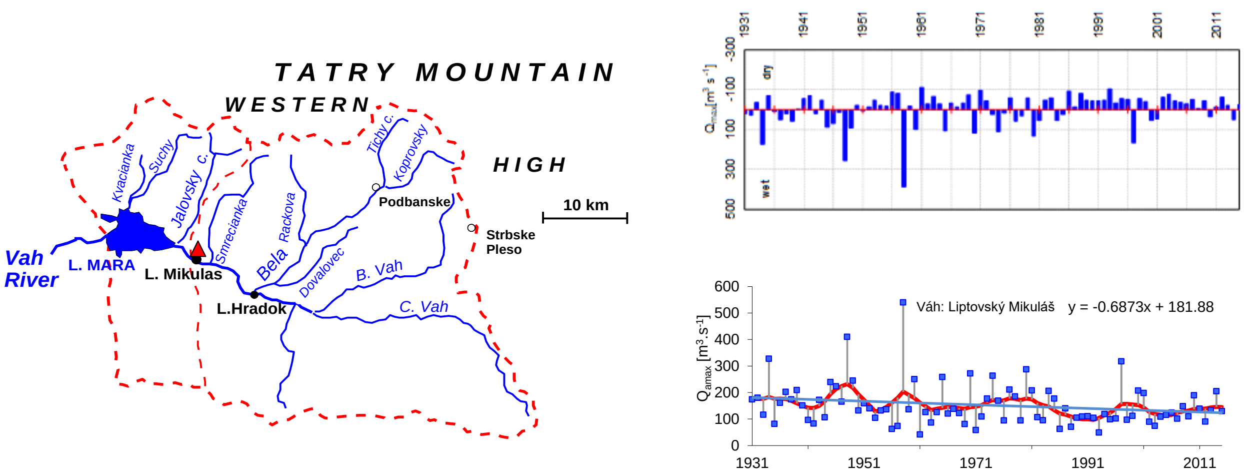

Fig. 1 The location of the selected Váh River section and right-up: deviation from long-term mean annual discharge during the period of 1931–2015 and right-down: maximum annual discharges, Váh: Liptovský Mikuláš (1931–2015), their linear trend and 5-year moving trend.

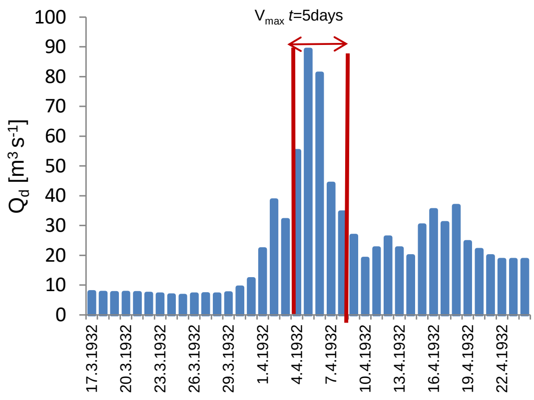

Fig. 2. Example of the determination of the maximum volume with a given runoff duration t=5 days on Váh River: Liptovský Mikuláš (1932).

estimate extremes in many natural processes and is one of the most commonly used probability distribution in hydrology (Phien and Jivajirajah, 1984; Pilon and Adamowski, 1993; Millington et al., 2011). The LPIII theoretical distribution belongs to the family of Pearson distributions, so called three parametric Gamma distributions, with logarithmic transformation of the data. This type of distribution is possible to proceed with regionalization of the LPIII distribution using the third parameter of this distribution – skew coefficient (asymmetry). The cumulative distribution function and probability distribution function according Hosking and Wallis (1997) are defined as:

If $\gamma \neq 0$ let $\alpha=4/\gamma^2$ and $\xi=\mu-2\sigma/\gamma$

If $\gamma>0$ then:

$$F(x) = G(\alpha, \tfrac{x-\xi}{\beta})/\Gamma(\alpha) \tag{1}$$

$$f(x) = \frac{(x-\xi)^{\alpha-1}e^{-(x-\xi)/\beta}}{\beta^{\alpha}\Gamma(\alpha)} \tag{2}$$

where
ξ – location parameter;
α – shape parameter;
β – scale parameter;
Γ – Gamma function.

If $\gamma<0$ then

$$F(x) = 1 - G(\alpha, \tfrac{x-\xi}{\beta})/\Gamma(\alpha) \tag{3}$$

$$f(x) = \frac{(\xi-x)^{\alpha-1}e^{-(\xi-x)/\beta}}{\beta^{\alpha}\Gamma(\alpha)} \tag{4}$$

The Kolmogorov-Smirnov test was performed to test the assumption that the discharge magnitudes follow the theoretical distributions. The *p*-value ($p\geq0.05$) was used as a criterion for rejection of the proposed distribution hypothesis. The empirical probability curve of the maximum volumes was calculated according equation (5):

$$P = \frac{m}{n+0{,}4} \tag{5}$$

where
m – variable order number – descending order to the statistical series;
n – number of variables.

The relationship between the probability of exceedance a given value in any year and its average return period T is (Szolgay et al., 1994):

$$p = 1 - e^{-1/T} \tag{6}$$

If $T \geq 10$ we can use simplified form of equation (6):

$$P = \frac{m}{T} \tag{7}$$

Results

Maximum annual runoff volumes V_{maxt} lasting 2-, 5-, 10-, 20-days

The annual maximum runoff volumes at a given runoff duration of the Váh River at Liptovský Mikuláš station during the period of 1931–2015 and their linear trends are presented in Figure 3. From the point of view of 2-days and 5-days annual maximum runoff volumes the highest values reached the flood in 1948 ($V_{maxt=2}$=39.1 mil.m^3 and $V_{maxt=5}$=71.4 mil.m^3). From the point of view of 10-days and 20-days annual maximum runoff volumes the highest values reached the flood in 1965 ($V_{maxt=10}$=106.2 mil.m^3 and $V_{maxt=20}$=175.2 mil.m^3). The maximal numbers of the annual peak discharges occurred in May. The maximum annual volumes show a slightly declining linear trend for 2-days and 5-days runoff duration. Figure 4 and Table 1 present T-year annual maximum runoff volumes of the Váh: Liptovský Mikuláš (Log-Pearson III).

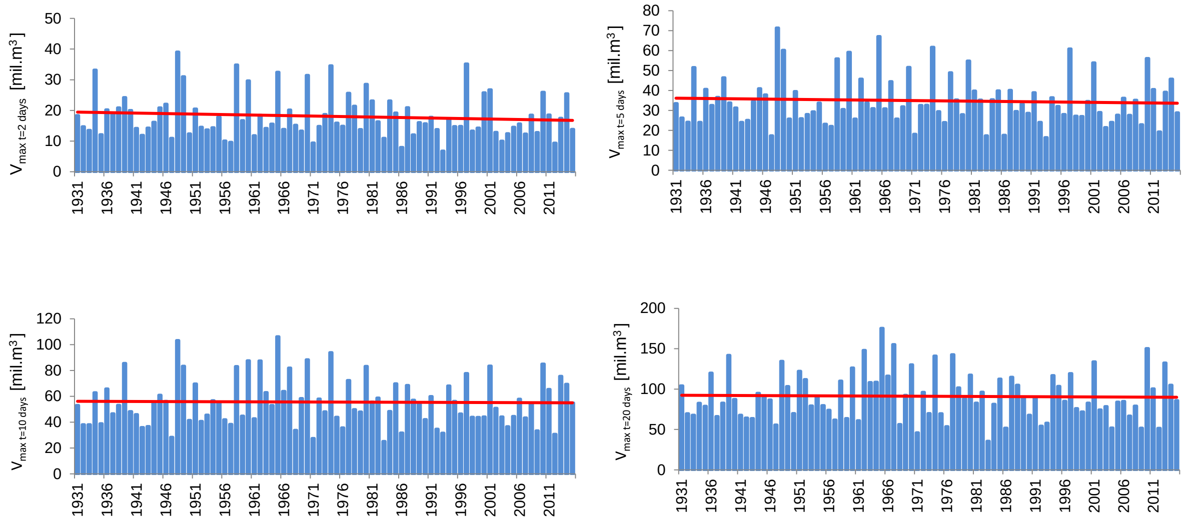

Fig. 3. Time course of annual maximum runoff volumes lasting 2-, 5-, 10-, 20-days, Váh River: Liptovský Mikuláš (1931–2015).

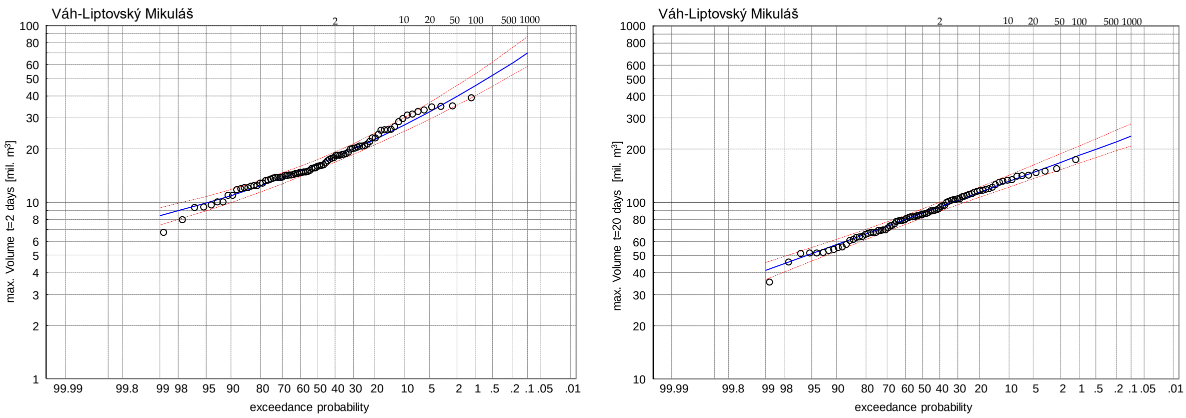

Fig. 4. The LPIII exceedance probability curve of the V_{max} for a given runoff duration t=2 days (left) and t=20 days (right), Váh: Liptovský Mikuláš (1931–2015).

Table 1. ***T*-year maximum discharges Q_{max} [m³ s⁻¹] and *T*-year annual maximum runoff volumes V_{maxt} [mil. m³], Váh: Liptovský Mikuláš (1931–2015) (Log-Pearson III)**

River: Gauging station	Q_T [m³ s⁻¹]	t=2 days	t=5 days	t=10 days	t=20 days
Váh: Liptovský Mikuláš	Q_{50}	V_{50maxt} [mil. m³]			
	426	41	79	108	171
	Q_{100}	$V_{100maxt}$ [mil. m³]			
	521	46	78	116	184
	Q_{500}	$V_{500maxt}$ [mil. m³]			
	809	62	99	143	221
	Q_{1000}	$V_{1000maxt}$ [mil. m³]			
	969	70	108	154	237

Maximum annual runoff volumes V_{maxt} lasting 2-, 5-, 10-, 20-days in two parts

With regard to the character of the upper part of the river Váh basin, where the seasonality of individual tributaries is manifested, we divided the data into two parts:

I. December–May;
II. June–November.

The maximum annual runoff volumes V_{maxt} lasting 2-, 5- , 10-, 20-days, show a constant or slightly decreasing linear trend for the I. part: December–May. The maximum annual discharges and maximum annual volumes for a given runoff duration t=2 days and t=20 days for selected periods I. are presented in Figure 5. The maximum annual runoff volumes V_{maxt} lasting 2-days have decreasing linear trend during the II. part: June-November. For V_{maxt} lasting 5-, 10- and 20-days the trend is approached to constant value.

Calculated *T*-year maximum annual volumes V_{maxt} for runoff duration t=2-days and 20-days calculated by LPII probability distribution for selected parts I. and II. are presented in Figure 6. *T*-year annual maximum runoff volumes V_{maxt} for selected parts are listed in Table 2.

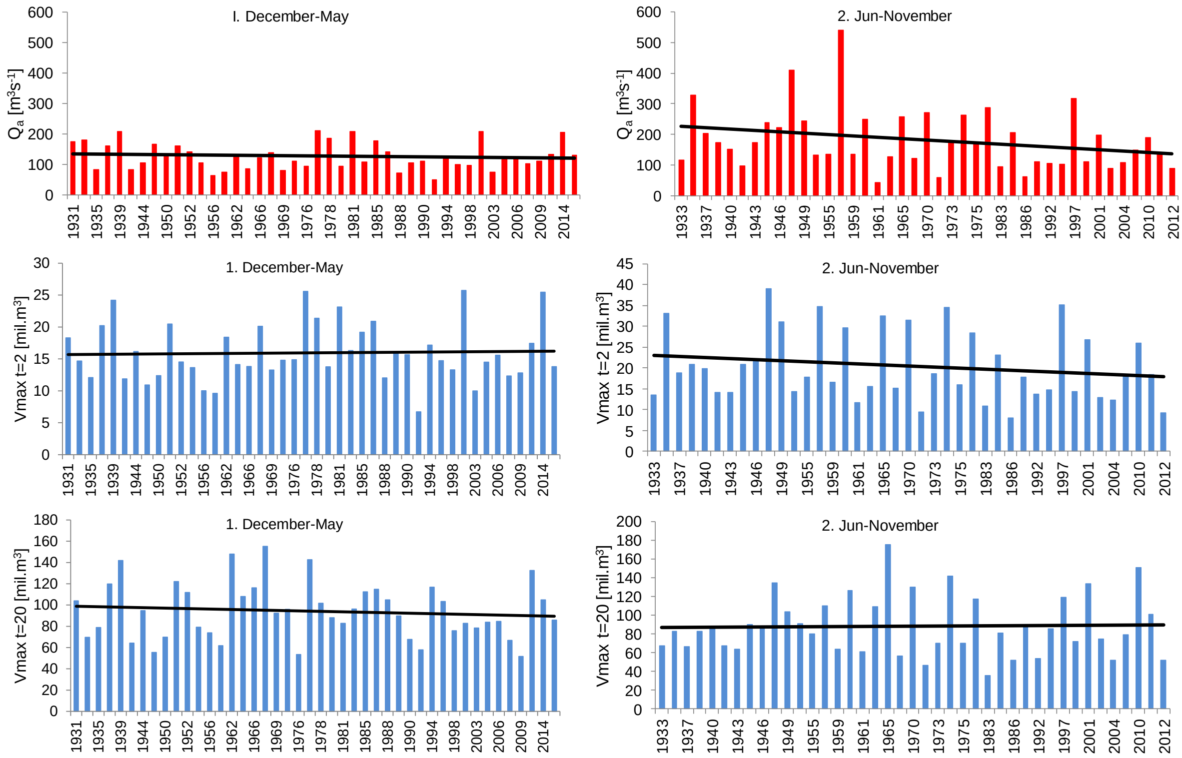

Fig. 5. The maximum annual discharges and maximum annual volumes for a given runoff duration t=2 days and t=20 days for selected parts I. and II., Váh: Liptovský Mikuláš (1931–2015).

Table 2. ***T*-year annual maximum runoff volumes V_{maxt} [mil. m^3] for selected parts, Váh: Liptovský Mikuláš (1931–2015) (Log-Pearson III)**

River: Gauging station	parts	t=2 days	t=5 days	t=10 days	t=20 days
Váh: Liptovský Mikuláš	V_{50maxt} [mil. m^3]				
	I.	27	51	91	160
	II.	44	80	117	172
	$V_{100maxt}$ [mil. m^3]				
	I.	29	54	98	172
	II.	49	89	130	190
	$V_{500maxt}$ [mil. m^3]				
	I.	33	60	114	200
	II.	63	112	161	232
	$V_{1000maxt}$ [mil. m^3]				
	I.	35	63	12	211
	II.	68	122	175	250

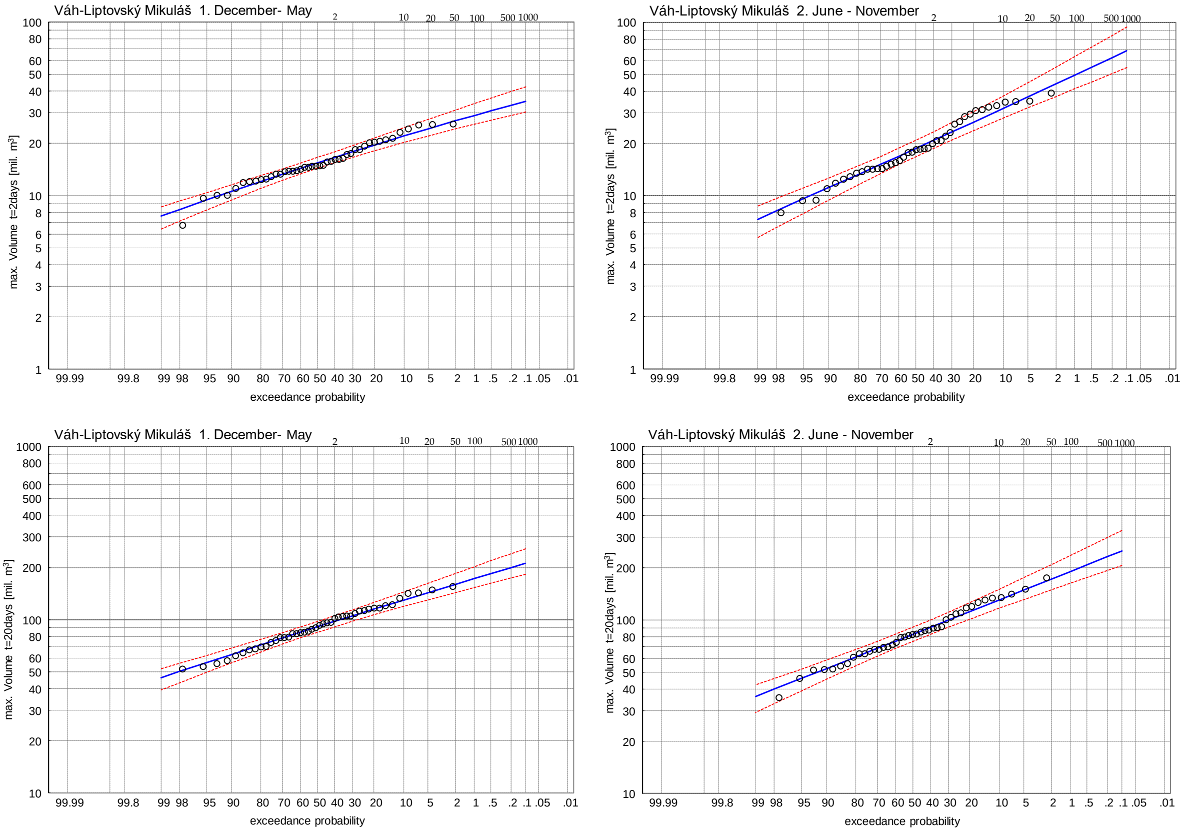

Fig. 6. The LPIII exceedance probability curve of the V_{maxt} for a given runoff duration t=2 days and t=20 days for selected parts I. and II., Váh: Liptovský Mikuláš (1931–2015).

Total annual runoff volumes of the wave belongs total annual maximum discharge

As mentioned above in our analysis, the beginning and end of the wave was determined approximately at the level of the long-term average daily discharge $\overline{Q}_d$=21 m^{3}s^{-1} (1931–2015). Figure 7 illustrates the total runoff duration and month of annual maximum discharge occurrence.

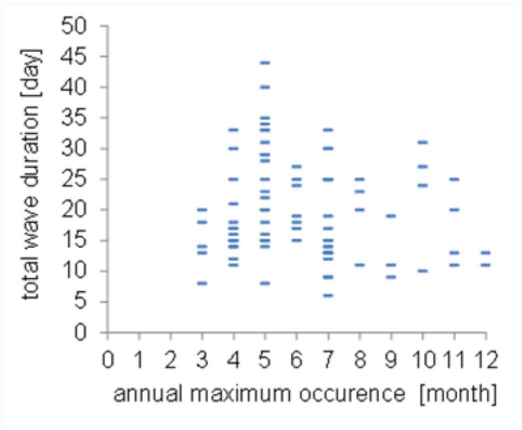

Fig. 7. Distribution of the total duration of the wave belongs to the annual discharges, Váh: Liptovský Mikuláš (1931–2015).

Figure 7 shows that the total wave durations above 25-days most often occur in May.

The mean total duration of the discharge waves with this limit was 20 days (Fig. 8a).The longest duration (t=43 days) with this criterion was identified for wave which occurred in April–May 2013 (Figure 8a). The maximum discharge of this wave was about 133.50 m^3 s^{-1}. In contrast, the wave belongs to the highest annual maximum discharges (years 1948 and 1958) lasted only 25 days (Figure 8a). Calculated total volumes of the identified wave belongs to maximum annual discharges of the river Váh: Liptovský Mikuláš for the period 1931–2015 are illustrated in Figure 8b. The total volume and duration of the waves show a slightly increasing trend during the selected period (Fig. 8).

Based on calculated total runoff volumes of the wave belongs to annual maxima the T-year total volumes were calculated by Log-Pearson type III. probability distribution (Fig. 9). Table 3 listed T-year maximum discharges Q_{max} and T-year annual total runoff volumes belong to annual maximum discharges in Váh: Liptovský Mikuláš (1931–2015) (Log-Pearson III).

Total annual runoff volumes of the wave belongs to the annual maximum discharge in two parts

The total runoff volumes V and total runoff duration t of the waves show a markedly increasing linear trend for the I. period: December–May (Fig. 10). The LPIII exceedance probability curve of the total runoff volumes of the wave belongs to annual maximum discharges of the Váh: Liptovský Mikuláš for part I. and part II. (1931–2015) were calculated by Log-Pearson type III. probability distribution. The exceedance curves of the total runoff volumes are presented in (Figure 11). *T*-year annual runoff volumes *V* for selected parts are listed in Table 4. The average difference of the *T*-year total volumes *V* and *T*-year total volumes V_I and V_{II} belongs to annual maximum discharges for Q_{100} can be 22% and for Q_{1000} the difference is 43%.

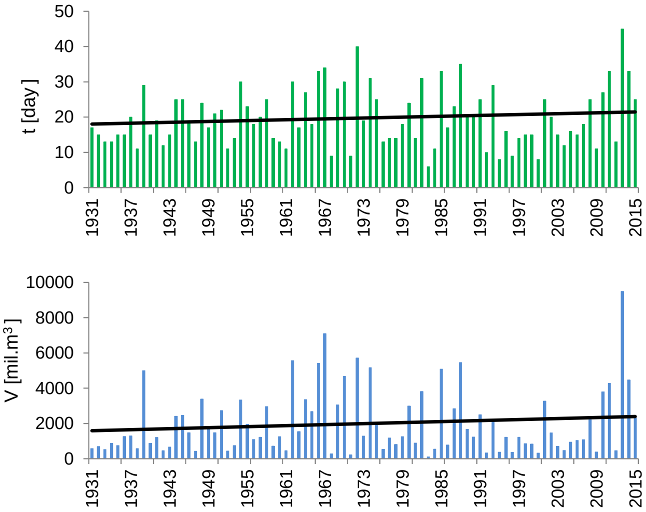

a)

b)

Fig. 8. Values of a) total duration of the waves annual maximum discharges, b) total runoff volumes of the wave belongs to annual maximum discharges, Váh: Liptovský Mikuláš (1931–2015).

Table 3. *T*-year maximum discharges Q_{max} [m^{3}s^{-1}] and *T*-year annual total runoff volumes *V* [mil. m^3] belongs to annual maximum discharges, Váh: Liptovský Mikuláš (1931–2015) (Log-Pearson III)

	Váh: Liptovský Mikuláš (1931–2015)			
	Q_{50}	Q_{100}	Q_{500}	Q_{1000}
Q_T [m^{3}s^{-1}]	426	521	809	969
V [mil. m^3]	8633	10978	17790	21389

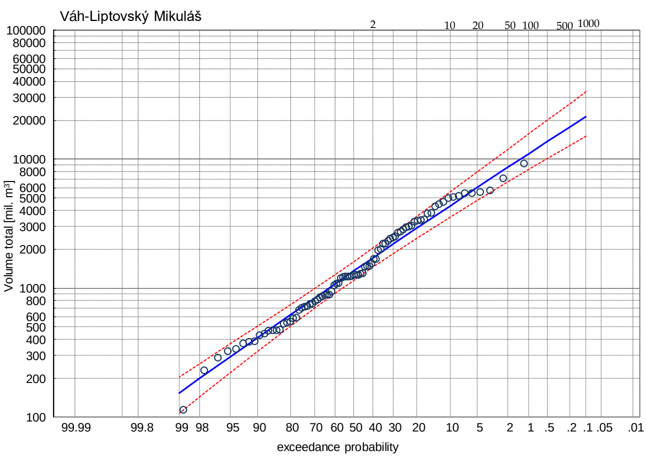

Fig. 9. The LPIII exceedance probability curve of the total runoff volume of the wave belongs to annual maximum discharges, Váh: Liptovský Mikuláš (1931–2015).

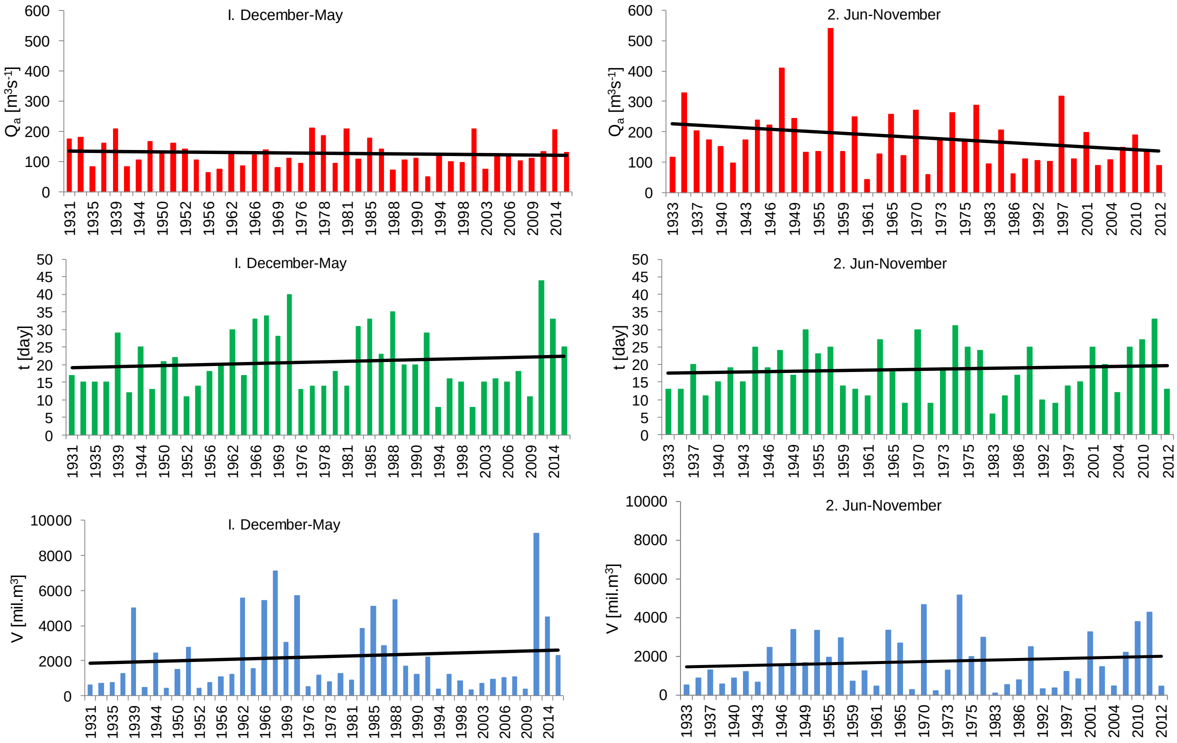

Fig. 10. Values of the anunual maximum discharges, total duration of the wave belongs to annual maximum discharges and total wave volumes belongs to annual maximum discharges, Váh: Liptovský Mikuláš (1931–2015) (left: part I. and right: part II.).

Table 4. ***T*-year annual total runoff volumes V_I [mil. m^3] and V_{II} [mil. m^3] for selected parts, Váh: Liptovský Mikuláš (1931–2015) (Log-Pearson III)**

Váh: Liptovský Mikuláš (1931–2015)				
	V_{50}	V_{100}	V_{500}	V_{1000}
I. December–May				
$V_{I.}$ [mil. m^3]	10760	14411	26502	33707
II. June–November				
$V_{II.}$ [mil. m^3]	6981	8503	12434	14293

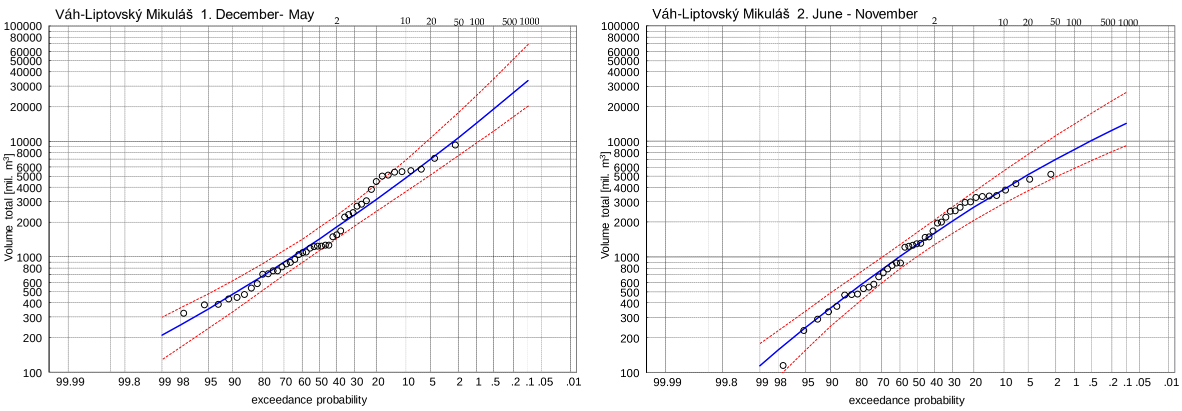

Fig. 11. The LPIII exceedance probability curve of the total runoff volumes of the wave belongs to annual maximum discharges, Váh: Liptovský Mikuláš (1931–2015) (left: part I and right: part II.).

Conclusion

Our analysis showed that in terms of the analyzed period 1931–2015, the maximum annual discharges have a decreasing linear trend and the annual maximum runoff volumes with a duration t=2 days have a slightly linear decreasing trend. Dividing the observed time period into two parts according to the occurrence of annual maximum discharges (I. December–May and II. June–November), the analysis showed a markedly decreasing trend at maximum annual discharges and a slightly decreasing trend in annual maximum runoff volumes with a duration t=2 days mainly in part II. June–November. On the contrary, the analysis of the total wave length and the total volume of wave belongs to annual maximum discharge showed an increasing linear trend in terms of the whole observed part 1931–2015. During the part I. December–May, the analysis showed a higher increasing trend of the total wave length and the total wave volume. The maximum annual discharges show only a slightly decreasing trend in the part I. December–May.

In conclusion, we can state that the given analysis showed on average decrease in annual maximum flows and also maximum annual volumes at t=2 days for the whole period. At the same time, an increase in the duration of the waves (according to our selected criteria) and the total volume of the waves was recorded. These changes are more pronounced especially for the part I. December–May. The snow melting in the mountain tributaries catchments and rainfall may cause such trend.

In addition to the analysis of volume changes, we focused on the use of one type of theoretical probability distribution – Log-Pearson distribution III. type. The LPIII probability distribution showed a high sensitivity to the inclusion of extremes in the underlying data series. We can state that this distribution is suitable for maximum flows with a longer repetition time.

Acknowledgement

This work was supported by the project VEGA No. 2/0004/19 "Analysis of changes in surface water balance and harmonization of design discharge calculations for estimation of flood and drought risks in the Carpathian region".

References

Beard, L. R. (1956): Statistical Evaluation of Runoff Volume Frequencies. Symposium Dorcy, IASA, Dijon.

Cunnane, C. (1989): Statistical distributions for flood frequency analysis. In Operational Hydrology Report (WMO); WMO: Geneva, Switzerland.

Halmova D., Pekarova P., Pekar J., Onderka M. (2008): Analyzing temporal changes in maximum runoff volume series of the Danube River. IOP Conf. Series: Earth and Environmental Science 4, IOP Publishing. 1–8. doi:10.1088/1755-1307/4/1/012007.

Helsel, D. R., Hirsch, R. M. (2002): Statistical Methods in Water Resources; US Geological Survey: Reston, VA, USA, Volume 323

Hladný, J., Doležal, F., Makeľ, M. and Sacherová, D. (1970): Peak runoff volumes of a given duration (in Czech) Hydrological conditions of the CSSR Volume III.

Hosking, J. R. M., Wallis, J. R. (1997): Regional Frequency Analysis. Cambridge University Press. Cambridge.

IACWD (1982): Guidelines for determining flood flow frequency, Bulletin 17-B. Technical report, Interagency Committee on Water Data, Hydrol. Subcommittee. 194 p.

Jeneiova, K., Kohnova, S., Sabo, M., (2014): Detecting Trends in the Annual Maximum Discharges in the Vah River Basin. Slovakia, Lign. Hung., Vol. 10, Nr. 2 (2014) 133–144, DOI: 10.2478/aslh-2014-0010 Acta Silv.

Langat, P. K., Kumar L., Koech R. (2019): Identification of the Most Suitable Probability Distribution Models for Maximum, Minimum, and Mean Streamflow. Water 2019, 11, 734, 1–24, doi:10.3390/w11040734

Millington, N., Das S., Simonovic S. P. (2011): The Comparison of GEV, Log-Pearson Type 3 and Gumbel Distributions in the Upper Thames River Watershed under Global Climate Models. Water Resources Research Report. Department of Civil and Environmental Engineering, The University of Western Ontario London, Ontario, Canada, 1–54.

Phien, H. N., Jivajirajah, T. (1984): Applications of the log Pearson type-3 distribution in hydrology, Journal of Hydrology, 73, 359–372.

Pekárová, P., Szolgay, J. (eds.) (2005): Scenarios of changes in selected hydrosphere and biosphere components in the Hrona and Vah catchment areas due to climate change. Press Bratislava: Veda, 496 p. ISBN ISBN 80-224-0884-0. In Slovak).

Pilon, P. J., Adamowski, K. (1993): Asymptotic variance of flood quantile in log Pearson type III distribution with historical information, J. of Hydrol., 143, 3–4, 481–503.

Szolgay, J., Dzubák, M., Hlavčová, K. (1994): Hydrology. Drainage process and hydrology of surface waters. Slovak faculty of Civil Engineering STU in Bratislava. 277 p. (In Slovak)

Szolgay, J., Kohnová, S., Bacigál, T., Hlavčová, K. (2012): Proposed flood: Joint probability analysis of maximum discharges and their pertaining volumes. Acta Hydrologica Slovaca. Vol. 13(2), 289–296.

Zatkalík, G. (1970): Calculation of the basic parameters of the flow waves. PhD. thesis. 71 p. (In Slovak)

Ing. Veronika Bačová Mitková, PhD. (*corresponding author, e-mail: mitkova@uh.savba.sk)
Ing. Dana Halmová, PhD
Institute of Hydrology SAS
Dúbravská cesta 9
84104 Bratislava
Slovak Republic

DOI: 10.31577/ahs-2020-0021.02.0024

ACTA HYDROLOGICA SLOVACA

Volume 21, No. 2, 2020, 197 – 204

THE DYNAMICS OF ANNUAL AND SEASONAL PRECIPITATION TOTALS IN THE CZECH REPUBLIC DURING 1961–2019

Jaroslav Rožnovský*, Jaroslav Střeštík, Petr Štěpánek, Pavel Zahradníček

The long-term change in precipitation has been estimated for 300 stations in the Czech Republic using values of monthly precipitation totals. Annual totals for the whole country show a very slight decrease, in units of mm, there can be significant fluctuation on a year-to-year basis. Long-term changes of annual totals vary at different stations and in different regions. In southern and western Bohemia, precipitation totals increased more, in Elbe lowlands and in large parts of Moravia, a rather small decrease in rainfall has been observed. Long-term changes depend only slightly on the absolute value of annual rainfall at the respective station or region. Summer precipitation totals increased more than annual averages, while spring precipitation totals decreased. During the remaining seasons, the change is negligible. In the meantime, the annual variation in precipitation has changed slightly: maximum values have shifted from June to July.

KEY WORDS: long-term change, regions, annual precipitation totals, seasons

Introduction

With regard to their significance, precipitation is studied from many points of view. Basically no large rivers flows into the Czech Republic. This means that all water sources are represented by atmospheric precipitation and springs. Their occurrence is affected by circulation (Labudová et al., 2013).

The amount of water in springs, however, also depends on atmospheric precipitation. It is therefore obvious that the precipitation amount, annual precipitation totals and their long-term changes are of major importance (Tolasz et al., 2007). In recent years, it has been very important to analyze climate changes, which manifest themselves especially by global warming (Zahradníček et al., 2020; Střeštík et al., 2014a). It is assumed that the global average air temperature will continue to rise and that the rate of this increase will be higher in the future. However, this means an increase in evaporation (Novák, 1995), and more frequent droughts (Rožnovský et al., 2012). Extremes of precipitation totals play an important role (Bhatia et al., 2019). Climate change analysis also includes precipitation. In contrast to air temperature, some authors believe that the precipitation amount will decrease (Räisänen et al., 2004; Střeštík, 2013), meaning drought periods will be more common. Information on the occurrence of precipitation is important, but also their estimates of its occurrence in the future (Jiang et al., 2017). Kožuchowski and Marciniak (1990) presented a study, which shows that precipitation amount in western and northern Europe is increasing and will continue to increase in the future, unlike in southern and eastern Europe where they believe precipitation amount has been decreasing and will continue to decrease. The Czech Republic lies in the region of expected precipitation decrease. This trend has also been proven by more recent studies (Střeštík, 2014b). Information on precipitation totals of both historical and current data can be found on the portal of the Czech Hydrometeorological Institute (http://portal.chmi.cz/). Precipitation affects processes in the soil, while soil moisture is crucial for plants (Guderle and Hildebrandt, 2015). Precipitation and their use represent a very wide range, from measurement methods, through quantification of water circulation phases, etc., to methods of maintaining water in the landscape. (Rožnovský, 2020).

Materials and methods

Assessment of precipitation dynamics is based on monthly values of the so-called technical series from 267 stations in the Czech Republic (Štěpánek, et al., 2011; 2013). This data was statistically processed and average annual and seasonal amount calculated for each station as well as average annual value for each year for the entire country as a whole, including trends etc.

Results and discussion

Average annual rainfall for the entire Czech Republic for the period 1961–2019 is 691.7 mm. However, the individual annual values are often quite variable. In the driest year 2003 only 513 mm was measured, in 2015 547 mm and 1982 it was 551 mm. The wettest year observed was 2010 894 mm, 1966 with 860 mm, followed by 2002 (854 mm) and 1981 (852 mm). The difference between the driest and wettest year is 381 mm, it is 43% of the wettest year, about 55% of the annual total.

Here are large differences in the precipitation amounts at different stations (Fig. 1). Highest precipitation amounts are observed at mountain stations, especially in the northern parts close to the borders. Stations with highest annual precipitation amount during the entire period were Labská bouda in Giant Mountains (1444 mm) and Lysá hora in Beskids (1422 mm). The absolute highest observed annual precipitation (in one year) was at the station Lysá hora in 2010 (2127 mm).

Lowest precipitation amounts are observed in lowlands, at stations Tušimice in Sub-Ore Mountains Lowland (444 mm) and in Prague-Karlov (445 mm). Absolute lowest observed annual precipitation amount in the entire period was 238 mm in 2008 in České Budějovice (Budweis). The wettest region is eastern Bohemia (average of 892 mm) and northern Moravia (average of 827 mm). Driest region is central Bohemia (average of 556 mm) and southern Moravia (average of 593 mm).

In general the precipitation amounts show a significant positive correlation with elevation (coefficient of 0.72), to a certain extent also with latitude (coefficient of 0.29), however, this is due to the fact that higher mountains are located mostly in the northern part of the country.

The trend during the 1961–2019 period shows a negligible increase in precipitation amount, supplemented by large fluctuations from year to year (Fig. 2). These do not display any regularity or periodicity (e. g. wet years are not usually followed by dry years). The same is valid also for decades and for the 20- or 30-year averages. Their values are given in Table 1.

The course of precipitation amounts for the individual stations or regions is in some extent similar to the course in the entire country. Individual maximums and minimums show a similar pattern. A dry year is a dry year in all regions and at all stations and similarly a wet year is a wet year everywhere. This is because the total area of the Czech Republic is not very large.

But the change in precipitation amount in the individual regions is different. Big differences appear among different regions though the total area of the country is relatively small. An example of different long-term change of precipitation amounts is given in Fig. 3. A strong increase is observed at the station Jirkov-Otvice in Sub-Ore-Mountains Lowland and a strong decrease appears at the station Nedvězí in Bohemian-Moravian Highlands. As a measure of the decrease or increase the slope of the respective regression line can be used. These slopes have been calculated for all stations and are presented in Fig. 4. The highest rate of increase is observed in Sub-Ore-Mountains Lowland and in southern and western Bohemia. In contrast, a decrease was observed in southern and in northern Moravia. The most significant increase was observed at the station Jirkov-Otvice, Sub-Ore-Mountains Lowland (slope 3.47), the largest decrease at the station Nedvězí in Bohemian-Moravian Highlands (slope -3.18). However, at most stations the respective increase or decrease is much weaker and remains far under the limit of the statistical significance.

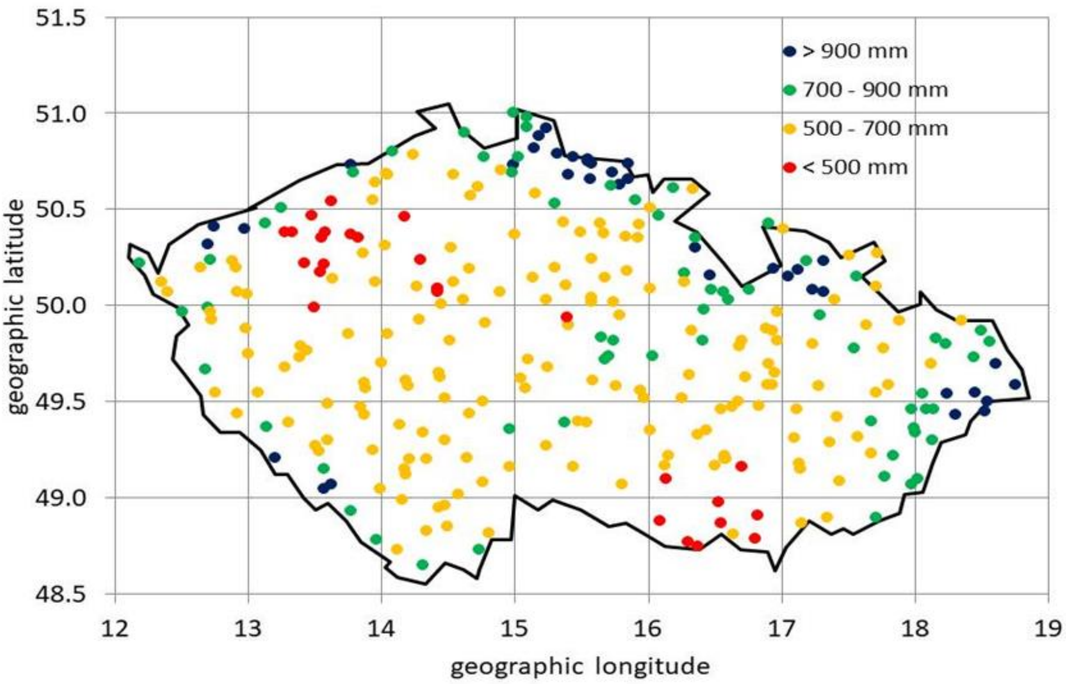

Fig. 1 Distribution of average annual precipitation in the Czech Republic (1961–2019).

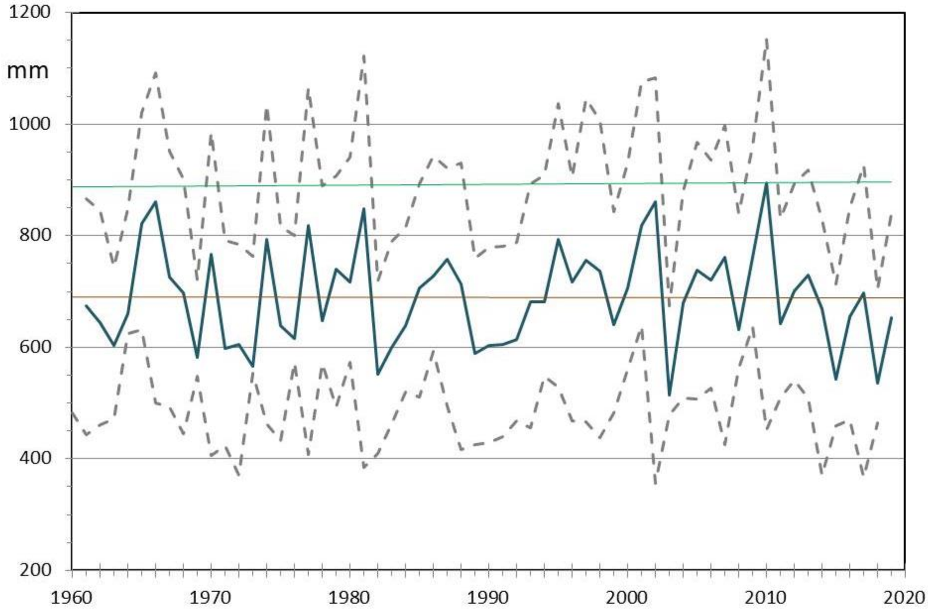

Fig. 2. Course of annual precipitation amounts in the Czech Republic (1961–2019). Dashed lines represent average ± standard deviation.

Table 1. Average precipitation amount [mm] in the individual decades and 20 and 30-year periods in the Czech Republic (1961–2019)

1961–1970	1971–1980	1981–1990	1991–2000	2001–2010	2011–2019
702	673	673	693	736	647
1961–1980	1971–1990	1981–2000	1991–2010	2001–2019	
687	673	683	715	695	
1961–1990	1971–2000	1981–2010	1991–2019		
683	680	701	694		

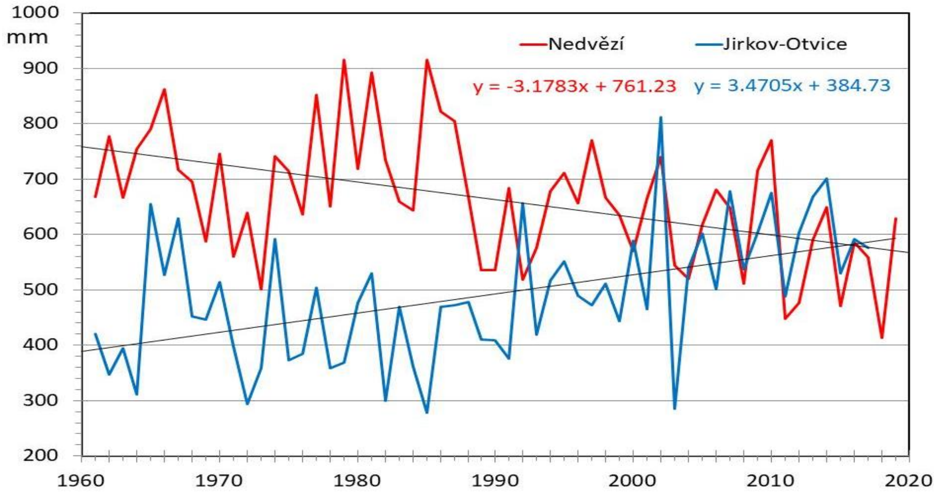

Fig. 3. Course of annual precipitation amounts in two selected stations in the Czech Republic (1961–2019), with regression lines and equations of these lines.

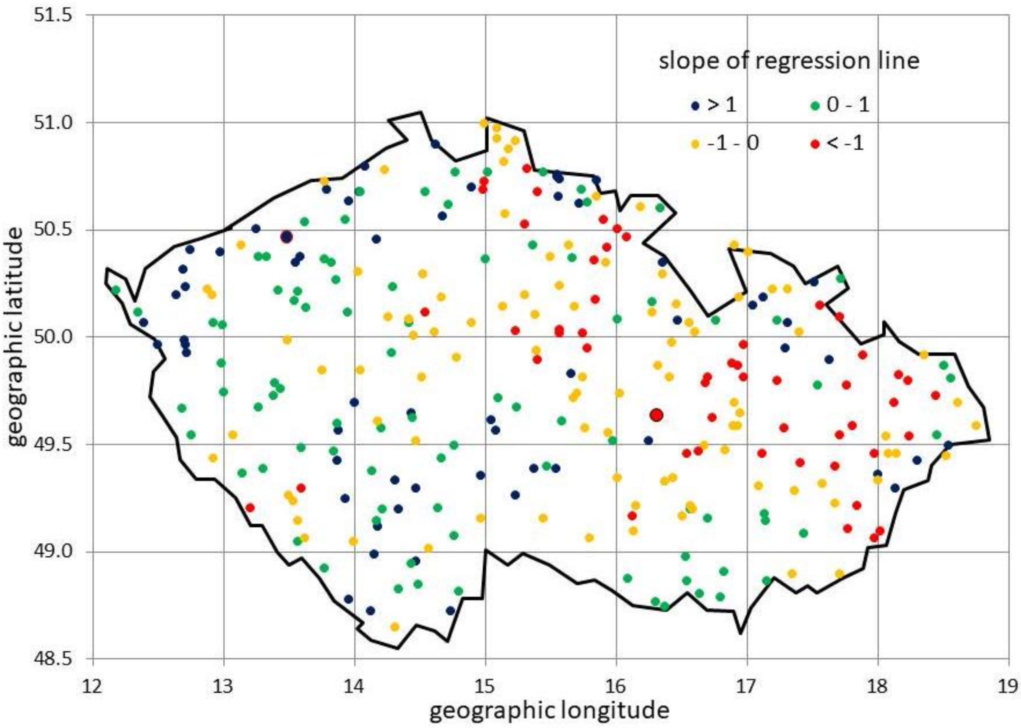

Fig. 4. Distribution of increase and decrease in annual precipitation amount in the Czech Republic (1961–2019). The stations used in Fig. 2 are marked by a bigger point with a boundary of another color.

Despite of these high slopes of the regression lines the real decrease or increase must not be necessarily significant. It is due to high fluctuation from year to year. The significance can be simply guessed when the whole period is divided into two parts (1961–1990 and 1991–1019) and the difference between average values of precipitation amounts in these parts (with respect standard deviations) is tested using the Student's *t*-test. For the stations given in Fig. 7 are the *t*-values 3.72 (Nedvězí) and 4.45 (Jirkov-Otvice). Hence, the change in these stations is statistically significant (the limit value for the 95% significance with 30 points in each part is t=2.04). Roughly said, the increase in precipitation totals at stations marked in Fig. 3 by a dark-blue point and the decrease at stations marked by a red point can be considered as statistically significant.

Despite the relatively small total area of the Czech Republic one can also see some pattern with regards to geographical longitude. Western half of the country shows mostly increase (with the exception of Elbe Lowland and its vicinity), whereas eastern half of the country shows either only very minor increase or, more frequently, a decrease in precipitation amount, with the exception of high-elevation regions of Jeseníky Mountains and Beskids. This means there is a significant negative correlation between precipitation amount and longitude (coefficient of -0.43). There is no significant correlation between absolute average annual precipitation amount and the trend (increase or decrease) (coefficient of just 0.06).

With regard to the need for water in the landscape, the occurrence of precipitation during the year is important. Their distribution into individual seasons for individual climatic areas is shown in Table 2. However, the differences among the regions are small, at most 1-2 percent more or less than the average for the entire Czech Republic.

Changes in seasonal precipitation amounts during 1961–2019 differ significantly from the course of annual precipitation amounts (Fig. 5). The individual maxima and minima do not correspond to each other and this can easily be explained. For example, an exceptionally dry or wet year might not be very dry or wet in each of its seasons. A dry spring can be (but not necessarily) compensated by a subsequent very wet summer or autumn. In fact even many weather sayings suggest that an exceptionally dry or wet season usually does not continue in the subsequent months. Different is also the long-term precipitation trend in the individual seasons (Fig. 5).

In the spring, precipitation totals fall slightly, which can be unpleasant for agricultural crops with a larger decline. The same applies to differences between regions in the case of seasonal precipitation as for year-round precipitation: greater growth is observed in the west, less growth or decline in the east, this also applies to individual stations. In the spring, when a nationwide decline is observed, precipitation totals increase only at a few stations in the border mountains.

Table 2. Proportion of seasonal precipitation amount from the annual total grouped by different regions [%]

Region	Spring	Summer	Autumn	Winter
Czech Republic	23.2	36.4	22.0	18.4
Sub-Ore Mountains Lowland	22.2	33.2	23.1	21.5
Western and Southern Bohemia	23.9	38.5	21.0	16.6
Central Bohemia	23.9	39.1	21.0	16.0
Eastern Bohemia	22.2	33.4	22.5	21.9
Bohemian-Moravian Highland	23.4	36.2	21.4	19.0
South Moravia	23.6	37.4	22.6	16.4
North Moravia	23.8	36.9	22.2	17.1

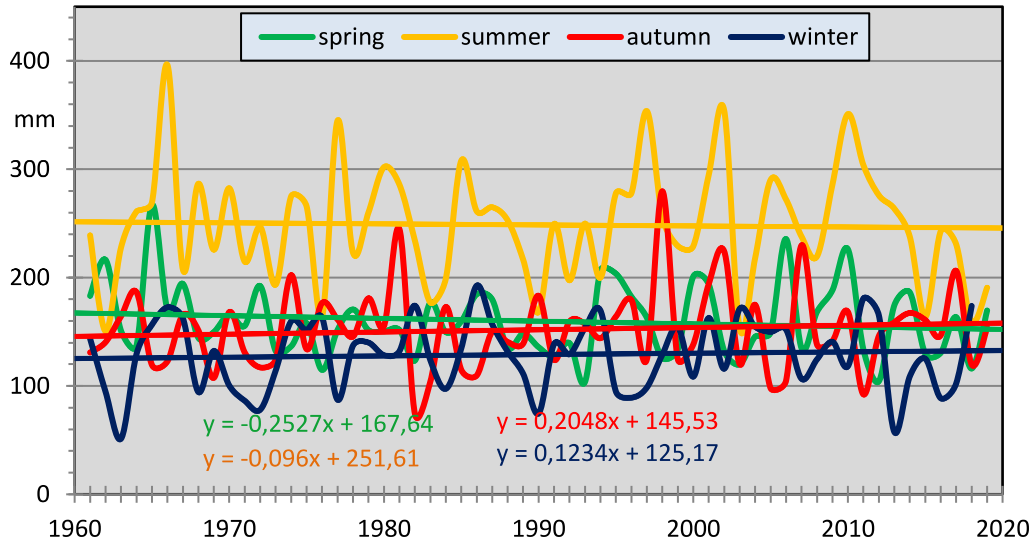

Fig. 5. Course of seasonal precipitation amounts in the Czech Republic (1961–2019). Figure shows approximate regression line in the same color.

The season with highest precipitation amount is summer (Jun-Aug), on average 36.4% of annual total. This value differs only very slightly in the individual regions. Relatively wettest summers are in central Bohemia (39.1%), relatively driest in Sub-Ore-Mountains Lowland (33.2%). The differences for the individual stations, however, are much more profound. Highest ratio of precipitation in summer is observed in Český Krumlov (44.6%), absolute highest was the summer of 1997 in Vítkov in Odra Hills (63.3%). In contrast, the long-term lowest ratio of summer precipitation is at the station Vrchlabí (25.5%), record low was the summer of 1983 at the station Rychorská bouda (8.6%), both in Giant Mountains. Percentage of summer precipitation amount also fluctuates from year to year (Fig. 6). Overall, driest summer was the one in 1962, when only 23.9% of the annual total precipitation amount was observed. On average, the highest summer precipitation ratio was in 1966 and 2011 (47.3%). Long-term change is negligible, based on the regression line the ratio of summer precipitation increased from 36.1% to 37.5%. There is also no periodicity.

The amount of precipitation in the summer does not change much, the curve shows a very small, statistically insignificant decrease. It should, however, be emphasized that there is a high variability in the summer precipitation. This is due to the occurrence of intense thunderstorms. Because they are limited to a certain place, they will not show as much in the overall average as might be expected. In the summer, when growth is higher nationwide, there are more stations in Western Bohemia with more significant growth, while there are fewer stations with a decline and they are concentrated mainly in the Moravian lowlands (Fig. 6). This Figure is prepared by the same way as Fig. 4 and the same statistical significance is valid too. In comparison with

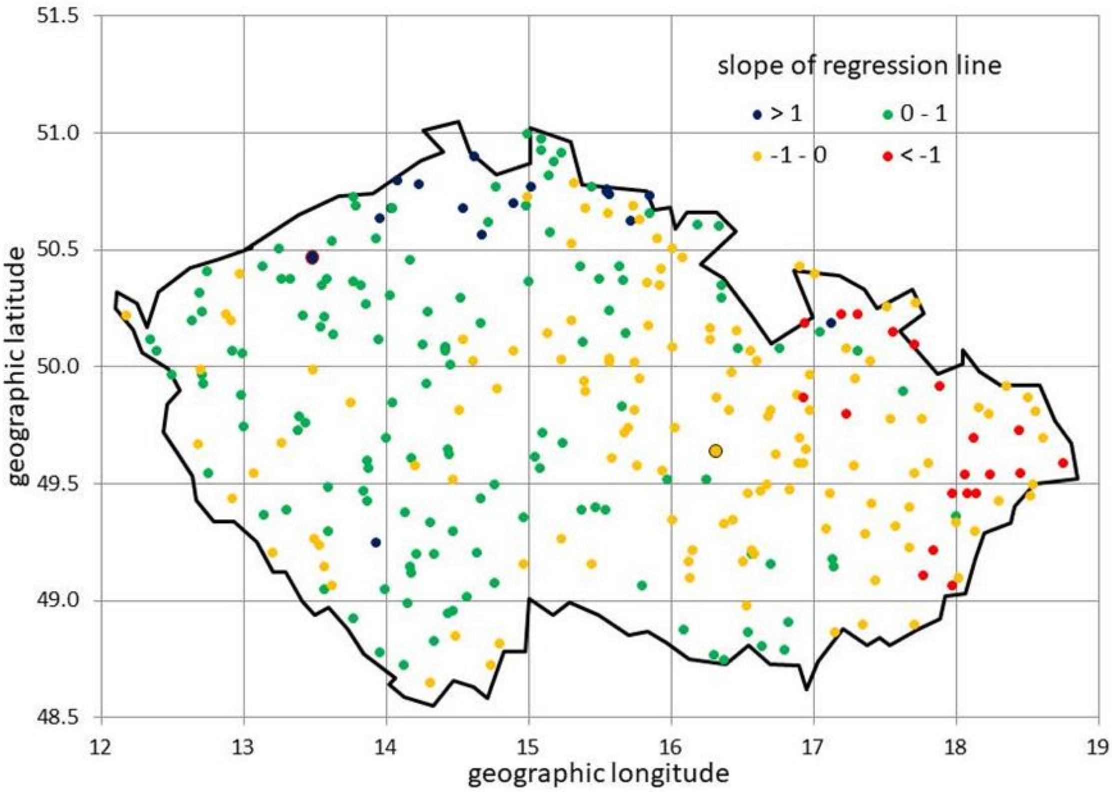

Fig. 6. Distribution of growth and decrease of summer precipitation totals on the territory of the Czech Republic in the period 1961–2019. The stations used in Fig. 2 are marked by a bigger point with a boundary of another color.

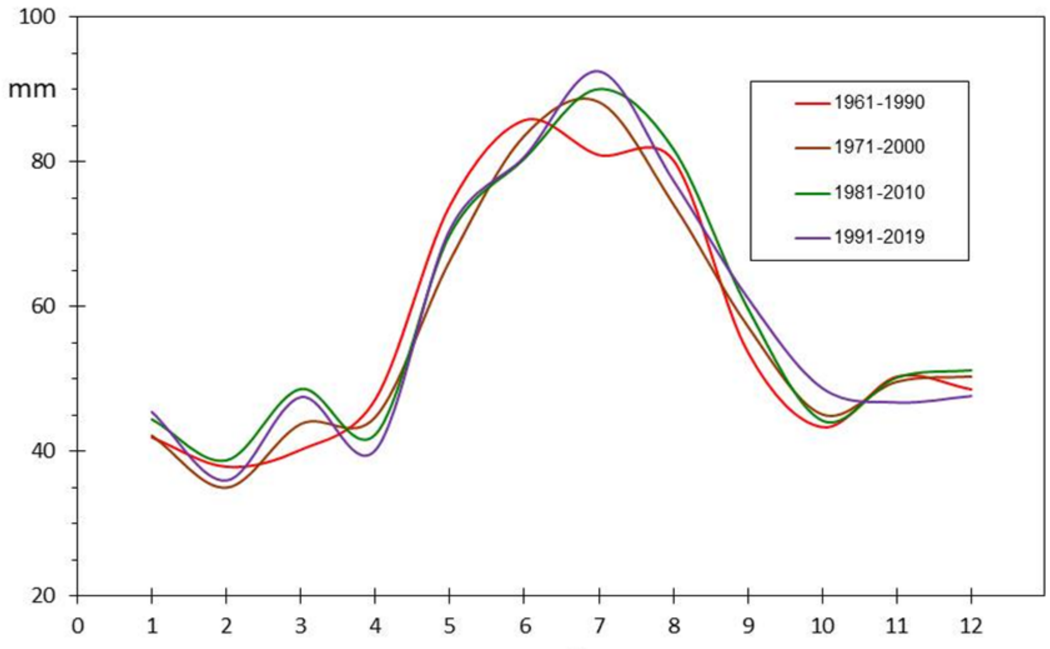

Fig. 7. Average monthly precipitation in the Czech Republic for four 30-year periods. In the recent period it is only 29 years (1991–2019).

annual data, the number of stations with big increase or decrease of summer precipitation totals (blue or red circles) is much lesser.

Just as the course of precipitation differs in individual seasons, the course also differs in individual months, even within the same season, but with the proviso that the three-month average must give the course shown in Fig. 4. The course of precipitation totals during the year for the observed 59 years is shown in Fig. 7 for four 30-year overlapping periods (in the last period, however, it is only 29 years).

It is surprising how the course of monthly precipitation totals during the year in the following 30-years periods differ from the first one (1961–1990). It is worth noting the gradual shift of the main summer maximum, when in the first period it was in June, over time it moved to July. This shift certainly has an impact on the emergence of drought in early summer. There are also some small changes in the spring and autumn: a small increase in March followed by a small decrease in April, and a small increase in October followed by a small decrease in November and perhaps in December. Due to the fact that precipitation amount in spring and autumn are much lower than those in summer, the meaning of the above mentioned changes is very small.

Conclusion

Annual precipitation amounts in the Czech Republic during the period from 1961 to 2019 show a negligible long-term change, i.e., no significant decrease or increase can be taken into account. Moreover, there are large differences of annual and seasonal totals among the individual years. In general, the highest total precipitation is in summer, the lowest in winter.

In the individual seasons the long-term change of precipitation totals are a little different. In the spring, there is a small decreasing trend in precipitation amount. This means that there can be water insufficiency at the beginning of the growing season, particularly in regions where the precipitation amounts are relatively low. Though in the summer a small increase appears (but less than the spring decrease), farmers and gardeners feel the continuing water deficit. Precipitation in the autumn and winter have lesser importance from the perspective of growing season, but are of major importance from the hydrological perspective as they saturate the soil profiles and subsequently ground waters. There are also differences in the regional precipitation amounts – a rather increase in the western regions and a rather decrease in the eastern regions, particularly in lowlands.

Due to the short period of observation used in this study and considerable fluctuations from year to year it is not possible to declare any prediction for the next decades. Nevertheless, the decrease of precipitation amounts in some regions, though with a low statistical significance, should not be neglected. Of course, there are many factors causing the drought in the last years, and precipitation totals are only one of them. But if the decrease of precipitation amounts would continue, and it is not excluded, this factor would be more and more important. And because the precipitations are the only source of water for our territory, it is necessary to pay great attention to their measurement and evaluation, and also to modeling their occurrence in the coming years.

Acknowledgement

The paper was prepared with the support of the project of the Technology Agency of the Czech Republic "Revitalization of agricultural land in areas of the Czech Republic threatened by drought "(TH02030073) and project "Innovation of the Evaluated Soil-Ecological Units (BPEJ) for state administration needs", QK1920280.

References

Bhatia, N., Singh, V. P., Lee, K. (2019): Variability of extreme precipitation over Texas and its relation with climatic cycles. Theor Appl Climatol 138, 449–467. https://doi.org/10.1007/s00704-019-02840-w

Guderle, M., Hildebrandt, A. (2015): Using measured soil water contents to estimate evapotranspiration and root water uptake profiles – A comparative study. Hydrology & Earth System Sciences Discussions, 11, 10859–10902.

Jiang, R., Gan, T. Y., Xie, J. et al. (2017): Historical and potential changes of precipitation and temperature of Alberta subjected to climate change impact: 1900–2100. Theor Appl Climatol 127, 725–739. https://doi.org/10.1007/s00704-015-1664-y

Kożuchowski, K., Marciniak, K. (1990): Tendencje zmian temperatury i opadów w Europie śródkowej w stuleciu 1881–1980. Acta universitatis Nicolai Copernici, Geografia, XXII, zesz. 73, 22–43

Labudová, L., Šťastný, P., Trizna, M. (2013): The North Atlantic Oscillation and winter precipitation totals in Slovakia. Moravian Geographical Reports, Vol. 21, No. 4, p. 38–49, DOI: 10.2478/mgr-2013-0019.

Novák, V. (1995): Vyparovanie vody v prírode a metódy jeho určovania. Bratislava: SAV, 260 s.

Portal ČHMÚ http://portal.chmi.cz/historicka-data/pocasi/zakladni-informace

Räisänen, J., Hansson, U., Ullerstig, A., Döscher, R., Graham, L. P., Jones, C., Meier, H. E. M., Samuelsson, P., Willén, U. (2004): European climate in late twenty first century: regional simulations with two driving global models and two forcing scenarios. Climate dynamics 27, 13–31.

Rožnovský, J. et. al. (2012): Agroklimatologická studie o výskytu sucha na území ČR v roce 2012 a za období srpen 2011 až srpen 2012. Zpráva pro Výzkumný ústav meliorací a ochrany půdy. Český hydrometeorologický ústav, pobočka Brno, 67 s.

Rožnovský J. (2020): Projekce změny klimatu v oběhu vody v krajině České republiky. In: Rožnovský, J. a Litschmann, T. (eds). Sborník abstraktů z mezinárodní konference „Hospodaření s vodou v krajině", Třeboň 9.–10. 9. 2020. Praha: Český hydrometeorologický ústav, s. 21. ISBN 978-80-7653-002-7.

Střeštík, J., Rožnovský, J., Štěpánek, P., Zahradníček, P. (2014a): Increase of annual and seasonal air temperatures in the Czech Republic during 1961–2010. In: J. Rožnovský a T. Litschmann eds. Mendel and Bioclimatology. Conference proceedings, Brno, [CD-ROM]. Brno: 2014. ISBN 978-80-210-6983-1.

Střeštík J., Rožnovský, J., Štěpánek P., Zahradníček, P. (2014b): Změna ročních a sezonních srážkových úhrnů

v České republice v letech 1961–2012. In: Extrémy oběhu vody v krajině, Mikulov. (CD-ROM).
Střeštík, J. (2013): The change of precipitation totals in different European localities during 1900–2000. Proceedings of the international conference "Environmental changes and adaptation strategies", Eds. Šiška, Nejedlík, Hájková and Kožnarová, Skalica.
Štěpánek, P., Zahradníček, P., Farda, A. (2013): Experiences with data quality control and homogenization of daily records of various meteorological elements in the Czech Republic in the period 1961–2010. Idöjárás 117: 123–141,
Štěpánek, P., Zahradníček, P., Brázdil, R., Tolasz, R. (2011): Metodologie kontroly a homogenizace časových řad v klimatologii. Praha. 118 s. ISBN 978-80-86690-97-1.
Tolasz, R. et al. (2007): Atlas podnebí Česka. Český hydrometeorologický ústav, Univerzita Palackého v Olomouci, 255 s. ISBN 978-80-86690-26-1 (CHMI), 978-80-244-1626-7 (UP).
Zahradníček, P., Brázdil, R., Štěpánek, P., Trnka, M. (2020): Reflections of global warming in trends of temperature characteristics in the Czech Republic, 1961–2019. In: J Climatol.; 1–19. https://doi.org/10.1002/joc.6791

RNDr. Ing. Jaroslav Rožnovský, CSc. (*corresponding author, e-mail: jaroslav.roznovsky@chmi.cz)
Mgr. Petr Štěpánek, Ph.D.
Mgr. Pavel Zahradníček, Ph.D.
Český hydrometeorologický ústav
Kroftova 43,
616 67 Brno
Czech Republic

RNDr. Ing. Jaroslav Rožnovský, CSc.
RNDr. Jaroslav Střeštík, CSc.
Mendelova univerzita v Brně
Zemědělská 1,
613 00 Brno
Czech Republic
roznov@mendelu.cz